

MARTIN MARIETTA ENERGY SYSTEMS LIBRARY

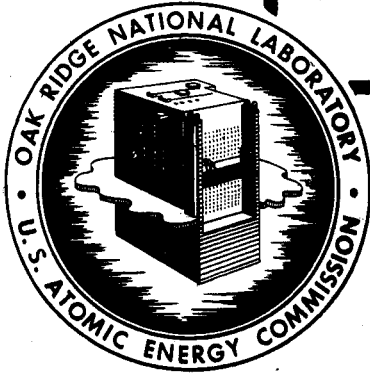


3 4456 0352772 5

ORNL 1053  
Progress Report



**CHEMISTRY DIVISION**  
**QUARTERLY PROGRESS REPORT**  
**FOR PERIOD ENDING MARCH 31, 1951**



**OAK RIDGE NATIONAL LABORATORY**  
OPERATED BY  
**CARBIDE AND CARBON CHEMICALS COMPANY**  
A DIVISION OF UNION CARBIDE AND CARBON CORPORATION



POST OFFICE BOX P  
OAK RIDGE, TENNESSEE



**SECRET**

ORNL-1053  
Progress Report

**DECLASSIFIED**

CLASSIFICATION CHANGED TO:

This document consists of 149 pages.

By: AEC List 8  
BY: D. Merson 7/11/57

Copy 8 of 132 copies. Series A.

Contract No. W-7405, eng. 26

**CHEMISTRY DIVISION**

S. G. Lind, Acting Director  
G. E. Boyd, M. A. Bredig, Associate Directors

**QUARTERLY PROGRESS REPORT**  
for Period Ending March 31, 1951

DATE ISSUED: OCT 5 1951

**OAK RIDGE NATIONAL LABORATORY**  
operated by  
**CARBIDE AND CARBON CHEMICALS COMPANY**  
A Division of Union Carbide and Carbon Corporation  
Post Office Box P  
Oak Ridge, Tennessee

**SECRET**

**SECRET**



3 4456 0352772 5

INTERNAL DISTRIBUTION:

- |                              |                       |                             |
|------------------------------|-----------------------|-----------------------------|
| 1. G. M. Felbeck (C&CCC)     | 25. J. A. Swartout    | 44. C. J. Borkowski         |
| 2-3. Chemistry Library       | 26. F. L. Steahly     | 45. G. H. Jenks             |
| 4. Physics Library           | 27. A. H. Snell       | 46. K. A. Kraus             |
| 5. Biology Library           | 28. A. Hollaender     | 47. H. A. Levy              |
| 6. Health Physics Library    | 29. M. T. Kelley      | 48. R. S. Livingston        |
| 7. Metallurgy Library        | 30. G. H. Clewett     | 49. T. E. Willmarth         |
| 8-9. Training School Library | 31. K. Z. Morgan      | 50. C. H. Secoy             |
| 10-13. Central Files         | 32. J. S. Felton      | 51. C. J. Hochanadel        |
| 14. C. E. Center             | 33. A. S. Householder | 52. O. K. Neville           |
| 15. C. E. Larson             | 34. C. S. Harrill     | 53. W. H. Baldwin           |
| 16. W. B. Humes (K-25)       | 35. C. E. Winters     | 54. A. R. Brosi             |
| 17. W. D. Lavers (Y-12)      | 36. D. W. Cardwell    | 55. R. N. Lyon              |
| 18. A. M. Weinberg           | 37. E. M. King        | 56. S. A. Reynolds          |
| 19. E. H. Taylor             | 38. J. A. Wethington  | 57. P. F. Thomason          |
| 20. E. J. Murphy             | 39. G. E. Boyd        | 58. E. H. Bohlmann          |
| 21. E. D. Shipley            | 40. A. Bredig         | 59. C. P. Keim              |
| 22. S. C. Lind               | 41. H. Stoughton      | 60. C. D. Susano            |
| 23. F. C. VonderLage         | 42. J. Lane           | 61. D. D. Cowen             |
| 24. R. C. Briant             | 43. G. W. Tucker      | 62. R. M. Reyling           |
|                              |                       | 63-65. Central Files (O.P.) |

EXTERNAL DISTRIBUTION

- 66-73. Argonne National Laboratory
- 74-81. Atomic Energy Commission, Washington
- 82-85. Brookhaven National Laboratory
- 86-89. Carbide & Carbon Chemicals Company (Y-12)
- 90-93. E. I. duPont de Nemours and Company
- 94-95. Knolls Atomic Power Laboratory
- 96-101. General Electric Company, Richland
- 102-105. Los Alamos
- 106. Mound Laboratory
- 107-109. New York Operations Office
- 110. Patent Branch, Washington
- 111. Savannah River Operations Office
- 112-126. Technical Information Service, Oak Ridge
- 127-130. University of California Radiation Laboratory
- 131-132. Westinghouse Electric Corporation

Chemistry Division quarterly progress reports previously issued in this series are as follows:

ORNL 65	March, April, May, 1948
ORNL 176	June, July, August, 1948
ORNL 229	September, October, November, 1948
ORNL 336	December, 1948, January and February, 1949
ORNL 286	Period Ending June 30, 1949
ORNL 499	Period Ending September 30, 1949
ORNL 607	Period Ending December 31, 1949
ORNL 685	Period Ending March 31, 1950
ORNL 795	Period Ending June 30, 1950
ORNL 870	Period Ending September 30, 1950
ORNL 1036	Period Ending December 31, 1950

## TABLE OF CONTENTS

ABSTRACT	11
1. CHEMISTRY OF SOURCE, FISSIONABLE, AND STRUCTURAL ELEMENTS	18
Solution Chemistry	18
Aqueous-benzene-TTA extraction method	18
Ultracentrifuge studies of inorganic systems	18
Electromigration on filter paper	19
Anion-exchange studies of metal complexes	19
Phase Studies	21
Vapor pressure—temperature relations of aqueous solutions of uranyl salts	21
The uranyl nitrate—water system above 180°C	22
The $UO_2SO_4 \cdot UO_3 \cdot H_2O$ system	25
Solubility of fission product sulfates	25
Corrosion Studies	26
Corrosion studies with synthetic HRE solutions	26
Electrochemical corrosion studies	27
2. NUCLEAR CHEMISTRY	31
Radionuclides of tin	31
Radionuclides of technetium	33
Radionuclides of niobium	43
Fission product decay schemes	43
Photoneutrons from energetic gamma rays emitted by fission product radionuclides	46
Use of hydrogen peroxide in a method for treating uranium metal dissolver off-gases	48
Hot-atom chemistry in the solid state	52
Chemistry of technetium: measurement of magnetic susceptibilities	53
3. RADIO-ORGANIC CHEMISTRY	56
Radiation, Analytical, and Preparative Chemistry	56
Radiation chemistry	56
Analytical chemistry	59
Preparative chemistry	61
Synthesis of High-Molecular-Weight Compounds Containing $C^{14}$	64
Aromatic polynuclear compounds	64
2-(Thenoyl- $\alpha$ - $C^{14}$ )-trifluoroacetone (TTA)	64
Isotope Effect Studies	65
Bromination of styrene- $\alpha$ - $C^{14}$ and styrene- $\beta$ - $C^{14}$	65
The dehydration of formic- $C^{14}$ acid	68
The absorption of $C^{14}O_2$ in alkaline media	73

Mechanism Studies of Organic Reactions	73
C <sup>14</sup> -tracer studies in the rearrangement of unsymmetrical α-diketones	73
Isotope exchange reactions involving the carbon-carbon bond	74
Synthesis and structure determination of C <sup>14</sup> -labeled 1- methylphenanthrene	75
Model runs with nonradioactive materials	76
Publications	77
4. CHEMISTRY OF SEPARATIONS PROCESSES	78
Volatility Studies	78
Removal of Pa <sup>233</sup> from neutron-irradiated ThF <sub>4</sub>	78
Solvent Extraction	83
Organic chemistry of solvents	83
Zirconium in aqueous HCl-HClO <sub>4</sub>	88
Ion Exchange	88
Ion-exchange kinetics	88
Ion-exchange separations	89
Electrochemical ion-exchange separations	90
5. CHEMICAL PHYSICS	93
Neutron Diffraction Studies	93
Neutron diffraction study of the crystal structure of ammonium bromide	93
Experiments in Chemical Kinetics with Molecular Beams	105
Radiofrequency Spectroscopy	106
Magnetic moment of I <sup>129</sup>	106
Spin of I <sup>131</sup>	106
Quadrupole moment ratio of Cl <sup>35</sup> and Cl <sup>37</sup>	106
Electronic nature of chlorine bonds in covalently bonded chlorine compounds	107
Calorimetry of Radioactivity	112
Test for storage of absorbed beta-ray energy in charcoal	112
Solids and High-Temperature Chemistry	114
X-ray-diffraction apparatus	114
Vacuum chamber for high (and subnormal) temperature X-ray diffraction	115
Remote-control X-ray-diffraction spectrometer for high-level radioactive specimens	115
Specific gravity of hafnium and zirconium	116
Effects of radiation on crystal structure	118
Carbonate and potassium apatites	119

6. RADIATION CHEMISTRY	131
Luminescence of alkali halides subjected to ionizing radiation	131
Effect of radiation on heterogeneous catalysts	131
Radiation decomposition of water and aqueous solutions	133
Radiation chemistry of aqueous organic solutions	133
Radiation stability of HRE components	134
7. INSTRUMENTATION	139
$4\pi$ proportional beta counter for absolute disintegration-rate measurements	139
Precision pulser circuit	148

## LIST OF FIGURES

		Page
Fig. 1.1	The Uranyl Nitrate--Water System	23
Fig. 2.1	Beta Proportional Counter Spectrometer Examination of 245-day Sn <sup>119m</sup> Source	32
Fig. 2.2	Coincidence Rate Determinations on 15-day Sn <sup>117m</sup>	34
Fig. 2.3	Positron Spectrum of 2.75-hr Tc <sup>93</sup>	35
Fig. 2.4	Conversion Electron Spectra from 2.75-hr Tc <sup>93</sup> Source	36
Fig. 2.5	Kurie Plot of Positron Spectrum of 2.75-hr Tc <sup>93</sup> , Assuming an Allowed Transition	37
Fig. 2.6	Gamma-Ray Spectrum of 2.75-hr Tc <sup>93</sup> Source	38
Fig. 2.7	Gamma-Ray Spectrum of 60.0-day Tc <sup>95</sup>	39
Fig. 2.8	Gamma-Ray Spectrum of Ruthenium Fraction from Mo <sup>92</sup> + $\alpha$	40
Fig. 2.9	Conversion Electron Spectrum on 4.20-day Tc <sup>96</sup> Source	41
Fig. 2.10	Gamma-Ray Spectrum of 4.20-day Tc <sup>96</sup>	42
Fig. 2.11	Aluminum Absorption Curve on Tc <sup>101</sup> from Natural Mo + $n_{th}$	44
Fig. 2.12	Gamma-Ray Spectrum of 13.5-min Tc <sup>101</sup>	45
Fig. 2.13	Apparatus for Stripping Uranium Dissolver Off Gases	50
Fig. 3.1	Constant-Level Device for the Dropping Mercury Electrode	60
Fig. 3.2	Isotope Effect in the Dehydration of HC <sup>14</sup> OOH	69
Fig. 3.3	Elution Curve for the Removal of Air from the Flow System Used in Measuring the Isotope Effect	72
Fig. 5.1	Neutron-Diffraction Pattern of ND <sub>4</sub> Br (-195°C)	97
Fig. 5.2	Neutron-Diffraction Pattern of ND <sub>4</sub> Br (23°C)	98
Fig. 5.3	Model of the Low-Temperature Ordered Structure of Deutero-Ammonium Bromide	103

	Page
Fig. 5.4 Views Showing Fissures in Hafnium Matrix	117
Fig. 5.5 X-Ray-Diffraction Patterns of Sodium Bitartrate Hydrate Before Irradiation	120
Fig. 5.6 X-Ray-Diffraction Patterns of Sodium Bitartrate Hydrate After Irradiation	121
Fig. 5.7 X-Ray-Diffraction Patterns of Carbonate Apatite and Hydroxyl Apatite	125
Fig. 7.1 $4\pi$ Proportional Counter	141
Fig. 7.2 $4\pi$ Proportional Counter	142
Fig. 7.3 $4\pi$ Proportional Counter — Details	146
Fig. 7.4 $4\pi$ Proportional Counter — Assembly	147
Fig. 7.5 Precision Pulser Circuit	149

## LIST OF TABLES

Table 1.1	Thermal Decomposition of Aqueous Uranyl Nitrate Solutions	24
Table 2.1	Reference Sources	47
Table 2.2	Uncharacterized Fission Product Sources	48
Table 3.1	H <sub>2</sub> O <sub>2</sub> Concentration vs. Current	61
Table 3.2	Specific Activities of Styrene Dibromides	67
Table 3.3	Values of the Rate Constant and the Isotope Effect at Different Temperatures	68
Table 3.4	Estimates of Slopes and Their Variances in the Calculation of Values of $k_{12}$ and of $100(k_{12} - k_{14})/k_{12}$	70
Table 4.1	Preliminary Run on Sample A	79
Table 4.2	Removal of Pa <sup>233</sup> from ThF <sub>4</sub> with Phosphorus Fluoride Regeneration Treatments	80
Table 4.3	Mean Holdup Times for Sample B	82
Table 4.4	Decontamination Tests with Trialkyl Phosphates	84
Table 4.5	Extraction of Uranium with Phosphorus Compounds	86
Table 5.1	ND <sub>4</sub> Br Data at -195°C	99
Table 5.2	Selected ND <sub>4</sub> Br Data at 23°C	101
Table 5.3	ND <sub>4</sub> Br Data at 23°C	104
Table 5.4	N-H or N-D Distances	105
Table 5.5	Measured Frequencies and Ratios for Solid Chlorine Compounds	107
Table 5.6	Pure Quadrupole Transitions for Solid Chlorine Compounds at 77°K	109

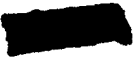


Table 5.7	Observed and Calculated Spacings from Powder X-Ray-Diffraction Spectrometer Data for Sodium Carbonate Apatite	126
Table 7.1	Effect of Methane Gas Pressure on Disintegration Rate	144
Table 7.2	Saturation Backscattering Using a $\text{Co}^{60}$ Source	144
Table 7.3	Comparison of $4\pi$ Disintegration Rates with Those Determined by Various Methods	145

## ABSTRACT

### CHEMISTRY OF SOURCE, FISSIONABLE, AND STRUCTURAL ELEMENTS

**Solution Chemistry.** A determination of the stability constant for the thorium-TTA complex which exists in aqueous solutions is in progress. TTA labeled with  $C^{14}$  will be used in some of the measurements required to solve this problem.

Further molecular weight determinations of the hydrolysis products of Zr(IV) and Hf(IV) present in chloride solutions have been performed. In a 1 M HCl + 1 M NaCl mixture the formation of monodispersed trimers of molecular weights 600 and 830, respectively, was demonstrated.

Electromigration studies of the complex chloride ions of Fe(III), Co(II), Cu(II), Zn(II), Cd(II), Hg(II), Pb(II), Th(IV), and U(VI) were made using filter paper as an immobile phase. Of these, only Th(IV) did not show any migration toward the anode, suggesting that it may not form a negatively charged complex chloride ion.

Measurements on the anion exchange equilibrium between Dowex-1 and hydrochloric acid solutions containing Fe(III) indicated that the hypothesis that the resin phase is a special concentrated electrolyte solution may be valid over fairly wide resin composition ranges.

Equilibrium exchange measurements on Ti(IV), Zr(IV), Hf(IV), and Th(IV) in chloride solutions using Dowex-1 showed that a ready separation of these elements from each other should be possible. Similar studies indicate that V(IV) is separable from both Ti(IV) and U(VI).

**Phase Studies.** Preliminary results from investigations on the  $UO_2(NO_3)_2$ - $H_2O$  and on the  $UO_2(NO_3)_2$ - $HNO_3$ - $H_2O$  systems above 100°C have become available. Measurements on the former system have now been extended over an appreciable concentration range and up to temperatures of thermal instability. Fundamental investigations on the  $UO_2SO_4$ - $UO_3$ - $H_2O$  system at 25 and 100°C have been continued.

A research project has been initiated to determine the vapor pressures of all volatile species above aqueous solutions of  $UO_2F_2$ ,  $UO_2SO_4$ , and  $UO_2(NO_3)_2$  over a wide range in concentration and in temperature.

The solubilities of a number of the fission product sulfates in  $\text{UO}_2\text{SO}_4$  solutions at  $250^\circ\text{C}$  were determined using radioactive tracers. The solubilities of  $\text{SrSO}_4$  and  $\text{Y}_2(\text{SO}_4)_3$  in a  $\text{UO}_2\text{SO}_4$  solution containing 30 g of uranium per liter were 0.45 and 50 mg per 100 g of solution, respectively.

**Corrosion Studies.** A systematic study has been undertaken of factors such as pH, stainless steel corrosion products, U(IV) concentrations, and kind of graphite, which affect the stability of aqueous  $\text{UO}_2\text{SO}_4$  solutions (HRE solution types). The effectiveness of several corrosion inhibitors will be determined. Although for cogent reasons these experiments will be conducted in quartz tubes, it is believed that the results to be found will still be of value in practical HRE situations.

An electrochemical investigation of the corrosion of type 347 stainless steel in  $\text{UO}_2\text{SO}_4$  solutions has also been initiated. A "matched" electrochemical cell using two test samples of passivated stainless steel as electrodes has been devised and found applicable to the detection of corrosion processes at  $250^\circ\text{C}$  in  $\text{UO}_2\text{SO}_4$  solutions. This technique should be of considerable use in the evaluation of corrosion inhibitors. The promising preliminary observation has been made that the addition of a few hundred parts per million of silica to the  $\text{UO}_2\text{SO}_4$  solution will greatly increase the corrosion resistance of passivated type 347 stainless steel to chloride ions.

#### NUCLEAR CHEMISTRY

Use of the technique of beta-gamma coincidence spectrometry was initiated by connecting a scintillation-counter spectrometer to a thin-magnetic-lens beta spectrometer through a fast coincidence circuit. Currently, measurements of the energy distributions of beta rays coincident with gamma rays of known energy can be made. An increased transmission in the thin-lens spectrometer, an improved energy resolution in the scintillation spectrometer, and a shorter resolution time-coincidence circuit were also achieved. Preliminary measurements on the  $\text{I}^{131}$  decay with the coincidence spectrometer have indicated the existence of two low-energy beta groups of 250 and 330 Kev maximum energy which are in coincidence with 720- and 640-Kev gamma rays, respectively.

Further studies on the two-step decay postulated for the isomeric 245-day  $\text{Sn}^{119m}$  and 15-day  $\text{Sn}^{117m}$  confirmed the existence of this process in the latter but not in the former radionuclide.

Measurements of beta and conversion electron distribution, of gamma-ray spectra, and of beta-gamma coincidence rates were conducted on several of the technetium radionuclides, including the 2.75-hr  $Tc^{93}$ , 60.0-day  $Tc^{95m}$ , 20-hr  $Tc^{95}$ , 4.20-day  $Tc^{96}$ , and the 13.5-min  $Tc^{101}$ , as a part of a general program to determine the character of the nuclear energy surface in the technetium region. As a part of this study measurements were also made on 15-hr  $Nb^{90}$  and 10-day  $Nb^{92}$ .

The presence of gamma rays of energies exceeding the photoneutron thresholds in both beryllium and deuterium in the decay of the 2.4-hr  $I^{132}$  was confirmed. Evidence for the possible occurrence of high-energy quanta in very low abundance in the decay of the 30-hr  $Te^{131m}$  + 25-min  $Te^{131}$  isomers was also found.

Experimental investigations of methods for the recovery of 9.4-year  $Kr^{85}$  formed in fission have led to a new procedure for the treatment of uranium metal dissolver off-gases involving the use of hydrogen peroxide.

Investigations of the fate of the radioactive recoil  $Br^{82}$  atoms produced in crystalline  $KBrO_3$  by neutron capture have indicated that a variety of back-reactions, thermal and radiation-induced, may cause these products to return to the parent compound. A novel interpretation for the observation that even at zero time some radiobromine remains combined as bromate is proposed, based upon assumptions about the capture gamma-ray spectrum and upon a stochastic calculation of the probability that the resultant momentum imparted to the  $Br^{82}$  will not exceed the bond energies of the bromate radical.

The availability of gram amounts of technetium now recovered from Chalk River wastes has given impetus to studies on the chemistry of this element. Magnetic susceptibility measurements are planned, and apparatus for these has been constructed.

#### **RADIO-ORGANIC CHEMISTRY**

**Radiation, Analytical, and Preparative Chemistry.** Three separate irradiation experiments have been performed using  $C_6H_5C^{14}OOH$  in aqueous solution as a target material and  $Co^{60}$  (300 curies) as the radiation source. Certain reaction products have been identified. The utility of  $C^{14}$  as an analytical tool in radiation chemistry studies has been demonstrated.

A polarographic method has been developed for the determination of hydrogen peroxide concentrations in an extremely dilute sulfuric acid solution containing a constant concentration of uranyl sulfate.

The following millicurie amounts of low- and intermediate-molecular-weight labeled compounds have been prepared: methanol- $C^{14}$ , 690.4 mc; potassium cyanide- $C^{14}$ , 70 mc; acetic-2- $C^{14}$  acid, 20 mc; benzoic-7- $C^{14}$  acid, 65 mc. In addition, syntheses have been studied or worked out for the following labeled compounds: glycine-2- $C^{14}$ ; malonic-2- $C^{14}$  acid; glycerol-1- $C^{14}$ ; and glycerol-2- $C^{14}$ .

**Synthesis of High-Molecular-Weight Compounds Containing  $C^{14}$ .** The following millicurie amounts of aromatic polynuclear hydrocarbons have been prepared: phenanthrene-9- $C^{14}$ , 10.6 mc; 1-methylphenanthrene-9(10)- $C^{14}$ , 10 mc; benz(a)anthracene-5-6- $C_1^{14}$ , 6 mc.

The compound 2-(thenoyl- $\alpha$ - $C^{14}$ )-trifluoroacetone (TTA), 17.3 mc, has been prepared from acetic-1- $C^{14}$  acid in overall yield of 65%.

**Isotope Effect Studies.** The bromination of styrene- $\alpha$ - $C^{14}$  and of styrene- $\beta$ - $C^{14}$  has been shown to proceed with no isotope effect.

Certain supplementary experiments in the dehydration of formic- $C^{14}$  acid have ruled out the possibility of an erroneous isotope effect. In addition, mean values of the isotope effects and their 95% confidence intervals at four temperatures were obtained for the dehydration of formic- $C^{14}$  acid.

It has been shown that under certain experimental conditions no isotope effect can be demonstrated in the absorption of  $C^{14}O_2$  by alkaline media.

**Mechanism Studies of Organic Reactions.** The rearrangement of *p*-methoxybenzylidene(aceto-1- $C^{14}$ )-phenone oxide has been shown to proceed without phenyl group migration.

Several substituted acetophenones have been shown to exhibit no exchange with  $C^{14}$ -labeled acyl halides in the presence of Lewis acids. 1-Methylphenanthrene labeled with  $C^{14}$  has been prepared prior to determination of the position of its labeling.

#### CHEMISTRY OF SEPARATIONS PROCESSES

The removal of  $Pa^{233}$  from neutron-irradiated  $ThF_4$  ( $\sigma = 0.077 \text{ m}^2/\text{g}$ ) by gaseous extraction has been investigated. The gases  $F_2$ ,  $PF_3$ , and  $PF_5$  and

mixtures of these gases were used as extractants at temperatures from 375 to 650°C for 1 to 4 hr. The fractions of activity removed varied from 0.0002 to 0.058; holdup times varied from  $1.8 \times 10^4$  to  $2.4 \times 10^5$  days. Nickel containers were more resistant than platinum.

Among the organic orthophosphates tested for extracting uranium from solution, tri-*n*-butyl phosphate was found to compare quite favorably with the others when considering the factors uranium distribution ratio, separation of uranium from fission products, and solvent stability. Tri-*sec*-propyl phosphate, tri-*sec*-butyl phosphate, and dibutylphenyl phosphate were found, however, to extract somewhat more uranium than TBP from an aqueous phase under a standardized set of conditions. The use of TBP labeled with  $P^{32}$  has materially facilitated the analytical determination of this compound and its decomposition products. Commercially available TBP was shown to possess at least a 98% *n*-butyl radical content.

Fundamental studies on the kinetics of ion-exchange reactions have continued. An investigation of the effect of ion-exchange capacity on the self-diffusion rate of ions through an ion exchanger while the polymer structure was maintained constant showed this variable to be of an importance comparable to ionic charge and polymer cross-linking. Lowering of the exchange capacity at first served to increase the rate until a critical capacity was reached, after which a dramatic slowing down occurred.

A number of new ion-exchange column separations of the fission product radioisotopes and other radionuclides of importance to nuclear chemical research were accomplished using strong-base anion exchangers and various elutriants, including nitrate, perchlorate, thiocyanate, and hydrochloric acid. Group separations included fluorine, chlorine, bromine, and iodine; manganese, technetium, and rhenium; selenium and tellurium, arsenic and antimony; manganese, iron, cobalt, nickel, copper, and zinc. Separations of tin and indium and of cadmium and indium were devised to assist in other work on the radiochemistry of tin.

Investigations on the electrochemical properties of granular ion-exchange beds were continued. Measurements of the conductances of the lithium, sodium, and hydrogen forms of Dowex-50 indicated that either the cation mobilities in the resin are restricted or the dissociation of the resin salt or acid is incomplete.

## CHEMICAL PHYSICS

A neutron diffraction study of the crystal structure of  $\text{ND}_4\text{Br}$  at 195 and 23°C has been completed. Decisive confirmation was obtained for the conclusion, previously based on indirect evidence, that at low temperatures the structure is ordered, whereas at room temperatures there is an orientational disorder of the ammonium ions. The structures, which are based on the CsCl lattice, indicate that an attraction between hydrogen and bromine is effective in determining the atomic arrangement. The ordered phase is probably stabilized by weak repulsive forces between hydrogen atoms of neighboring ions. This stabilization is overcome at higher temperatures by the increased entropy of the disordered structure.

A precise value,  $1.26878 \pm 0.00015$ , for the chlorine isotope quadrupole moment ratio,  $Q(\text{Cl}^{35})/Q(\text{Cl}^{37})$ , was determined; it was found to be independent of the type of chlorine-containing compound in five instances.

New and interesting information on carbon-chlorine bond characters was derived from quadrupole spectrum measurements on a variety of compounds using microwave techniques. It was concluded from the observed value for the quadrupole coupling in  $\text{Cl}_2$  that the bonding in this molecule is predominantly P type with little or no S character. Interesting inductive effects on the carbon-chlorine bond caused by the substitution of atoms of varying electronegativity in other parts of the molecules examined were found.

A calorimetric measurement at liquid-helium temperatures of the amount of beta-ray energy stored in charcoal exposed to a  $\text{Au}^{198}$  source indicated the absence of any such process to within 1.3%. Accordingly, this possible source of error in the previously reported  $\text{C}^{14}$  decay energy measurement is believed to be absent.

A program for the study of the high-temperature chemistry of solids has been initiated, and several X-ray-diffraction spectrometers of special design are being assembled. Results of interest were obtained on the effects of fast neutrons on the crystal structure of organic acid salts.

## RADIATION CHEMISTRY

The alkali halides ( $\text{KCl}$ ,  $\text{NaCl}$ ,  $\text{LiF}$ ) have been irradiated at low temperatures by an intense (300°C)  $\text{Co}^{60}$  gamma-ray source. Infrared emission was

observed at characteristic temperatures and wavelengths during slow warming from low to room temperature.

Work was continued on the catalytic activity of ZnO observed after irradiation with gamma rays. The hydrogenation of ethylene at 0°C was again used to test the decrease in activity after irradiation with Co<sup>60</sup> gamma rays at 15,000 r/min. Positive results were obtained, which remain to be interpreted.

The kinetics of the decomposition of liquid water by intense gamma radiation has been investigated in pure water and in the presence of dissolved H<sub>2</sub>O<sub>2</sub>, O<sub>2</sub>, and H<sub>2</sub> and mixtures of the three. Acid FeSO<sub>4</sub> solution was used as an actinometer. The minimum yield is estimated to be 3.66 moles of H<sub>2</sub>O per 100 ev.

A study has been initiated on the protective action of organic solutes in biological systems. The formation of phenol upon irradiation of an aqueous benzene solution is now being studied.

Experiments have continued on the stability of uranyl sulfate solution at temperatures up to 250°C in a type 347 stainless steel container with or without radiation. From analytical results and examination of corrosion specimens the results of 22 experiments may be classified as "good," "indifferent," or "bad." Radiation appears to be beneficial. Failures due to reactor shutdown may be attributed to reduction and precipitation of uranium incident to cessation of oxidizing conditions. "Good" experiments correlate with low concentration of chloride ion. In nonradioactive experiments bomb performance was improved by eliminating silver solder and by ensuring perfect passivation of the stainless steel walls above as well as below the waterline.

#### INSTRUMENTATION

A previously described 4π proportional counter method devised for the determination of absolute disintegration rates of beta-emitting radionuclides has been tested and shown to give rates agreeing to within 2% with those found by beta-gamma coincidence-rate measurements.

A modified and improved circuit design was devised for a precision pulse generator to be used in the calibration of beta-proportional and scintillation-counter spectrometers, as well as for the checking of pulse amplifiers in general. This latest model has given quite satisfactory performance during the past six months.

## 1. CHEMISTRY OF SOURCE, FISSIONABLE, AND STRUCTURAL ELEMENTS

### SOLUTION CHEMISTRY

**Aqueous-Benzene-TTA Extraction Method** (W. C. Waggener and R. W. Stoughton). Study has continued on the determination of the stability constant for the aqueous-thorium-TTA complex. Of present concern are: (1) the rate of transfer of TTA from benzene phase to aqueous phase and (2) the stability of aqueous monothonyltrifluoroacetone thorium ion, both as a function of ionic strength.

The complex nature of the aqueous-benzene-TTA system makes the reliability of spectrophotometric measurements of TTA concentration questionable. It is planned to check these results by an independent method, using  $C^{14}$ -labeled TTA recently prepared by V. F. Raaen under the direction of C. J. Collins and O. K. Neville.

**Ultracentrifuge Studies of Inorganic Systems** (J. S. Johnson and K. A. Kraus). During the past quarter further molecular weight determinations on zirconium(IV) and hafnium(IV) hydrolysis products have been carried out. This work has now been discontinued and a final report will be issued soon. The results to date are summarized below.

Both zirconium and hafnium are trimeric and monodispersed in 1 M HCl—1 M NaCl with observed molecular weights of 600 and 830 for the two trimers, respectively. Assuming a composition  $M(OH)_{2.33}Cl_{1.67}$ , the corresponding theoretical molecular weights are 570 and 830.

At higher acidity (3 M) the molecular weights of the zirconium compounds are lower and the systems are no longer monodispersed in both chloride and perchlorate solutions. However, the molecular weights are still higher than those of monomeric zirconium.

At considerably lower acidity (0.1 M) further polymerization occurs. Thus the zirconium polymer in perchlorate solutions at  $\mu = 1$  has a molecular weight of about 1400 (possibly a hexamer or heptamer). The molecular weight of the hafnium polymer in chloride solutions is somewhat lower (910 to 1040), indicating a lower degree of polymerization.

Several experiments were also carried out with zirconium in 1 M  $HClO_4$ —1 M  $NaClO_4$  which indicate that a trimeric hydrolysis product is present at this acidity.

**Electromigration on Filter Paper** (G. W. Smith and K. A. Kraus). The complexing of a number of metal ions by chloride ions has been investigated by electromigration on filter paper. This work has been temporarily discontinued, and the results to date are being assembled for a final report.

The following elements have been studied: Fe(III), Co(II), Cu(II), Zn(II), Cd(II), Hg(II), Pb(II), Th(IV), and U(VI). The range of chloride concentration was approximately 0.01 to 8 M. Thorium(IV) shows no migration toward the anode, suggesting that it does not form a negatively charged complex. Mercury(II) shows no migration toward the cathode, which indicates that it is a neutral or negatively charged complex. All other elements showed migration toward both the cathode and anode. In the following tabulation they are given in order according to the chloride concentration at which they showed no migration, i.e., where the mobility changed from cathodic to anodic:

ELEMENT	[Cl <sup>-</sup> ]
Hg(II)	<0.005
Cd(II)	0.75
Pb(II)	0.9
Zn(II)	2
Cu(II)	5.2
U(VI)	5.6
Fe(III)	8
Co(II)	8

**Anion-Exchange Studies of Metal Complexes** (K. A. Kraus, G. E. Moore, and F. Nelson). *Activity Coefficient Ratios in the Resin Phase*. The ion-exchange equilibrium for a negatively charged complex M<sup>-</sup> and chloride ions can be represented by the equation

$$K_{ar}^0 = \frac{(M^-)_r (Cl^-)}{(M^-)(Cl^-)_r} \frac{\gamma_M^r \gamma_{Cl^-}}{\gamma_M \gamma_{Cl^-}^r} = K_{ar}^m \frac{\gamma_M^r \gamma_{Cl^-}}{\gamma_M \gamma_{Cl^-}^r} \quad (1)$$

where parentheses indicate concentrations;  $\gamma$ , activity coefficients; and sub- and superscript  $r$ , the resin phase. When  $\gamma_{Cl^-}/\gamma_M$  is known, or can be considered constant, variations of  $K_{ar}^m$ , for example, as a result of loading, can be ascribed to changes in the activity coefficient ratio  $\gamma_M^r/\gamma_{Cl^-}^r$  of the species in the resin phase.

Neglecting changes in the hydration of the resin in going from R-Cl to R-M we could consider a series of distribution coefficient measurements as a function of loading to be carried out at constant total molality in the resin. Considering, in addition, the resin to behave like a concentrated electrolyte solution we would expect the following equations to be applicable:

$$\log \gamma_{C_1}^r = a_{C_1} + b_{C_1}L \quad (2a)$$

$$\log \gamma_M^r = a_M - b_M L \quad (2b)$$

where  $a_{C_1}$  and  $a_M$  are the values of  $\log \gamma$  for the pure forms of R-Cl and R-M,  $b_{C_1}$  and  $b_M$  are constants, and  $L = (M)_r/C$  is the loading (fraction of capacity  $C$  of resin occupied by  $M^-$ ). Combination of Eqs. (1) and (2) yields

$$\log K_{ar}^m \frac{\gamma_{C_1}}{\gamma_M} = \log K_{ar}^0 + (a_{C_1} - a_M) + (b_M + b_{C_1})L \quad (3a)$$

or

$$\log K_{ar}^m = \log K_{ar}^0 \frac{\gamma_M}{\gamma_{C_1}} + (a_{C_1} - a_M) + (b_M + b_{C_1})L \quad (3b)$$

when  $\gamma_M/\gamma_{C_1}$  is constant. Thus a plot of  $\log K_{ar}^m$  or  $K_{ar}^m \gamma_{C_1}/\gamma_M$  vs.  $L$  should yield a straight line with slope  $(b_M + b_{C_1})$ .

Using the exchange of  $FeCl_4^-$  vs.  $Cl^-$ , Eq. (3b) was tested for 4, 6, 8, and 12 M HCl assuming  $\gamma_M/\gamma_{C_1} = \text{constant}$  for each molarity of HCl. It was found that  $\log K_{ar}^m$  varies linearly with loading in the range  $L = 0.2$  to  $0.8$  in accordance with Eq. (3b). Furthermore,  $(b_M + b_{C_1})$  was practically independent of the molarity of HCl of the aqueous solution. For values of  $L$  less than  $0.2$  considerable deviations from the linearity principle (Eq. 3a) were found. Since these deviations could easily be due to nonhomogeneity of the resin, it appears that considering the resin as a special concentrated electrolyte solution has considerable merit.

*Ti(IV), Zr(IV), Hf(IV), and Th(IV) in Chloride Solutions.* The adsorbability of these elements by Dowex-1 in hydrochloric acid solutions was studied from 1 to 12 M. Their behaviors are sufficiently different to permit their ready separation. Thus Th(IV) was not appreciably adsorbed even in 12 M HCl. Titanium(IV) showed no appreciable adsorption below 9 M HCl, but

strong adsorption in 12 M HCl. The adsorption of Zr(IV) and Hf(IV) was negligible below 6 M HCl, but very strong in 9 and 12 M HCl.

*Separation of Titanium and Vanadium by Anion Exchange in Chloride Solutions.* As mentioned in the previous section, titanium(IV) can be adsorbed by Dowex-1 from hydrochloric acid solutions more concentrated than 9 M. In a similar series of measurements on vanadium, vanadium(IV) could not be adsorbed even from 12 M HCl. Thus the separation of these elements can readily be accomplished by adsorption from hydrochloric acid solutions more concentrated than 9 M.

Vanadium(V) is adsorbed at very high HCl concentrations on Dowex-1. Fortunately reduction of the adsorbed vanadium to vanadium(IV) occurs readily on the resin. The adsorption of the element in the higher oxidation state thus introduces little difficulty, and it is believed that reduction of all vanadium(V) to vanadium(IV) before adsorption is not necessary.

*Separation of Vanadium and Uranium.* Since vanadium(IV) is not adsorbed by Dowex-1, it can readily be separated by anion exchange from those elements which show some adsorption, e.g., most transition elements, zirconium, and the elements found in group V-A (niobium, etc.). Of particular interest in this connection is its separation from uranium. Since this element had earlier been found<sup>(1,2)</sup> to be strongly adsorbed from HCl solutions more concentrated than approximately 4 M, the separation of these two elements is very simple and effective.

## PHASE STUDIES

**Vapor Pressure—Temperature Relations of Aqueous Solutions of Uranyl Salts** (H. O. Day and C. H. Secoy). The problem as it stands at present is the determination of the vapor pressures of solutions of uranyl fluoride, sulfate, and nitrate over a wide range of concentrations and temperatures. The problem is being approached from two directions: (1) investigation of the relatively low-pressure region from room temperature to 175 or 200°C, and (2) investigation from 175 or 200°C to the critical point of H<sub>2</sub>O. The equilibrium pressures

- (1) K. A. Kraus and G. E. Moore, *Chemistry of Protactinium. V. Separation of Thorium, Protactinium and Uranium with Anion Exchange Columns in HCl Solutions*, ORNL-330 (April 27, 1949).
- (2) K. A. Kraus and G. E. Moore, "Anion Exchange Studies of Uranium(VI) in HCl-HF Mixtures. Separation of Pa(V) and U(VI)," *Chemistry Division Quarterly Progress Report for Period Ending June 30, 1950*, ORNL-795 (Oct. 3, 1950).

of any substances produced by solution decomposition will also be measured in these studies.

After an extensive literature survey it was decided to measure the pressures in the low-pressure region by an absolute method involving a compound manometer system. Suitable apparatus has been designed and is being constructed.

A preliminary study has been made of the second phase of these investigations. The literature has been reviewed, and a few experimental tests have been made in a search for a confining metal container if compressibility data should be desired in addition to vapor pressure data.

**The Uranyl Nitrate—Water System Above 180°C** (W. L. Marshall, J. S. Gill, and C. H. Secoy). Results from preliminary investigations of the uranyl nitrate—water and of the uranyl nitrate—nitric acid—water systems above 100°C are given elsewhere.<sup>(3)</sup> The study of the uranyl nitrate—water system has now been extended from dilute to concentrated solutions, and up to temperatures of thermal instability.

*Experimental.* Mallinckrodt, c.p., uranyl nitrate hexahydrate was used in the experiments. The procedure described earlier<sup>(4)</sup> was used. In summary, solutions of known concentrations of uranyl nitrate were degassed and sealed in 4-mm-I.D. silica tubing of 10 cm length. At room temperature the liquid-to-vapor volume ratio was approximately unity. The solutions were rocked in a cylindrical heating device. In this particular investigation the temperature was held constant for given lengths of time before proceeding to a higher temperature in order to fix within limits precipitation and vapor phase coloration phenomena. The temperature was measured with an iron-constantan thermocouple.

*Results and Discussion.* The experimental data are given in Table 1.1. In Fig. 1.1 data are shown graphically together with previous solubility data<sup>(5,6)</sup> in order to indicate the complete condensed system. Region A represents the aqueous solution in which solubility curves BC, CD, DE, and EF and the precipitation curve FGH are the boundary limits.

- (3) W. L. Marshall and J. S. Gill, "Aqueous Uranyl Nitrate and Uranyl Nitrate—Nitric Acid—Water Solutions Above 100°C," *Homogeneous Reactor Experiment Quarterly Progress Report for Period Ending February 28, 1951*, ORNL-990, p. 136 (May 18, 1951).
- (4) W. L. Marshall, J. S. Gill and C. H. Secoy, "The Uranyl Fluoride—Water System," *Chemistry Division Quarterly Progress Report for Period Ending June 30, 1949*, ORNL-795, p. 22 (Oct. 3, 1950).
- (5) O. Guempel, "Équilibres hétérogènes au sein des mélanges d'eau, d'éther et d'un sel métallique," *Bull. soc. chim. Belg.* 38, 443 (1929).
- (6) W. L. Marshall, J. S. Gill and C. H. Secoy, *The Uranyl Nitrate—Water System Above 60°C*, ORNL-797 (Aug. 15, 1950).

-1053  
3/51

UNCLASSIFIED  
DWG. 10868

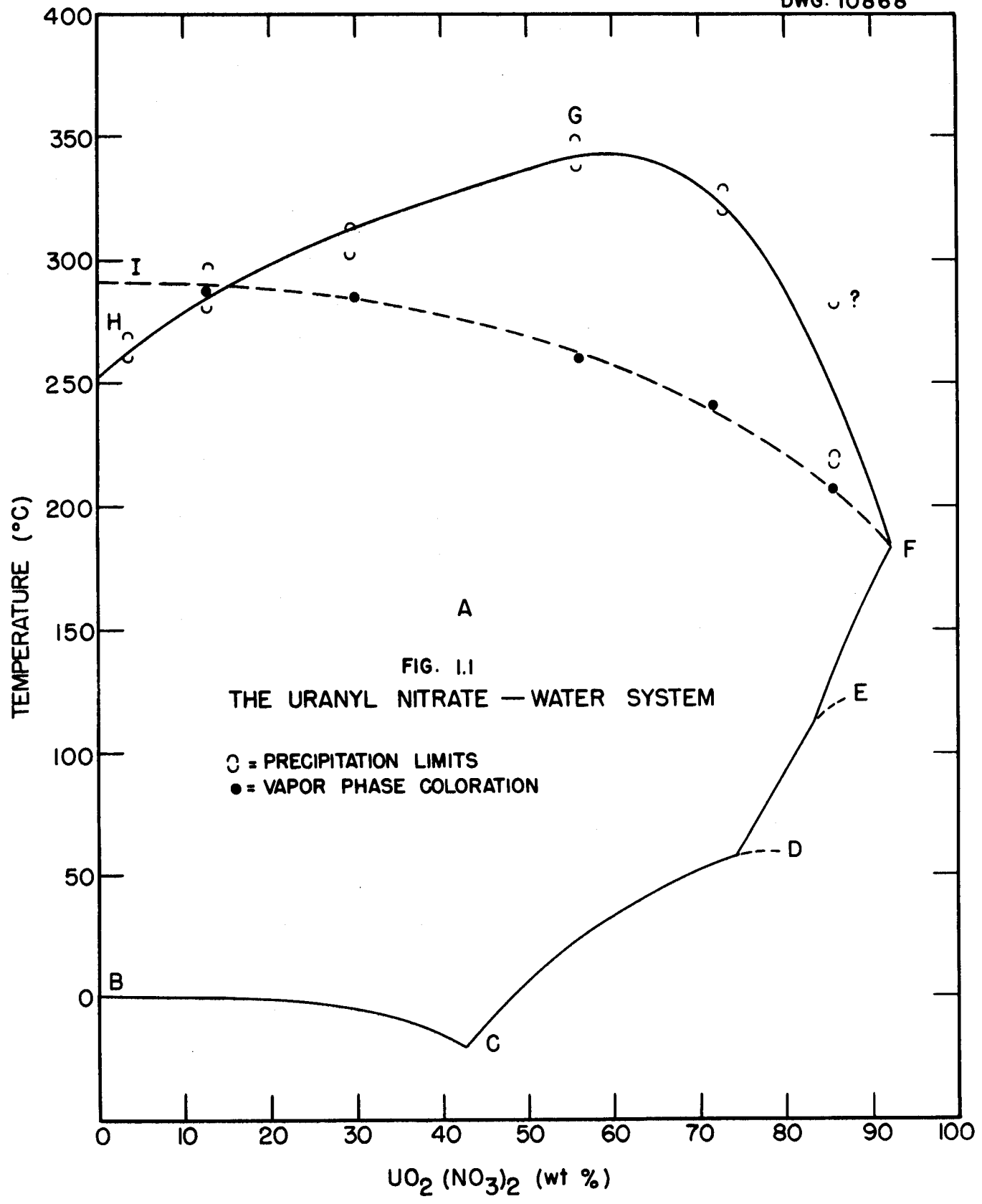


TABLE 1.1

## Thermal Decomposition of Aqueous Uranyl Nitrate Solutions

UO <sub>2</sub> (NO <sub>3</sub> ) <sub>2</sub> ·6H <sub>2</sub> O (wt. %)	RUN NO.	TEMPERATURE (°C)	MIXING TIME (hr)	OBSERVATIONS	
				SOLUTION	VAPOR
3.24	1	250	18	Clear	Colorless
		260	4	Clear	Colorless
		270	4	Yellow solid appeared	Colorless
12.52	2	280	18	Clear	Colorless
		288-295	2	Clear	Slight yellow-brown
		295	2	Yellow solid appeared	Yellow-brown
30.53	3	285	3	Clear	Slight yellow-brown
		300	4	Clear	Yellow-brown
		314	18	Yellow solid appeared	Red-brown
54.78	4	250	18	Clear	Colorless
		260	2	Clear	Slight yellow-brown
		270	18	Clear	Yellow-brown
	5	320	64	Clear	Red-brown
		338	4	Clear	Intense red-brown (tube explosion)
		350	2	Yellow solid precipitated	Intense red-brown
72.48	6	240	3	Clear	Slight yellow-brown
		275-300	42	Clear	Red-brown
		312	18	Clear	Intense red-brown
	7	328	6	Yellow solid appeared	Intense red-brown
		330	18	Yellow solid appeared	Intense red-brown
85.83	8	208	2	Clear	Slight yellow-brown
		215	5	Clear	Red-brown
		222	8	Yellow solid appeared	Red-brown
		280	4	No increase in precipitation (?)	
91.62 <sub>3</sub>	9	184		Melting point of UO <sub>2</sub> (NO <sub>3</sub> ) <sub>2</sub> ·2H <sub>2</sub> O	Red-brown above 184°C

The precipitations along curve FGH were rather slow to appear and were irreversible under the conditions of this investigation. Therefore it was not possible to fix the precipitation temperatures by slowly raising the tube temperature over a short period of time and still maintain equilibrium, although this procedure had been feasible in previous studies of quickly reversible solubility phenomena. The precipitation is explained in terms of a hydrolysis process.<sup>(3)</sup>

The observed reversible vapor phase coloration due to nitrogen oxides is indicated by curve FI of Fig. 1.1. The vapor phase containing nitrogen oxides was, in all probability, present below curve FI, but was not visible as such in the silica tubes.

The experimental data taken in these studies were found to be strongly dependent upon complete mixing of solution at all times and upon the liquid-to-vapor volume ratio. For example, in the preliminary work<sup>(3)</sup> capillary tubing was used in which mixing could not be achieved below about 305°C, and a slight amount of solid separated from the saturated solutions at about 290 to 300°C in the dry end of the capillary. In this investigation good mixing of the solution was realized at all times, and solid appeared only as indicated in Fig. 1.1.

**The  $\text{UO}_2\text{SO}_4\text{-UO}_3\text{-H}_2\text{O}$  System** (W. L. Marshall, J. S. Gill, and C. H. Secoy). A fundamental investigation of the  $\text{UO}_2\text{SO}_4\text{-UO}_3\text{-H}_2\text{O}$  system at 25 and 100°C is in progress. This work is reported in detail elsewhere.<sup>(7)</sup>

**Solubility of Fission Product Sulfates** (B. Zemel). The determination of the high-temperature solubilities of the more insoluble fission product sulfates, by means of radioactive tracers, has been continued using stainless steel bombs and filter disks; this has permitted the separation of solution and precipitate at an elevated temperature. To avoid corrosion, especially in determining solubilities in the presence of uranyl sulfate solutions, the bombs were provided with platinum liners, and the stainless steel filter disks were replaced by alundum disks.

Solubility studies were made on  $\text{SrSO}_4$ ,  $\text{Y}_2(\text{SO}_4)_3$ , and  $\text{BaSO}_4$  in  $\text{UO}_2\text{SO}_4$  solutions, and on  $\text{Ag}_2\text{SO}_4$  and  $\text{La}_2(\text{SO}_4)_3$  in water. The measurements on  $\text{SrSO}_4$  and  $\text{Y}_2(\text{SO}_4)_3$  in  $\text{UO}_2\text{SO}_4$  and of  $\text{Ag}_2\text{SO}_4$  in water were completed up to about 350°C; the others are not yet complete. The values for  $\text{Ag}_2\text{SO}_4$  were checked by potentiometric titration.

(7) W. L. Marshall and J. S. Gill, "The Uranyl Sulfate--Uranium Trioxide--Water System," *OPNL-990*, *op. cit.*, p. 134.

At 250°C the solubility of  $\text{SrSO}_4$  in  $\text{UO}_2\text{SO}_4$  (30 g of uranium per liter) was found to be 0.45 mg per 100 g of solution; for  $\text{Y}_2(\text{SO}_4)_3$  in  $\text{UO}_2\text{SO}_4$ , 0.05 g per 100 g of solution; and for  $\text{Ag}_2\text{SO}_4$ , 0.2 g per 100 g of solution. As a further check an attempt was made to determine at least part of the  $\text{Ag}_2\text{SO}_4$  solubility curve by the quartz-tube method, but this compound proved to be too photosensitive and the results were considered unreliable.

A detailed account of this work will be presented in the HRE quarterly report (ORNL-1057).

### CORROSION STUDIES

**Corrosion Studies with Synthetic HRE Solutions** (M. H. Lietzke). A series of experiments has been started in an effort to determine what factors influence the HRE solution stability in stainless steel vessels. The effects of pH, corrosion products of the stainless steel, uranium(IV) concentration, graphite, etc. on the stability of the uranyl sulfate solution are being investigated. Corrosion inhibitors such as nitric acid, tungstates, and molybdates are being added to uranyl sulfate solutions to determine their effects.

A comparison of the stability of uranyl phosphate solution in 1.5 M  $\text{H}_3\text{PO}_4$  and of the uranyl sulfate solution is also being undertaken.

These solutions, with and without pieces of passivated or unpassivated steel, will be sealed in quartz tubes which will be heated to 250°C and rocked during the heating process. Visual observations on the tubes will be made periodically. After a suitable length of time (usually 100 hr) the tubes are to be removed from the furnace, the solutions and any precipitates formed will be analyzed, and the effects upon the steel will be noted.

It is realized that because the experiments are being carried out in quartz tubes the results may not be strictly comparable to those obtained in the stainless steel test loops. Dissolved silica present in the former solution may act as a corrosion inhibitor, and hence a solution stabilizer. It is believed, however, that the beneficial or harmful effects of the variables listed above can still be observed even though quantitative limits may be different.

Experimental results will be reported in detail in the next HRE quarterly report.

**Electrochemical Corrosion Studies** (J. C. Griess and M. H. Lietzke). An electrochemical investigation of the corrosion of 347 stainless steel in uranyl sulfate solutions has been initiated. The study was limited to steel which had been rendered passive by pretreatment in nitric or chromic acid and to date has been confined to emf measurements on steel specimens passivated by J. English in a manner previously described.<sup>(8)</sup> Briefly, the steps in this pretreatment and passivation were (1) degreasing in an organic solvent, (2) etching in either a mixture of hydrofluoric and nitric acids, or a saturated solution of ferric chloride in concentrated hydrochloric acid, and (3) heating at 250°C for 24 hr in either 1% nitric or 2% chromic acid.

A number of specimens have been examined using the cell "passivated stainless steel |  $\text{UO}_2\text{SO}_4$  solution | S.C.E.," where the  $\text{UO}_2\text{SO}_4$  solution contained 30 g of uranium per liter. Since cells of this type are easily polarized it was necessary to use a vacuum-tube potentiometer for the measurements, which were made at either room temperature or 100°C. The results from these experiments can be summarized as follows: Potentiometrically there is essentially no difference between a steel specimen which has been passivated in nitric acid and one passivated in chromic acid. The potential of the cell "passive stainless steel |  $\text{UO}_2\text{SO}_4$  solution | S.C.E. is about 0.4 to 0.5 volt with the steel the positive electrode. Any one specimen gives a constant value but no two specimens give identical values. Changes in temperature cause only slight changes in potential. If untreated steel is substituted for the passivated steel, the potential of the cell is approximately equal to zero.

When a passivated steel surface is scratched below the liquid level, the potential of the cell changes instantly to approximately zero. However, there is a tendency toward self-healing, even in a uranyl sulfate solution, and the potential of the cell approaches its original value after a short period of time. The presence of a small amount of nitric acid increases the rate of self-healing; a very small amount of dichromate brings about extremely rapid self-healing. An increase in temperature from 25 to 100°C has no noticeable effect on the rate of self-healing.

In general a passivated steel surface behaves much like an oxygen electrode, i.e., it is sensitive to the pH of the solution as well as to oxygen pressure. A few of the surfaces were photosensitive but this was not generally true.

(8) Summary of section on corrosion, *Homogeneous Reactor Experiment Quarterly Progress Report for Period Ending August 31, 1950*, ORNL-826, p. 107 (Oct. 24, 1950).

-1053  
3/51

At room temperature the passivated steel retains its passivity (potential about +0.5 volt vs. S.C.E.) for at least five days in a uranyl sulfate solution containing as much as 0.1 M potassium chloride. At 100°C under the same conditions the passivity of the steel is destroyed (potential about 0 vs. S.C.E) within a few minutes.

All the above experiments were carried out at 100°C or less, at which temperature no difficulty was encountered in using a reference electrode. Since it was desirable to measure changes in potentials at 250°C and since there were no suitable reference electrodes available, a new system of detecting changes in potential was necessary. It was decided to utilize the cell "passive stainless steel |  $\text{UO}_2\text{SO}_4$  | passive stainless steel." If the two electrodes were identical, the potential of the cell would be zero; if one electrode lost its passivity there would be a change in potential. By determining the polarity of the cell it would be possible to determine which electrode had become active. If both electrodes should become active at the same time, there would be no detectable difference in cell potential and the cell would be useless. However, previous experiments indicated that it was highly unlikely that two separate pieces of steel would lose their passivity at exactly the same time.

Using the above system, the potential of a cell at 100°C was followed overnight by means of a vibrating-reed electrometer combined with a Brown recorder. The potential remained essentially at zero but fluctuated  $\pm 5$  mv. In the morning enough solid potassium chloride was added to make the chloride ion concentration 0.05 M. About 15 min after adding potassium chloride there was a sudden change in potential amounting to about 450 mv. The cell remained in this state for a 10-min period; then the potential again changed to approximately zero. By means of a saturated calomel electrode it was shown that each electrode had, lost its passivity. Hence our interpretation of the potential changes was as follows: At the end of the first 15-min period one electrode became active and the other retained its passivity, thereby changing the cell to "active stainless steel |  $\text{UO}_2\text{SO}_4$  | passive stainless steel"; 10 min later the breakdown of the passivity of the second electrode occurred, after which the two electrodes were again equivalent and hence the cell potential was zero. Several identical experiments have given similar results and have confirmed the belief that a cell of this type would be useful to detect changes in passivity.

When the electrodes were removed from the cell after a potential measurement had shown them to be no longer passive, it was possible to observe active corrosion at a few localized areas. If the electrodes were removed shortly after they had lost their passivity, it was necessary to use high magnification to observe the corrosion. If the electrodes were allowed to remain in the solution for several hours, the corroded areas were visible without magnification.

To test the described electrode system at 250°C an American Instrument Company bomb was used. In the head of the bomb was incorporated an electrical connector (American Instrument Catalog No. 406-101) to allow the introduction of an electrically insulated lead. For the first run a glass liner was used to protect the interior of the bomb. Each electrode consisted of 1.5-mm-diameter passivated stainless steel (347) rod. One electrode was introduced through the head of the bomb; the second was inside the glass liner, with the top of the wire pressed firmly against the inside wall of the bomb. The walls of the bomb thus served as one terminal of the cell and the electrically insulated lead served as the other. Inside the glass liner was placed 60 ml of  $\text{UO}_2\text{SO}_4$  solution (30 g of uranium per liter). After the electrodes were adjusted, the bomb was sealed and heated to 250°C for 12 hr and the potential was recorded. The potential remained essentially at zero, with a few minor fluctuations, during the entire run. At the end of this time the bomb was cooled and opened, and enough solid potassium chloride was added to make the chloride ion concentration 300 ppm. The bomb was again sealed and heated to 250°C and the potential was recorded. After 90 min there was a sudden change in potential, indicating that one electrode was undergoing corrosion. About 15 min later there was another change in potential of approximately equal magnitude but in the opposite direction, and the cell potential was again nearly zero. Following this there was a period of about 1 hr during which the potential fluctuated erratically ( $\pm 100$  mv), and at the end of this time the potential remained zero until the bomb was cooled and opened 12 hr later. Visual observation showed that each electrode had undergone corrosion at localized areas.

The results of this experiment indicated that the cell "passivated stainless steel |  $\text{UO}_2\text{SO}_4$  | passivated stainless steel" could be used at 250°C. No other experiments at 250°C have been carried out, but future experiments have been planned.

ORNL-1053  
3/51

Work has just begun on a determination of the effect of various inhibitors on the corrosion resistance of passivated steel. To date the effect of soluble silica in the electrolyte has been partially investigated. Preliminary data indicate that the presence of a few hundred parts per million of silica greatly increases the corrosion resistance of passivated 347 stainless steel to chloride ions.

## 2. NUCLEAR CHEMISTRY

**Radionuclides of Tin** (G. E. Boyd). Further investigations using a scintillation-counter spectrometer and absorption measurements have established the existence in low abundance of a  $1.90 \pm 0.05$  Mev gamma ray in the decay of the 9.4-day  $\text{Sn}^{125}$  previously suggested by the work of Hayward<sup>(1)</sup> and by our own work.<sup>(2)</sup>

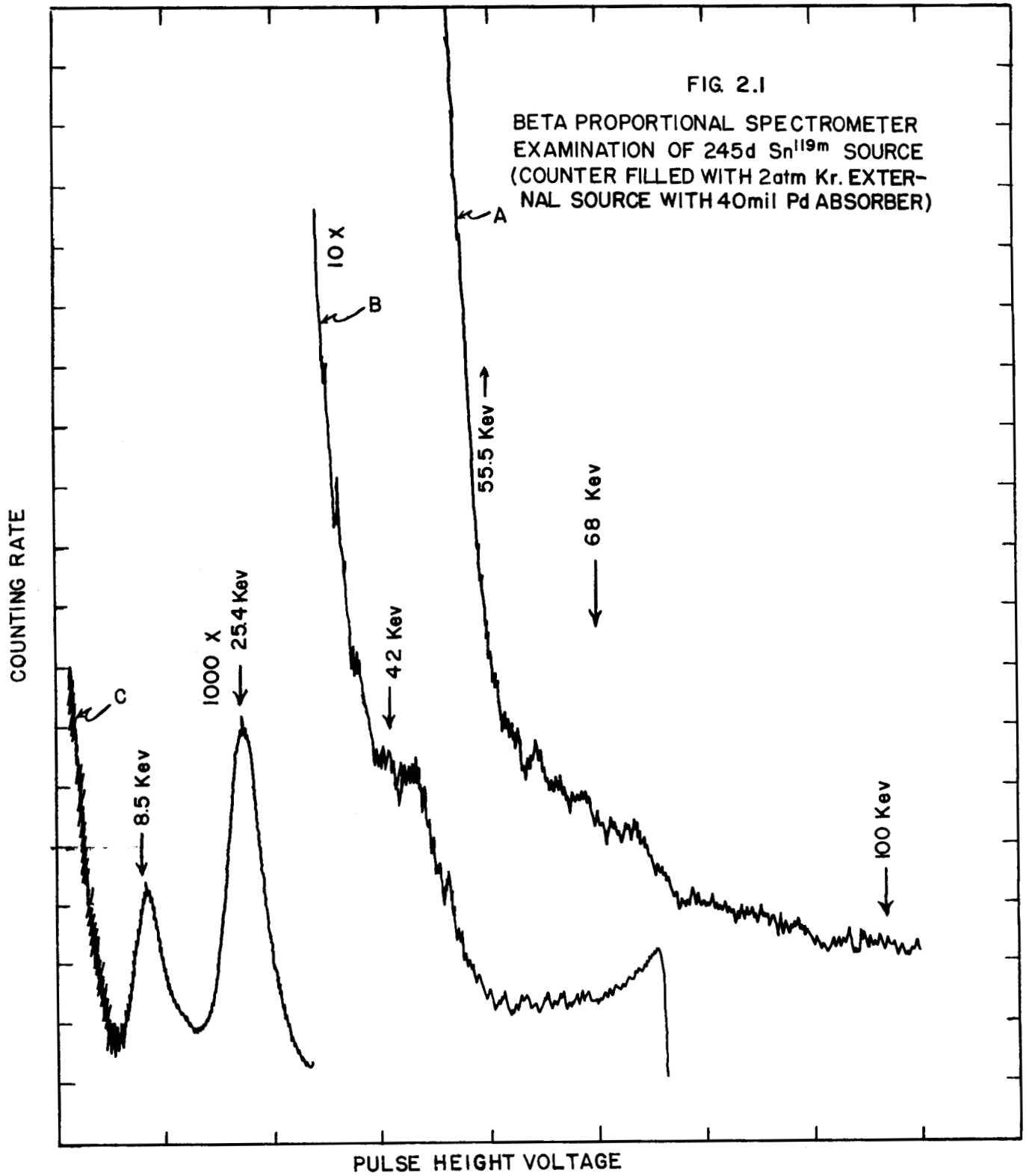
Since our first report on the 245-day  $\text{Sn}^{119m}$ , Hill and Mihelich<sup>(3)</sup> have published their results on this same radionuclide. They proposed that this isomeric activity may decay by a two-step process, presumably by analogy with the isomeric tellurium periods; however, no experimental data were given to support this contention. Accordingly, in collaboration with C. J. Borkowski a further search was made for a low energy relatively unconverted gamma ray in the decay of an intense 245-day  $\text{Sn}^{119m}$  source using a beta-proportional-counter spectrometer filled with 2 atm of krypton. The source was placed outside a beryllium window in the wall of the counter, and 4 mils of palladium was used to critically absorb and thereby reduce the strong Sn K X-rays emitted. Results from such an investigation are shown in Fig. 2.1. Possibly there is a very-low-intensity gamma ray at 42 Kev. Coincidence-rate measurements were made on this same source using the mica end-window beta-proportional-counter arrangement described below in the studies on the 15-day  $\text{Sn}^{117m}$ . No net  $e^-$ -gamma or X-gamma coincidences were observed. Accordingly it was concluded that if the 245-day  $\text{Sn}^{119m}$  decays by a cascade process, this process must occur in such a way that the radiations emitted in the second step were not detected in our experiments.

Hill and Mihelich also proposed a two-step decay for the 15-day  $\text{Sn}^{117m}$ , and, although again no supporting data were presented, preliminary coincidence-rate measurements were cited as supporting this hypothesis. In view of our inability to detect coincidences in the decay of the 245-day  $\text{Sn}^{119m}$ , it was considered desirable to see if coincidences could be observed with a 15-day  $\text{Sn}^{117m}$  source. Accordingly, coincidence-rate measurements were conducted

(1) R. W. Hayward, "The Beta-Spectrum of  $\text{Sn}^{125}$ ," *Phys. Rev.* 79, 409 (1950).

(2) C. M. Nelson, B. H. Ketelle, and G. E. Boyd, *Studies on the Nuclear Chemistry of Tin*, ORNL-828 (Nov. 10, 1950).

(3) J. W. Mihelich and R. D. Hill, "Radioactive Isomers of  $\text{Sn}^{117}$  and  $\text{Sn}^{119}$ ," *Phys. Rev.* 79, 781 (1950).



using two mica-end-window beta proportional counters, one of which had a gold cathode to give improved gamma-ray detection. The results given in Fig. 2.2 confirm the two-step process in  $\text{Sn}^{117m}$  and show that the conversion electrons are in coincidence with a 0.15-Mev gamma ray. Coincidence absorption measurements using aluminum to remove the conversion electrons in coincidence with the gamma ray showed that their energy was also about 150 Kev, as was expected. We are indebted to A. R. Brosi for the use of his coincidence tubes in these measurements.

**Radionuclides of Technetium** (G. E. Boyd and B. H. Ketelle). New observations on the radiations emitted by  $\text{Tc}^{93}$ ,  $\text{Tc}^{95}$ ,  $\text{Tc}^{96}$ , and  $\text{Tc}^{101}$  have been made using a magnetic-lens beta spectrometer and a scintillation-counter spectrometer. In a number of cases coincidence-rate determinations were also made. Measurements on the positron and conversion-electron spectra of a 2.75-hr  $\text{Tc}^{93}$  source prepared by the irradiation of enriched  $\text{Mo}^{92}$  (92.07% mass 92) with 14-Mev deuterons are shown in Figs. 2.3 and 2.4. It may be seen in Fig. 2.5 that the Kurie plot, assuming an allowed transition for the positron spectrum, is a straight line and that the maximum energy is  $0.800 \pm 0.005$  Mev. The gamma-ray spectrum for the 2.75-hr  $\text{Tc}^{93}$  is shown in Fig. 2.6. Measurements of the K capture--positron branching ratio indicated that 93% of the disintegrations occur by the former and 7% by the latter route. Coincidence absorption measurements indicated that the positron spectrum was simple and that the positrons are followed by a 1.34-Mev gamma transition.

Measurements of the gamma-ray spectrum of the 60.0-day  $\text{Tc}^{95m}$  are given in Fig. 2.7. These data are in excellent agreement with the recent observation of Medicus, Preiswerk, and Scherrer.<sup>(4)</sup> However, the spectrum for the 20-hr  $\text{Tc}^{95}$ , shown in Fig. 2.8, does not agree entirely with the findings of Medicus *et al.* Our results differ in that only 0.76- and 1.07-Mev gamma rays were seen; a 0.93-Mev transition, reported to be of equal intensity to the 1.07-Mev transition, was not found.

The conversion-electron and gamma-ray spectra for the 4.20-day  $\text{Tc}^{96}$  activity are given in Figs. 2.9 and 2.10. These results are in good agreement with those of Medicus *et al.* except that additional crossover transitions of 1.65, 1.89, and possibly 2.39 Mev energy were found. A determination of the

(4) H. Medicus, P. Preiswerk, and P. Scherrer, "Untersuchungen über den radioaktiven Zerfall bei Isotopen des Technetiums," *Helv. Phys. Acta* 23, 299 (1950).

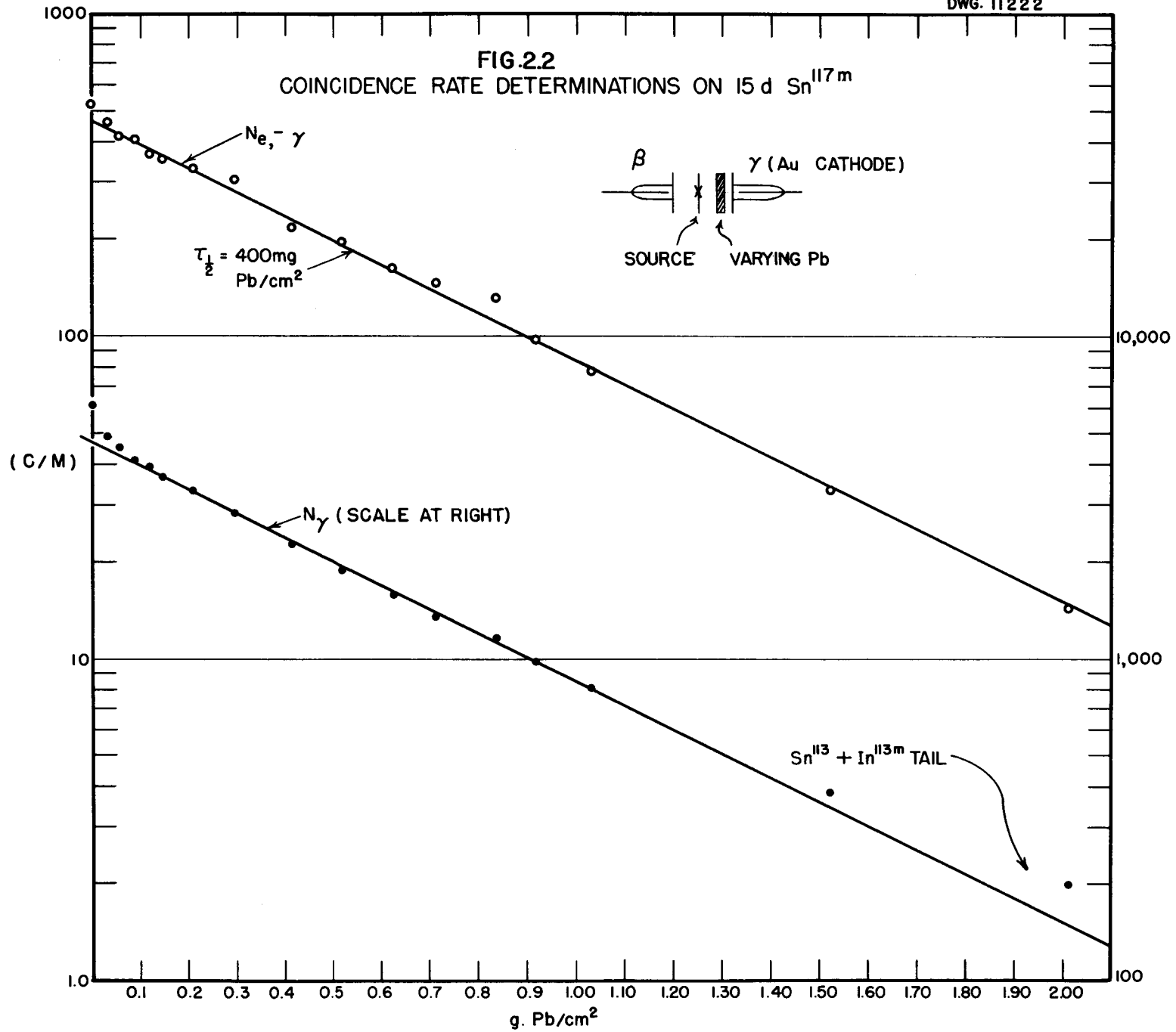
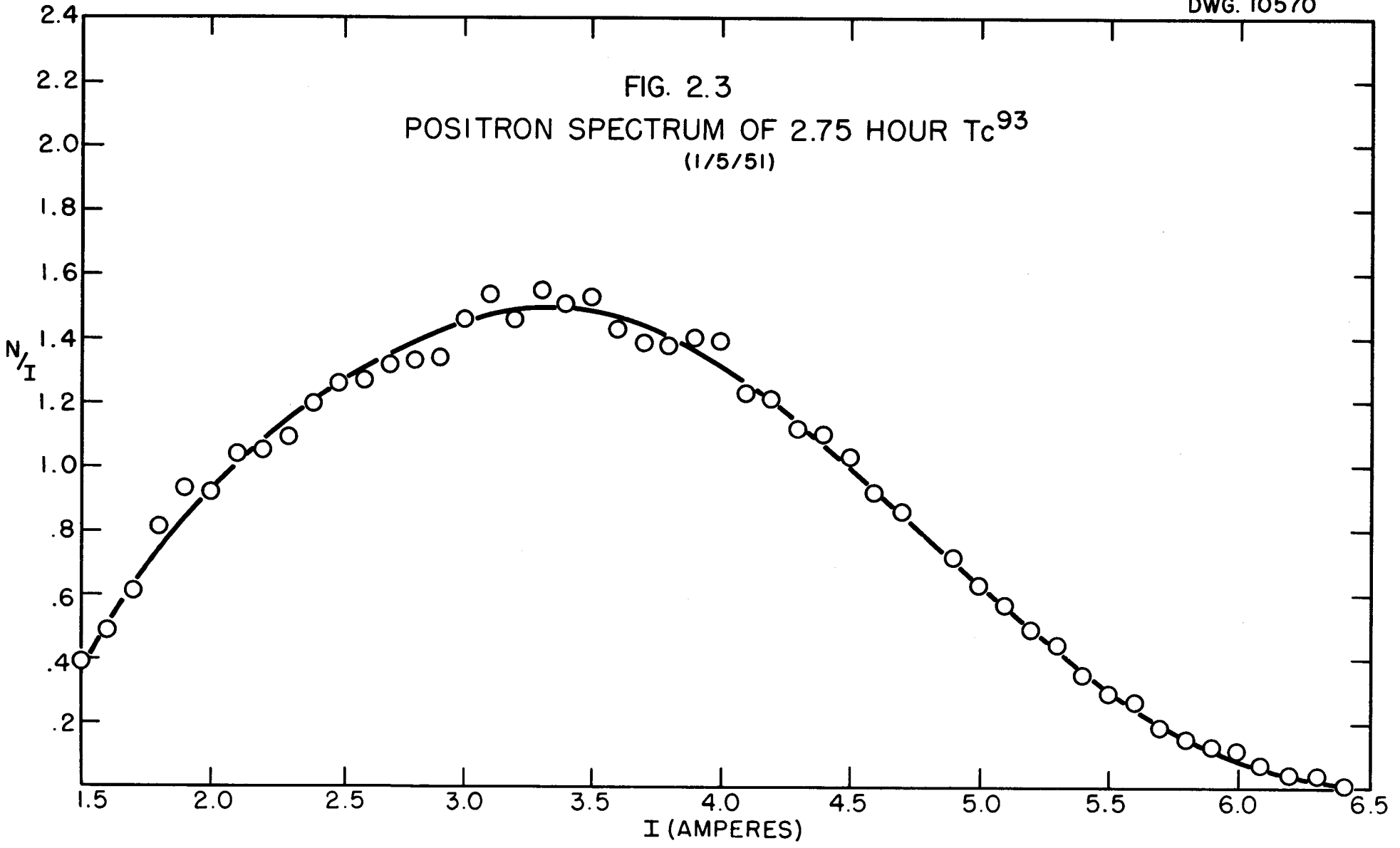


FIG. 2.3  
POSITRON SPECTRUM OF 2.75 HOUR  $Tc^{93}$   
(1/5/51)



35

FIG. 2.4  
CONVERSION ELECTRON SPECTRA FROM  
2.75 HOUR  $Tc^{93}$  SOURCE

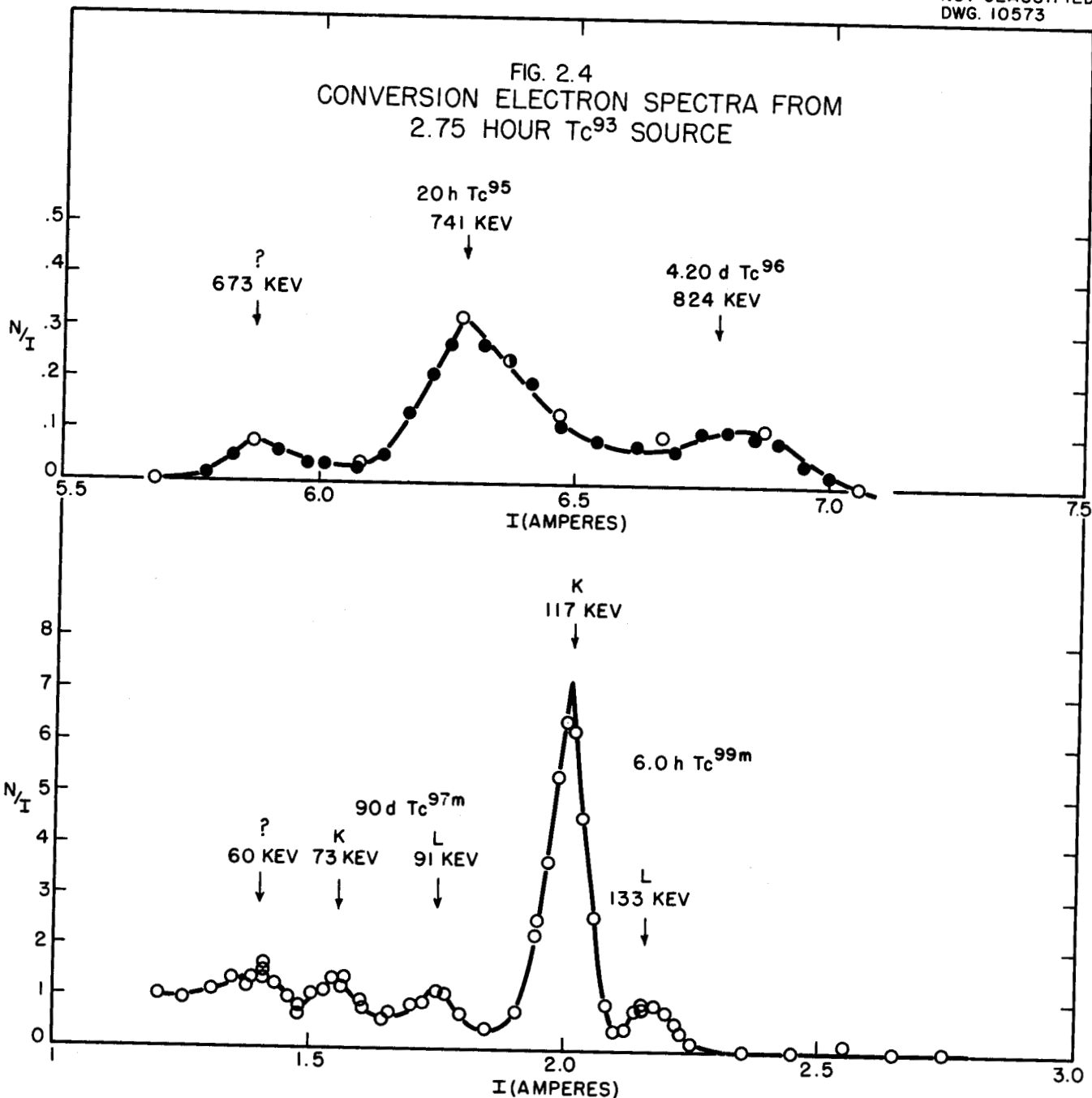
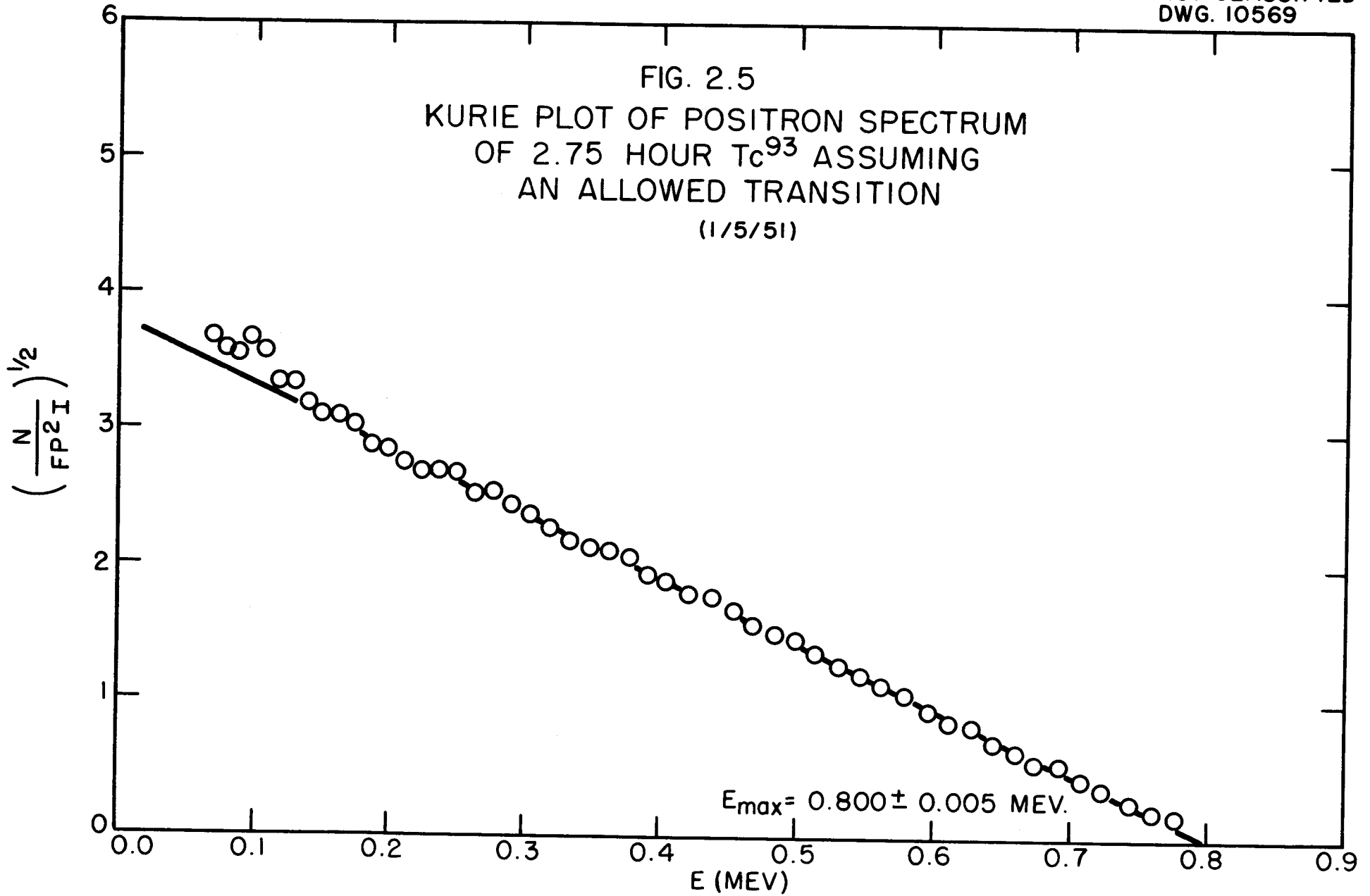
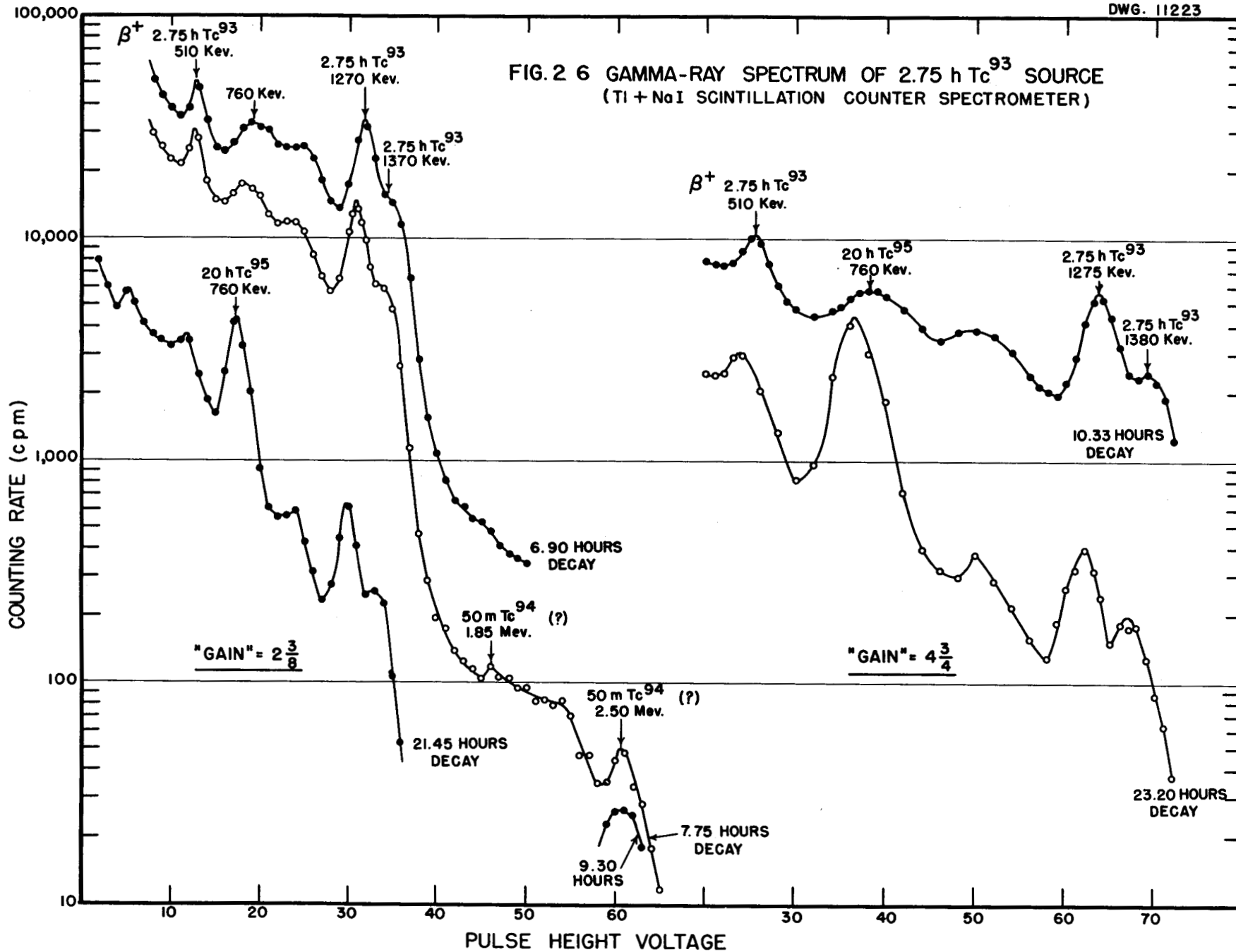
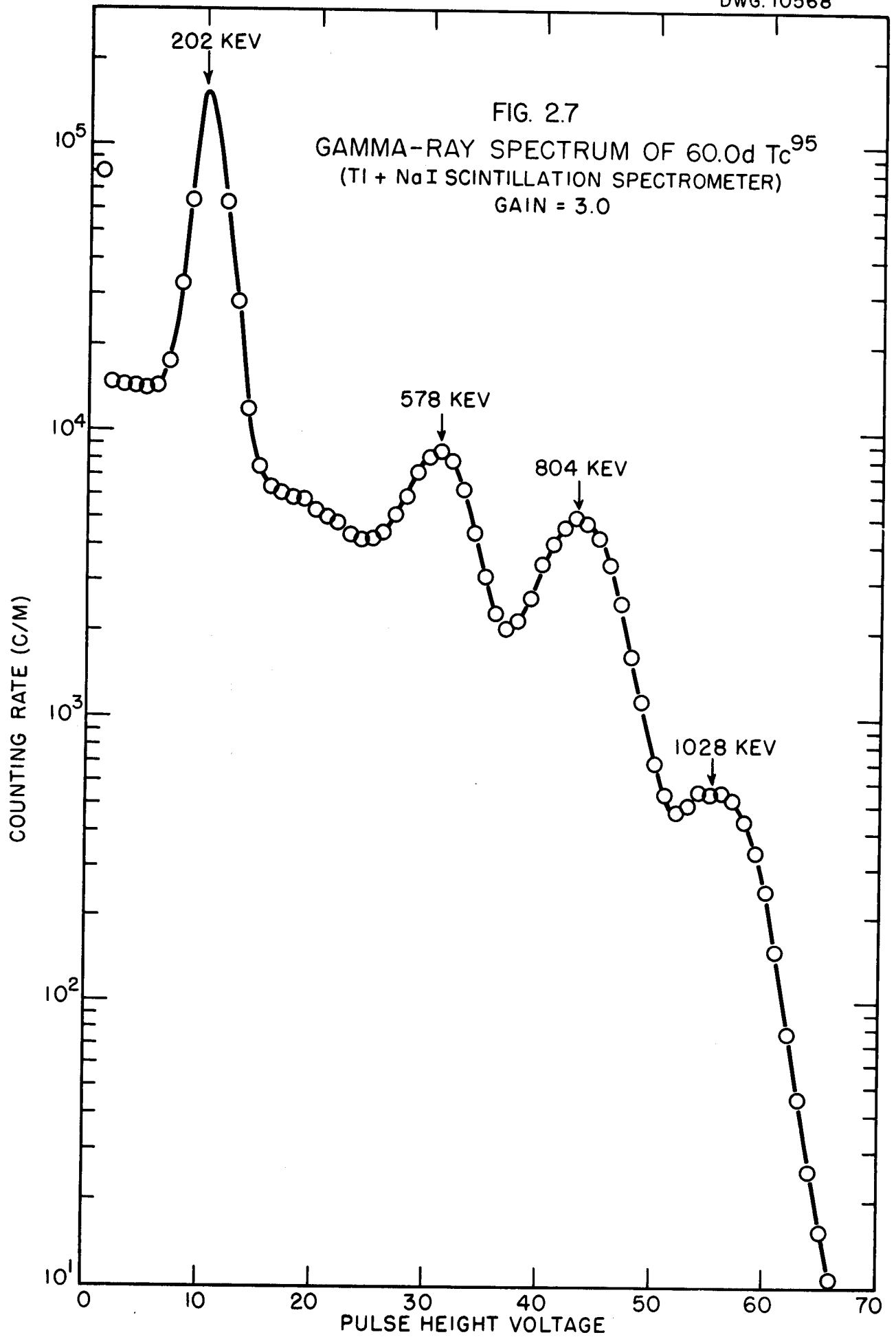
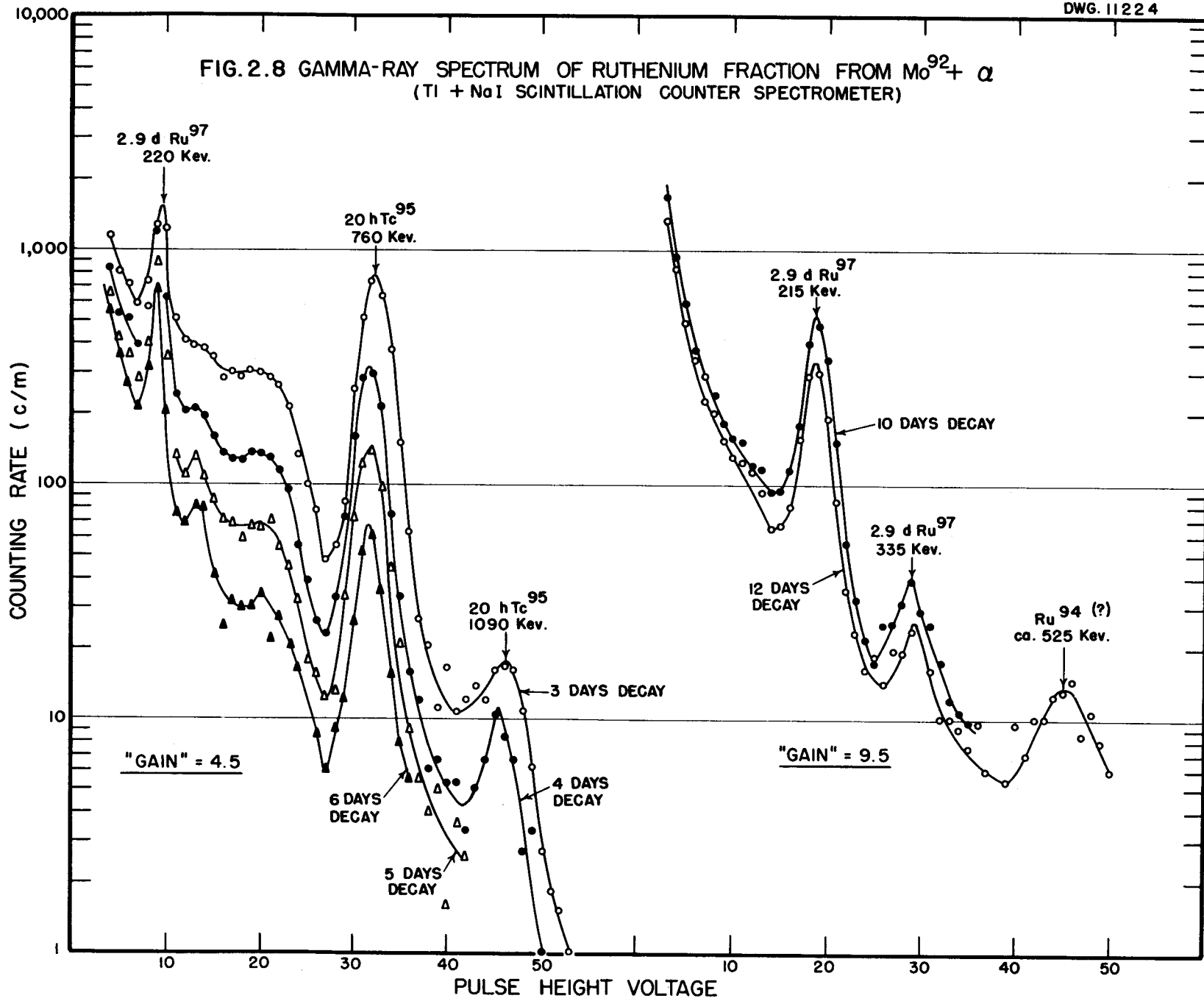


FIG. 2.5  
KURIE PLOT OF POSITRON SPECTRUM  
OF 2.75 HOUR  $Tc^{93}$  ASSUMING  
AN ALLOWED TRANSITION  
(1/5/51)









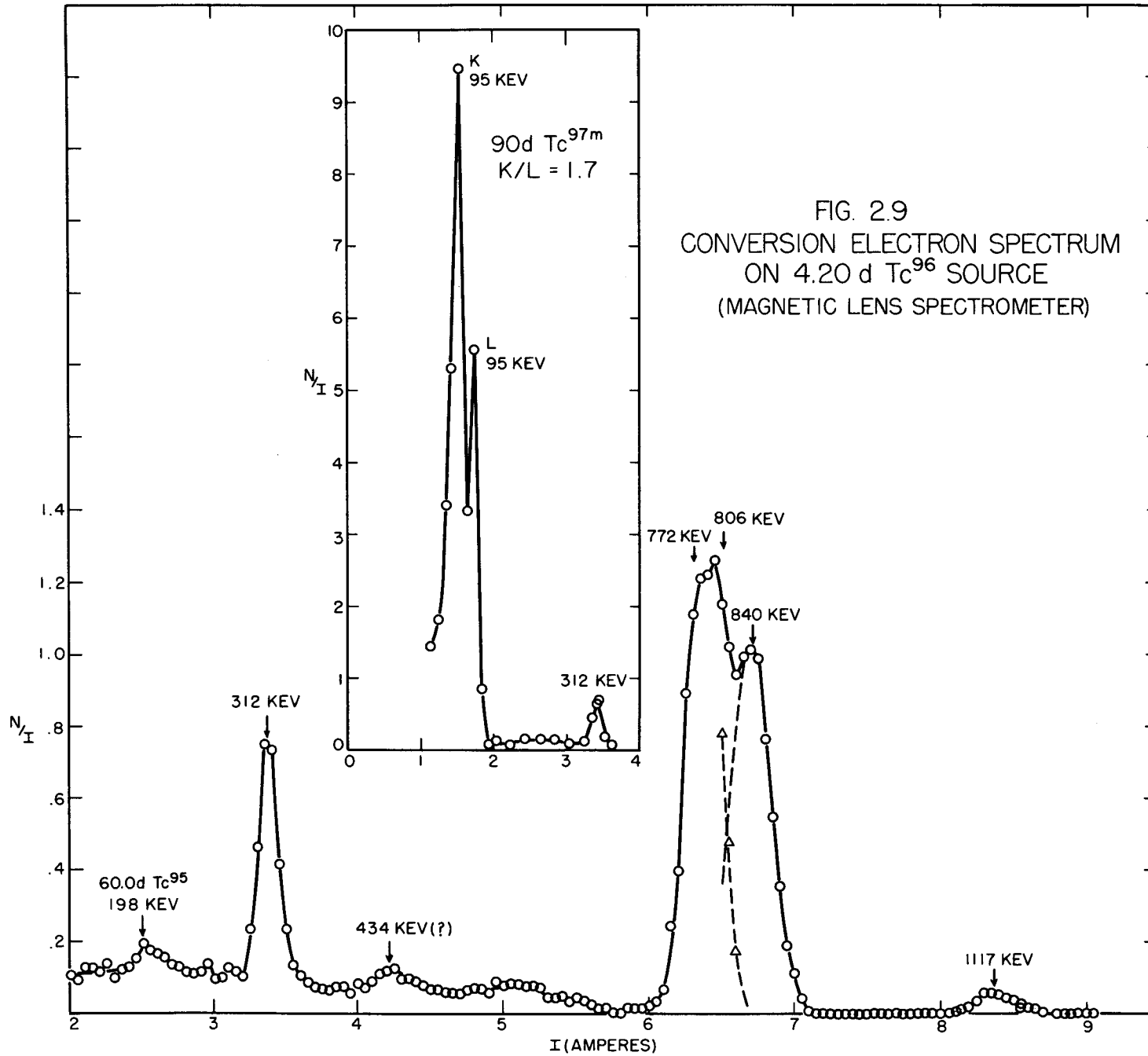


FIG. 2.9  
CONVERSION ELECTRON SPECTRUM  
ON 4.20 d Tc<sup>96</sup> SOURCE  
(MAGNETIC LENS SPECTROMETER)

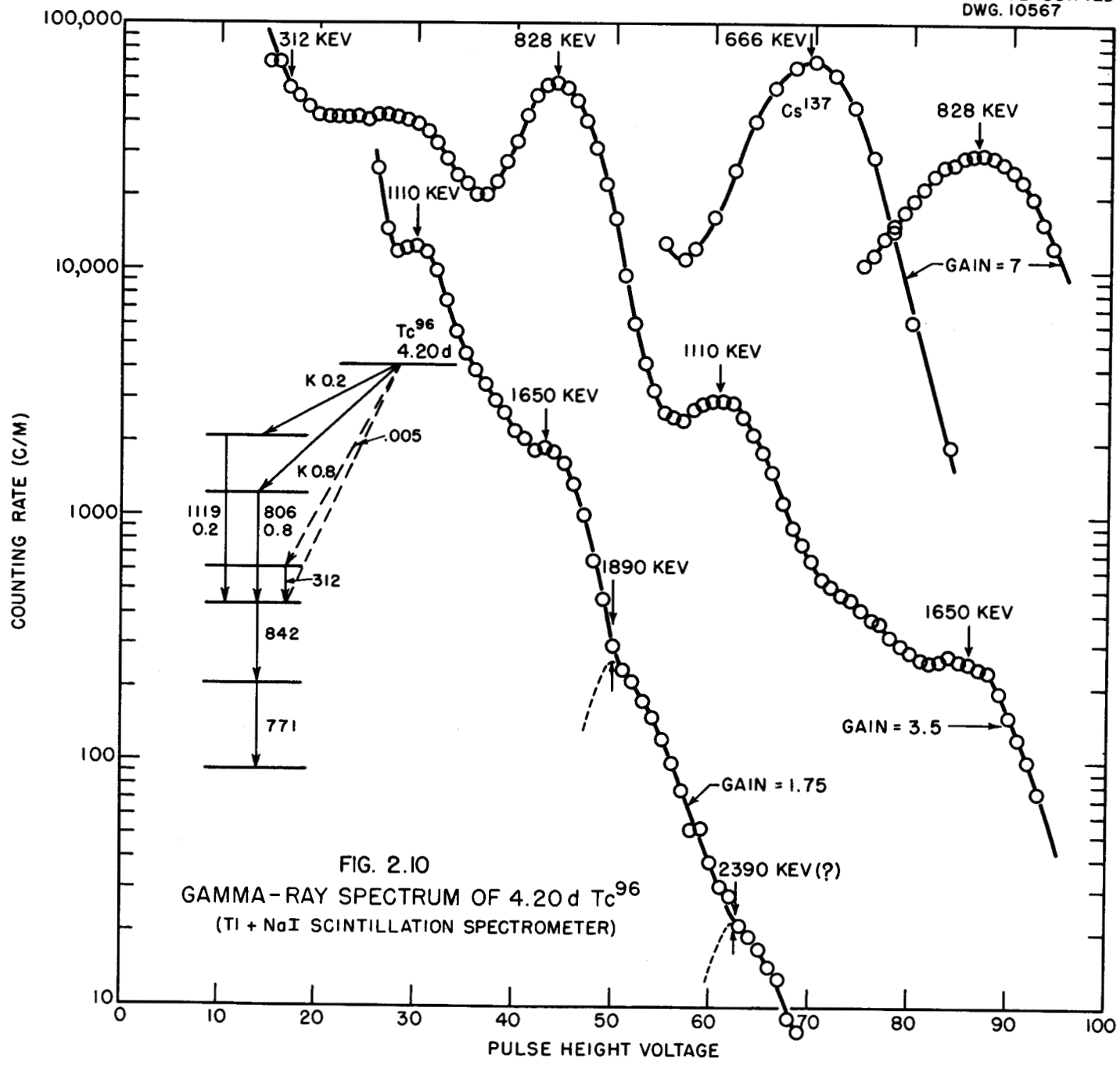


FIG. 2.10  
GAMMA-RAY SPECTRUM OF 4.20 d Tc<sup>96</sup>  
(TI + NaI SCINTILLATION SPECTROMETER)

gamma energy emitted per disintegration in the 4.20-day  $Tc^{96}$ , using a calibrated coincidence counting arrangement, was found to be in good agreement with the decay scheme proposed by Medicus *et al.*

Aluminum absorption measurements on the beta radiations (see Fig. 2.11) emitted by the 13.5-min  $Tc^{101}$  gave a maximum energy of  $1.20 \pm 0.05$  Mev. The gamma-ray spectrum is shown in Fig. 2.12. Coincidence-rate measurements showed that over 95% of the disintegrations of  $Tc^{101}$  proceed through the 1.20-Mev beta followed by a 0.30-Mev gamma.

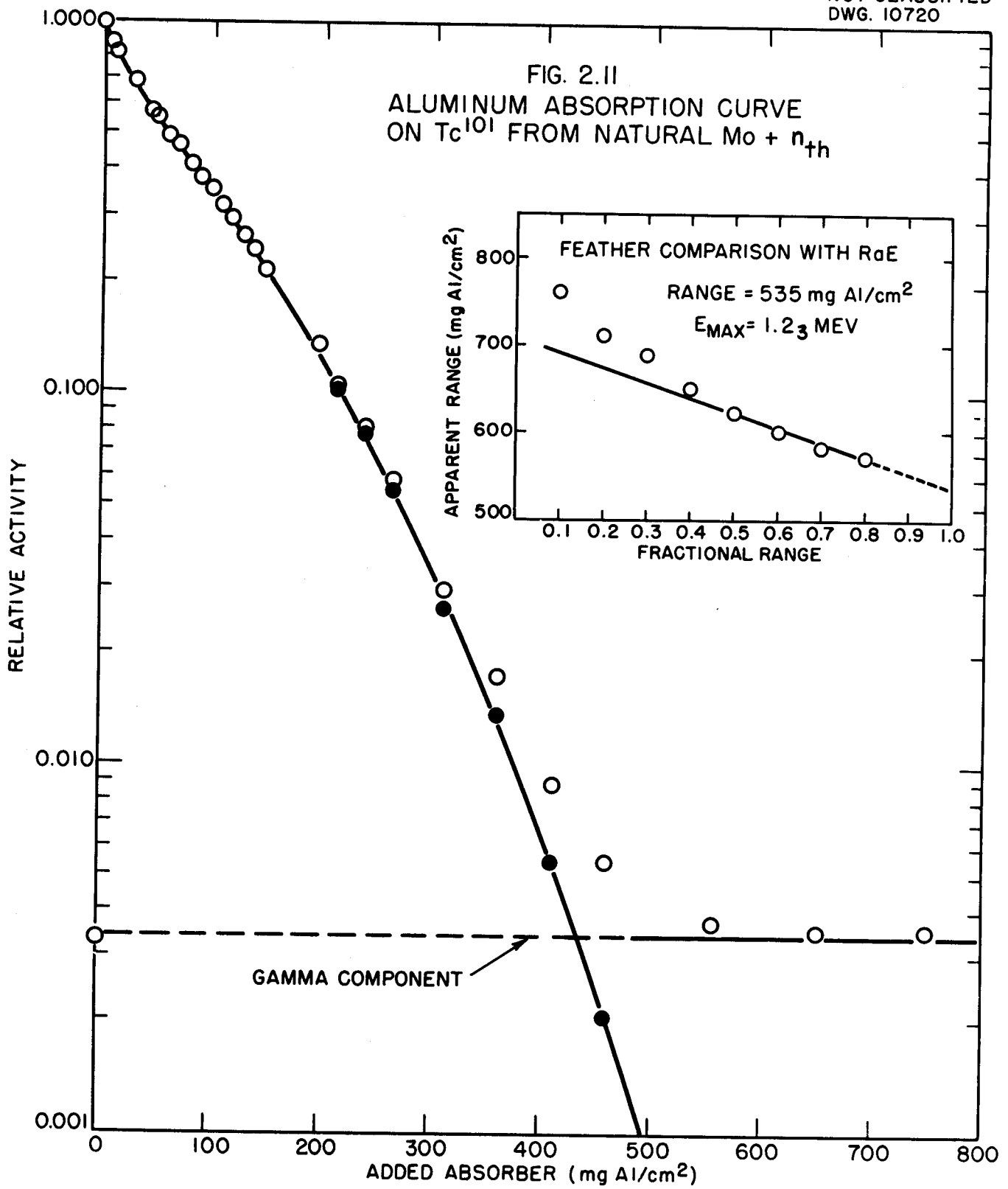
**Radionuclides of Niobium** (G. E. Boyd). Incidental to our cyclotron irradiations of enriched molybdenum isotopes with deuterons to produce technetium activities by a  $(d, 2n)$  reaction, several of the niobium periods also formed in the competing  $(d, \alpha)$  reaction were examined. In particular, measurements were conducted on the radiations from 15-hr  $Nb^{90}$  and 10-day  $Nb^{92}$ .

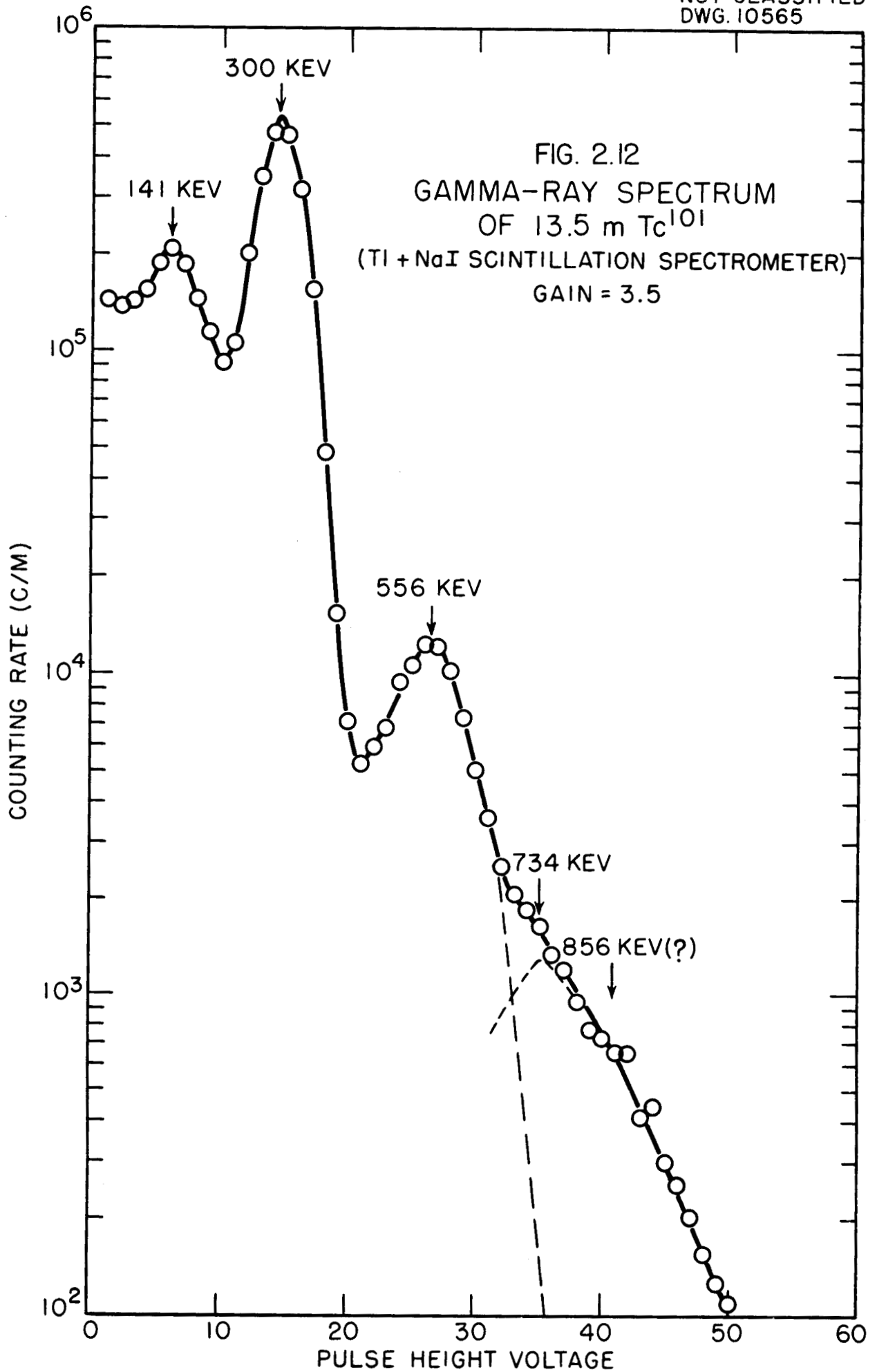
An investigation, using a scintillation-counter spectrometer, of the gamma-ray spectrum of the positron emitting 15-hr  $Nb^{90}$  revealed the presence of 2.23-, 1.14-, and 0.14-Mev transitions. Coincidence-rate measurements, however, suggest that the positron spectrum is simple and followed by approximately 2.2 Mev of gamma-ray energy.

Observations on the gamma spectrum of the 10-day  $Nb^{92}$  indicated a prominent 0.91-Mev transition together with a much weaker 0.20-Mev line. Coincidence-rate measurements showed that the 0.91-Mev transition occurs in  $Zr^{92}$  following K capture in the 10-day  $Nb^{92}$ .

**Fission Product Decay Schemes** (B. H. Ketelle, H. Zeldes, and A. R. Brosi). Work has been concentrated on equipment to determine the energy distributions of beta rays coincident with gamma rays of a given energy. Beta-energy distributions are measured with a thin-magnetic-lens spectrometer, while gamma-ray energies are selected with a scintillation spectrometer.

Some preliminary measurements have indicated that in  $I^{131}$  decay there are two soft-beta groups with maximum energies of 250 and 330 Kev in coincidence with 720- and 640-Kev gamma rays, respectively. To confirm these preliminary measurements further improvements in instrumentation have been made. Among these improvements are increased transmission in the thin-lens spectrometer, improved resolution in the scintillation-counter spectrometer, and shorter resolution times in the coincidence circuit.

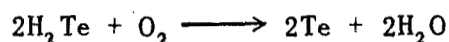
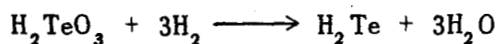
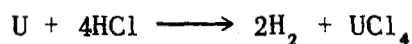




**Photoneutrons from Energetic Gamma Rays Emitted by Fission Product Radionuclides** (G. W. Parker). *Summary.* Using a technique and apparatus described in detail by Levy and Feldman,<sup>(5)</sup> energetic gamma rays in 2.4-hr  $I^{132}$ , whose decay is controlled by the 77-hr tellurium, have been found to account at least in part for the long photoneutron period previously reported by Bernstein *et al.*<sup>(6)</sup>

The initial result of a recent investigation by Ergen<sup>(7)</sup> was the detection of a 2.03-Mev gamma ray by scintillation spectrometry in samples of the 2.4-hr iodine. In an independent effort, while preparing sources for Ergen, evidence was obtained for a less abundant gamma of greater energy than 2.17 Mev, which is consistent with the data obtained by Bernstein *et al.* Supporting observations have also been made by Brosi and Ketelle<sup>(8)</sup> with both beta- and gamma-ray spectrometers.

*Isolation of 77-hr Te<sup>132</sup>.* While references to the formation of hydrogen telluride were subsequently found in published literature, it was not expected in the hydrochloric acid dissolution of uranium metal. However, in tracer experiments conducted prior to high-level runs, elemental carrier tellurium was observed to deposit in a glass reflux condenser connected to the dissolver. The mechanism responsible may possibly be described by the following approximate reactions:



This unusual chemistry presented the opportunity to obtain fairly pure tellurium in one step, and it was arranged to have the uranium dissolver off-gases scrubbed in an ammoniacal packed column for collection of the tellurium precipitate. Uranium slugs irradiated for three days, cooled for one week, and treated in this manner gave fairly good yields of very pure 77-hr  $Te^{132}$ .

(5) H. A. Levy and M. H. Feldman, "Hard Gamma Measurements," *Report of the Chemistry Division for the Months September, October and November, 1947*, MonN-432, p. 100 (Dec. 15, 1947).

(6) S. Bernstein, W. M. Preston, G. Wolfe, and R. E. Slattery, *Yield of Photoneutrons from U<sup>235</sup> Fission Products in Heavy Water* (Appendix by E. Greuling), MonP-172 (Sept. 24, 1946).

(7) W. K. Ergen, ORNL Physics Division, private communication, March, 1951.

(8) A. R. Brosi and B. H. Ketelle, private communication, March, 1951.

Separation of 2.4-hr  $I^{132}$  from 77-hr  $Te^{132}$ . After carrier plus active tellurium had been collected, the scrubber solution was transferred remotely to a glass reactor, carefully acidified to 3 M HCl, and treated with  $SO_2$  to precipitate tellurium metal. The black coagulated product was washed and then dissolved in a minimum volume of warm 8 M  $HNO_3$ . This solution was transferred to a still and diluted with subsequent washings. In order to "milk" the carrier-free 2.4-hr iodine daughter from its 77-hr tellurium parent it was necessary only to add 15%  $H_2O_2$  and to distill into an alkaline trap. The alkaline condensate was then concentrated or diluted as required for source preparation.

Calibration of the Photoneutron Apparatus. Using both a beryllium sphere (10 in. in diameter) obtained from Bernstein, and a  $D_2O$  tank (150 lb of  $D_2O$ ) and a  $U^{235}$  fission counter obtained from Levy, approximate counting rates of reference samples were made as a relative standard for instrument sensitivity. Besides various radium sources,  $Co^{60}$ ,  $Na^{24}$ , and fission products  $Cs^{137}$  and  $I^{131}$  were examined for energetic gammas. Source strengths and observed counting rates are given in Table 2.1. The sensitivity found with radium, as well as the  $Na^{24}$  efficiency, was about the same as reported by Levy.<sup>(5)</sup> While some rather important disadvantages are recognized as inherent in this method of characterizing gamma rays, the increasing number of available sources, the very low instrument background (0.2 c/m), and the fair reproducibility of the method has seemed to assure a place for measurements of this type.

TABLE 2.1  
Reference Sources

SOURCE	AMOUNT	COUNTS WITH Be (c/m)	COUNTS WITH $D_2O$ (c/m)	KNOWN HARD GAMMAS (% of disintegrations)
$Ra^{226}$ (RaC)	100 mg	~1380	~180	~10 (1.7 - 1.8 Mev) ~1 (2.2 - 2.4 Mev)
$Na^{24}$	3-4 mc	~88	380	100 (2.78 Mev)
Ba-La <sup>140</sup>	~30 mc	6.5	46	~70 (1.65 Mev) ~3 (2.5 Mev)
$I^{131}$	100 mc	~1.0		None
$Co^{60}$	250 mc	0		None
$Cs^{137}$	30 mc	0		None

*Energetic Gamma Rays in I<sup>132</sup> and Te<sup>131</sup>.* I<sup>132</sup> sources of nearly 200 mc strength were measured and observed for decay to identify the origin of the photoneutrons. An appreciable counting rate was obtained with both the beryllium and D<sub>2</sub>O absorbers, indicating the presence of photons of energies greater than the respective thresholds for each of these. An attempt was made to estimate the percent abundance of these rays; however, precise answers which are dependent on such variables as the change of ( $\gamma, n$ ) cross-section with energy cannot be given without further calibrations. The estimates given in Table 2.2 were made chiefly on the basis of a very crude understanding of the origin of photoneutrons from RaC.

TABLE 2.2

Uncharacterized Fission Product Sources

SOURCE	AMOUNT (mc)	COUNTS WITH Be (c/m)	COUNTS WITH D <sub>2</sub> O (c/m)	ESTIMATED GAMMA ABUNDANCE (% of disintegrations)	OBSERVED DECAY (hr)
2.4-hr I <sup>132</sup>	160	312	56	1 - 2 (>1.67 Mev) ~0.5 (>2.17 Mev)	~2.3
2.4-hr I <sup>132</sup>	100	200	36	Same	~2.3
30-hr (25- min) Te <sup>131</sup>	~5	6	2	Unreliable	~30

Because of the very low ( $n, \gamma$ ) cross-section of tellurium for the production of 30-hr Te<sup>131</sup>, only a relatively weak source was obtained. There was, however, an indication that energetic gamma rays are also present here (possibly in the 25-min isomer). At a later date tellurium samples will be irradiated at higher flux in the LITR, or possibly Te<sup>131</sup> will be separated from the fission products.

Investigation with other fission sources are being considered.

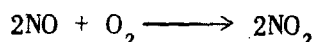
**Use of Hydrogen Peroxide in a Method for Treating Uranium Metal Dissolver Off-Gases** (G. W. Parker and G. E. Creek). *Summary.* In a previous quarterly report<sup>(9)</sup> a proposed method of treating the current large-scale dissolver-

(9) G. W. Parker, G. E. Creek, G. M. Hebert, P. M. Lantz, and W. J. Martin, "Feasibility Test of the Large Scale Collection of Fission Rare Gases," *Chemistry Division Quarterly Progress Report for Period Ending September 30, 1949*, ORNL-499 (Dec. 6, 1949).

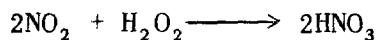
operations off-gases in order to permit an efficient recovery of both the fission iodine (principally I<sup>129</sup>) and the fission gases containing 10-year Kr<sup>85</sup> was described.

Recently interest in fumeless chemical operations for new processing plants has led to a number of gas-treatment designs<sup>(10)</sup> for specific gas mixtures, including the use of scrubbing systems of oxygen and water for NO and NO<sub>2</sub>, and gas compression and storage for mixtures containing N<sub>2</sub> and N<sub>2</sub>O. In our work, a process based on the well-known absorption quality of hydrogen peroxide for the acidic gases NO and NO<sub>2</sub> was demonstrated successfully in laboratory bench-scale glass equipment using tracer levels of Kr<sup>85</sup>. Although efficient iodine recovery was not proved, there is no serious doubt that it could be. In addition, the method was found capable of performing well for "acid recovery" and may give quite high HNO<sub>3</sub> concentrations.

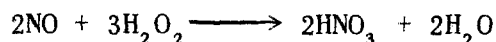
*Apparatus and Scrubber Solutions.* In the accompanying diagram (Fig. 2.13) a single-slug dissolver (5 moles of uranium) is shown connected with a reflux condenser, a gas rotameter for measuring the rate of production of NO, and a mixing chamber to which tank oxygen may be added at a proportional rate for the oxidation of NO to NO<sub>2</sub>, the reaction being



The oxidized mixture, containing either a slight excess or deficiency of oxygen, is then drawn through a sintered glass gas washer containing a catalyzed scrubbing solution of 5 to 10% H<sub>2</sub>O<sub>2</sub> in 0.5 to 5 M HNO<sub>3</sub>. In series with this is a second H<sub>2</sub>O<sub>2</sub> scrubber and a third scrubber containing either water or dilute alkali. Measurement of the consumption of H<sub>2</sub>O<sub>2</sub> established that near stoichiometric quantities are involved in the reaction



or



A fairly striking illustration of what is presumed to be autocatalysis has been encountered with the absorption of NO<sub>2</sub> in H<sub>2</sub>O<sub>2</sub>: During the start-up

(10) A. T. Gresky, private communication.

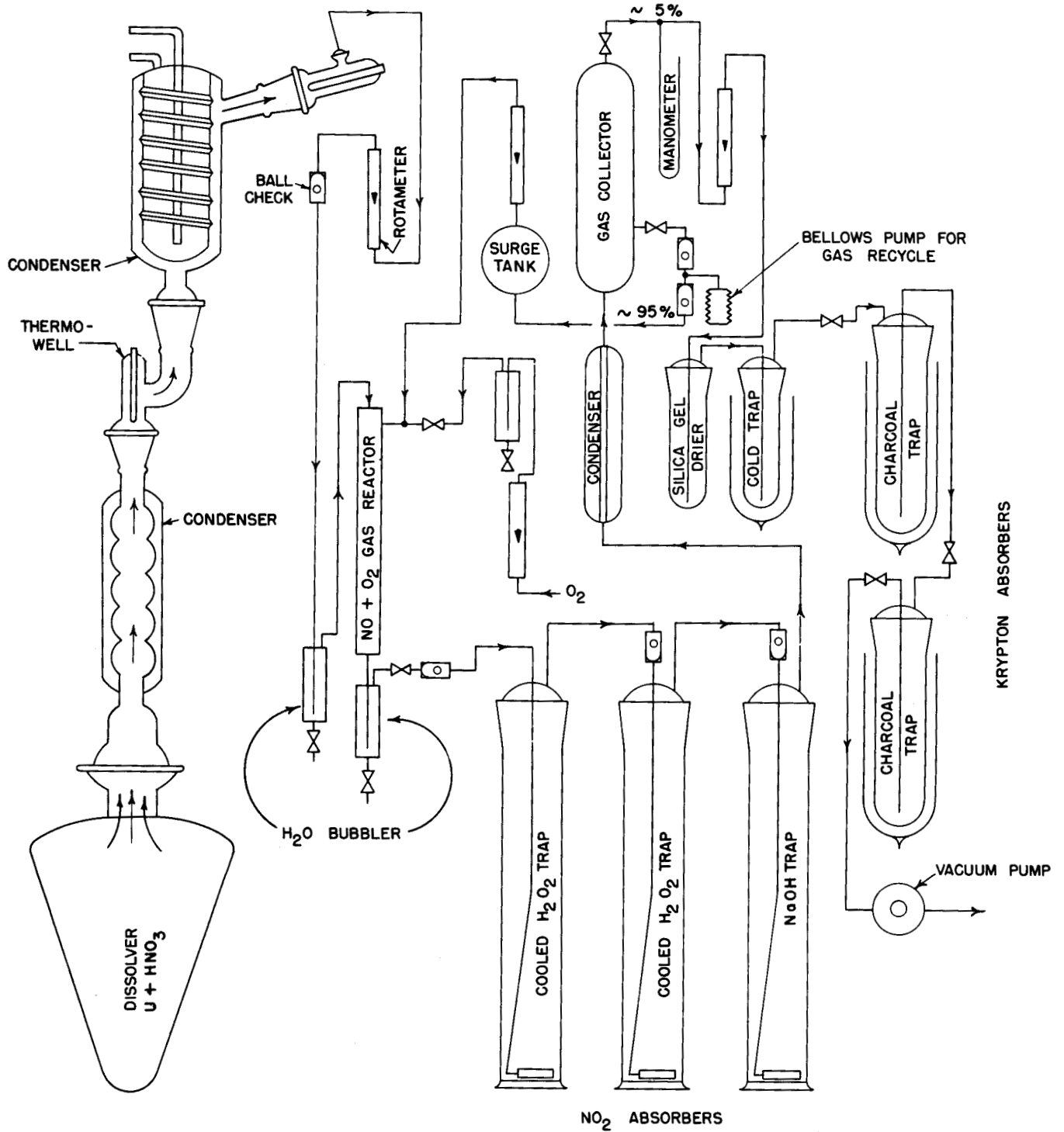
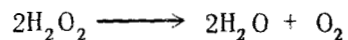


FIG. 2.13 APPARATUS FOR STRIPPING URANIUM DISSOLVER OFF GASES

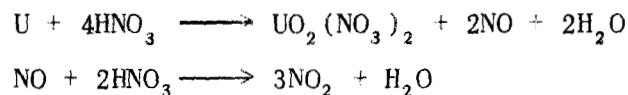
of the gas treatment, when pure materials were placed in the scrubber (usually 10% H<sub>2</sub>O<sub>2</sub> and 0.5 M HNO<sub>3</sub>) a period of poor absorption was observed. Brown fumes (NO<sub>2</sub>) apparently escaped both traps and accumulated in the free space above the solution. Then, after a few minutes, a large pressure drop occurred in the system which was interpreted as resulting from a rapid absorption of this gas. From this stage to the completion of the dissolving no brown gases escaped the first scrubber; however, an appreciable amount of effervescence was soon observed in the peroxide solution as a result of apparent decomposition:



The rate of production of oxygen was fairly constant at about 200 cc/min while about 1000 cc/min of NO<sub>2</sub> was being absorbed. Therefore, perhaps 20% of the H<sub>2</sub>O<sub>2</sub> was being decomposed. A sample removed from this catalyzed scrubber continues to effervesce for some time although ordinary mixtures of H<sub>2</sub>O<sub>2</sub> and HNO<sub>3</sub> of the same strength do not effervesce. In order to circumvent this loss of oxygen most of it was recirculated to the NO-O<sub>2</sub> gas reactor. In order to avoid the sluggish period in the scrubber it may be necessary to use a "seeded" scrub solution or to encourage catalytic decomposition with additives or with platinum black.<sup>(11)</sup>

*Controlled Dissolving Rate.* Most of the current dissolver operations are performed on a maximum rate basis; i.e., all the metal, including "heels," is exposed at one time to all the acid, and the dissolving is continued to a predetermined solution specific gravity or to a minimum residual free acid content.

In order to scrub the evolved gases effectively large extremes in the rate of dissolution had to be avoided. This was done by starting with dilute acid (actually, 4.5 moles of nitric acid per mole of uranium):



(11) H. H. Willard, private communication

The procedure was to add 500 ml of water to the dissolver and then heat to boiling. This displaced much of the air with H<sub>2</sub>O vapor before the addition of about 1500 ml of 70% HNO<sub>3</sub>. The acid was added slowly and continuously over a period of at least 2 hr while the solution was maintained at the boiling point (110 to 114°C). Dissolution in the presence of a 100% heel was accomplished in about 12 hr.

A negative pressure of about 3 cm Hg on the dissolver was maintained by means of a controlled vacuum pump which served to draw the residual gases through a silica drier, a rotameter, and two 250-g dry-ice-cooled charcoal traps for adsorbing xenon and radiokrypton from the O<sub>2</sub> and N<sub>2</sub> (about 1.5% of the total NO).<sup>(10)</sup> The total pressure drop was about 10 cm Hg.

*Adsorption of Kr<sup>85</sup> on Activated Charcoal.* While using slugs estimated to contain approximately 1 mc of Kr<sup>85</sup> it was found that about 200 cc/min of mixed O<sub>2</sub> and N<sub>2</sub> was adequately depleted of krypton activity by passage through one 250-g charcoal trap kept at dry-ice temperature. When dry ice was used instead of liquid N<sub>2</sub> a possible condensation of O<sub>2</sub> on the charcoal together with its attendant hazards was avoided.

At the completion of the extraction the rare gases were displaced successively into two smaller charcoal traps, each decreasing the adsorbent by a factor of 5. Finally, the 20-ml charcoal trap was connected to a 200-ml evacuated bulb and allowed to degas into it.

Using an ion chamber calibration furnished by Zeldes and coworkers,<sup>(12)</sup> a 0.6-mc yield of Kr<sup>85</sup> was determined. After corrections for decay had been made, this yield appeared to be quantitative. This was confirmed by checking all losses through a back-up charcoal trap. No losses were found within the limit of detection of the krypton activity (approximately 5%).

**Hot-Atom Chemistry in the Solid State** (G. E. Boyd and J. W. Cobble). The fate of the radioactive recoil Br<sup>82</sup> atoms produced in crystalline KBrO<sub>3</sub> by neutron capture was studied with the view to furthering an understanding of solid-state processes in ionic crystals. Measurements of the variation with time of the retention of radiobromine as bromate showed a limiting retention at zero time of 9 ± 1% which increased to and remained almost constant at

(12) H. Zeldes, B. H. Ketelle, and A. R. Brosi, "Radiations of Long-Lived Kr<sup>85</sup> and A<sup>39</sup>," *Chemistry Division Quarterly Progress Report for Period Ending June 30, 1950*, ORNL-795, p. 48 (Oct. 3, 1950).

32 ± 1% after about 16 hr of neutron irradiation. Heating the irradiated potassium bromate after removal from the pile induced a thermal reaction which increased the retention of Br<sup>82</sup>. A radiation-induced recombination of Br<sup>82</sup> to bromate was also observed when these crystals were exposed to the gamma rays from an approximately 1500-curie Co<sup>60</sup> source. No simple rate law was found capable of describing the thermal back-reaction, which showed a positive temperature coefficient. The radiation-induced back-reaction obeyed a first-order velocity equation and was found proportional to the source intensity. Furthermore, the reaction could be stopped completely at liquid-nitrogen temperatures. An activation energy of 8.5 kcal/mole between 10 and 150°C was found.

An interpretation of the finite retention observed at zero time was attempted, based upon assumptions concerning capture gamma-ray spectra. Calculations were made, using a stochastic procedure, of the probability that the resultant momentum possessed by a radiobromine atom after the emission of three, four, or six capture gamma rays in cascade would exceed the bond energies of the bromate radical. Estimates of the "cage" effect were made using the lattice dimensions for KBrO<sub>3</sub>. Those recoiled radiobromines which escape the bromate radical and do not immediately recombine by collision with neighboring bromate groups are subsequently trapped in the crystal in an energy-rich state. Further reaction of these "hot" atoms may involve trapped electrons (i.e., quenching), oxygen atoms produced by radiation decomposition, impurities such as water and its decomposition products, or an exchange with the bromate radicals in the crystal.

**Chemistry of Technetium: Measurement of Magnetic Susceptibilities** (C. M. Nelson, G. E. Boyd, and W. T. Smith\*). Research work during the past six months has been aimed at determining the bond character of several simple solid compounds of technetium by means of magnetic susceptibility measurements. Preparation of the halides and oxides of the several oxidation states of technetium will be attempted and their structures identified when possible by X-ray-diffraction methods. Analogous manganese and rhenium compounds will be examined also to compare the technetium results with atomic and electronic structural changes.

Although other compounds of technetium (e.g., the sulfates) might give more information regarding interatomic forces and other interactions, it was felt that the simple compounds should be investigated first in the hope that

\*Professor of Inorganic Chemistry, University of Tennessee, Knoxville.

the magnetic properties might be of help in elucidating the oxidation states of this new element. In its compounds manganese follows the Curie law rather well so that the "spin only" equation for the magnetic susceptibility  $\chi$  gives a good approximation to experimentally determined values. Although not many rhenium compounds have been investigated, it has been reported that in some compounds (e. g.,  $\text{Re}_2\text{O}$ ,  $\text{ReO}_3$ , and  $\text{ReO}_2$ ) a small temperature-independent paramagnetism may appear.<sup>(13)</sup> In other compounds rhenium appears to have normal magnetic properties. Since rhenium follows the rare earth series, and hence the "lanthanide contraction" in atomic radii, it might be expected to have abnormal magnetic properties. It will be of interest to see how  $\chi$  changes from manganese to technetium to rhenium in analogous compounds.

An attempt will be made to prepare  $\text{TcO}$  and  $\text{ReO}$  and to measure  $\chi$  down to very low temperatures in an effort to see if any "antiferromagnetism" exists in these compounds analogous to that of  $\text{MnO}_2$ .<sup>(14)</sup> This latter compound, as well as other compounds of Mn(II) with the Group VI-A elements, shows a "hump" in the specific heat and magnetic susceptibility curves at various temperatures.

A magnetic susceptibility-measurement apparatus has been designed and its assembly has been completed. Since only small samples of technetium will be available, the method used to measure  $\chi$  had to be adaptable to milligram-size samples. Consequently a nonhomogeneous magnetic field will be used in which a small sample will be acted upon by a force,  $F$ , defined by the equation

$$F = m\chi H (dH/dx)$$

where  $m$  is the mass of sample,  $H$  is the magnetic-field strength, and  $dH/dx$  is the gradient of the field. This force will be measured by the extension of a quartz spring. Sylphon bellows will be used to provide a vacuum-tight system and yet allow the quartz spring to be moved up and down.

The long-lived beta-emitting  $\text{Tc}^{99}$  is currently being separated by the Hot Laboratory Operations Group from Redox process waste solutions, and is now available for this research. This isotope emits a 0.3-Mev beta ray only in

(13) W. Schüth and W. Klemm, "Magnetochemische Untersuchungen. XI. 1. Über das Magnetische Verhalten einiger Rheniumverbindungen," *Z. anorg. u. allgem. Chem.* 220, 193 (1934).

(14) R. W. Tyler, "The Magnetic Susceptibility of  $\text{MnO}$  as a Function of the Temperature," *Phys. Rev.* 44, 776 (1933).

its radioactive decay, and has a half-life of at least  $2 \times 10^5$  years. These properties make it feasible for use in macrochemical research. As mentioned earlier, as many different oxides as can be prepared in a single oxidation state will be made, and their magnetic properties will be investigated. Several halides will also be synthesized. X-ray-diffraction measurements will be made to substantiate other evidence for the different structures. Counting techniques may be of aid in the analysis of the chemical composition. Bremsstrahlung from the beta rays can be counted in an ionization chamber.

### 3. RADIO-ORGANIC CHEMISTRY

#### RADIATION, ANALYTICAL, AND PREPARATIVE CHEMISTRY

E. J. Dowling      W. J. Skraba  
A. R. Jones        T. C. Weeks

**Radiation Chemistry.** Preliminary experiments on the effects of gamma radiation on aqueous solutions of organic compounds have been carried out using  $C^{14}$ -carboxyl-labeled benzoic acid. From the incomplete data the following conclusions may be drawn:

1. The use of  $C^{14}$ -labeled organic materials in radiation studies considerably simplifies the analytical difficulties encountered in determining the products formed in low concentration. By the addition of carrier amounts of the suspected products, purification, and subsequent radioactive assay the identity and the quantity of the various products may be determined. At the low concentrations employed such analyses would be almost impossible in any other way. In addition, from parallel experiments performed with the same organic compound labeled with  $C^{14}$  in different positions, the fate of each fragment, or carbon position, in the molecule may be determined.
2. Ninety percent of the benzoic acid in 25 ml of 0.0082 *M* aqueous solution was lost after 22 hr radiation in the 300-curie  $Co^{60}$  gamma source. After 3 hr of radiation the decomposition was 16%.
3. Approximately 25% of the loss of benzoic acid may be accounted for in the decarboxylation reaction. Carbon dioxide is formed in considerable preference to carbon monoxide.
4. Organic acids other than benzoic acid are produced.
5. Part of the benzoic acid is converted to neutral nongaseous products.

The radiation decomposition of organic compounds by gamma radiation of dilute water solutions involves the following considerations:

1. Spatially and energetically uniform radiation is obtained with gamma radiation from a  $Co^{60}$  source.
2. The rate of energy input is low enough to exclude temperature effects.
3. No stirring is necessary.

4. The large mass of water in comparison to the amount of organic material should cause the decomposition to be largely of a secondary and more homogeneous nature, i.e., most of the energy of the gamma rays would be used to ionize and activate water molecules.
5. The summation of such reactions would be the formation of hydrogen, oxygen, hydrogen peroxide, hydrogen ions, hydroxyl ions, hydrogen atoms, and hydroxyl radicals.<sup>(1,2)</sup> Since the actions of water solutions of H<sub>2</sub>, O<sub>2</sub>, H<sub>2</sub>O<sub>2</sub>, H<sup>+</sup>, and OH<sup>-</sup> on organic materials are fairly well understood and are found to be in general of a low rate, we might expect to obtain as products of the gamma radiation of dilute water solution those substances obtained by reaction between the organic molecules and the hydrogen and hydroxyl radicals.<sup>(3,4)</sup>

*Irradiation Experiment No. 1.* A 100-ml volume of water solution containing 99.3 mg of benzoic-7-C<sup>14</sup> acid (0.89 μc/mg) was prepared.

A 30.107-g aliquot of this solution, containing 29.9 mg (0.245 mmoles, 26.7 μc) of benzoic-7-C<sup>14</sup> acid, was irradiated for 3 hr in a vented bottle with gamma rays from the 300,000-r/hr Co<sup>60</sup> source at ORNL. The slightly cloudy solution was titrated to a pH of 8.0 with sodium hydroxide, and a clear solution was obtained. The titration showed 0.021 mmole (8.6%) of the carboxyl group to have disappeared, presumably in the form of carbon monoxide and/or dioxide. To the solution was then added 1.989 g of nonradioactive pure benzoic acid dissolved in sodium hydroxide, and the homogeneous solution was treated with sufficient hydrochloric acid to precipitate approximately one-third of the benzoic acid, which was removed by filtration. Another third of the benzoic acid was precipitated, dried, and weighed, and aliquots were burned. The radiochemical analyses indicated that 22.5 μc of benzoic-7-C<sup>14</sup> acid remained in the solution after irradiation (84.2%).

At the end of a 3-hr gamma irradiation, therefore, 84.2% of the starting material remained; during the radiation there was 8.6% decarboxylation and 15.8% loss of benzoic acid.

- (1) A. O. Allen, T. W. Davis, G. V. Elmore, J. A. Ghormley, B. M. Haines, and C. J. Hochanadel, *Decomposition of Water and Aqueous Solutions Under Pile Radiation*, ORNL-130 (Oct. 11, 1949).
- (2) A. O. Allen, *Radiation Chemistry of Aqueous Solutions*, MDDC-1056 (decl. June 23, 1947).
- (3) E. J. Hart, *Mechanism of the γ-Ray Induced Oxidation of Formic Acid in Aqueous Solution*, ANL-4434 (Apr. 4, 1950).
- (4) F. T. Farmer, G. Stein, and J. Weiss, "Chemical Actions of Ionising Radiations on Aqueous Solutions. Part I. Introductory Remarks and Description of Irradiation Arrangements," *J. Chem. Soc. London* 1949, p. 3241 (1949); G. Stein and J. Weiss, "Part II. The Formation of Free Radicals. The Action of X-Rays on Benzene and Benzoic Acid," p. 3245; "Part III. The Action of Neutrons and of α-Particles on Benzene," p. 3254; "Part IV. The Action of X-Rays on Some Amino-acids," p. 3256.

*Irradiation Experiment No. 2.* A second aliquot of the original solution weighing 27.235 g and containing 27.12 mg (0.222 mmole, 24.2  $\mu\text{c}$ ) of benzoic-7- $\text{C}^{14}$  acid was irradiated in the same manner for 22 hr. The same procedure was followed as in Expt. 1, and the white emulsion clarified completely on titration with sodium hydroxide. Because more extensive decomposition was expected, the isolated diluted benzoic acid was sublimed at 100°C before analysis.

At the end of the 22-hr gamma irradiation 10.9% of the starting material remained unchanged; there was 26.0% decarboxylation and 89% loss of benzoic acid.

*Irradiation Experiment No. 3.* Having now some idea of the extent of decomposition to be noted with time, 200 ml of a solution containing 176 mg of benzoic-7- $\text{C}^{14}$  acid (197  $\mu\text{c}/\text{mg}$ ) was prepared with double-distilled water.

A 25-g aliquot of this solution, containing 22.1 mg (0.181 mmoles, 434  $\mu\text{c}$ ) of benzoic-7- $\text{C}^{14}$  acid was placed in a specially constructed cell and purged with oxygen-free hydrogen for 15 min. The cell was then irradiated with gamma rays from the 300,000-r/hr  $\text{Co}^{60}$  source at ORNL for 21.3 hr. The irradiated solution was purged with oxygen, during which process much foaming was noted. The exit gas was passed through a spiral bubbler containing sodium hydroxide, then through a copper oxide furnace, and finally through a second sodium hydroxide spiral bubbler. It seems fairly certain that the organic gases produced would be only carbon dioxide and/or carbon monoxide because deep-seated disruption of the molecule would be necessary to produce any others. Of course, the only radioactive gases likely to be produced would be the same.

Acidification of aliquots of the contents of the first bubbler gave by radiochemical analysis 73  $\mu\text{c}$  of total activity, corresponding to 16.8% of the original activity of the benzoic acid.

Acidification of aliquots of the contents of the second bubbler gave by radiochemical analysis 0.8  $\mu\text{c}$  of total activity, corresponding to 0.2% of the original activity of benzoic acid.

The cell was washed thoroughly and the solution was titrated with standard sodium hydroxide. A loss of 0.081 mmole of carboxylic material out of 0.181 mmole before irradiation showed that 44.7% of the benzoic acid was decarboxylated.

To summarize, at the end of the 21.3-hr gamma irradiation there had been 44.7% loss of carboxyl carbon, 16.8% conversion of carboxyl to carbon dioxide, and 0.2% conversion of carboxyl to carbon monoxide. It is supposed that the carboxyl carbon lost but not found as carbon monoxide or carbon dioxide has been incorporated into product material as nonacidic carbon, such as carbonyl or carbinol carbon.

**Analytical Chemistry.** The determination of the concentration of hydrogen peroxide in extremely dilute sulfuric acid solutions containing a constant concentration of uranyl sulfate was found to be feasible polarographically. A straight line was obtained for such solutions for hydrogen peroxide concentrations of 50 to 500  $\mu$ moles/liter when determined in 0.1 *N* potassium chloride solution.

It was found that hydrogen peroxide solutions were not sufficiently stable in ordinary distilled water to allow time for standardization and dilution, but that in repurified water (distilled first from acidic and then from basic permanganate) the solutions were stable for several days.

To obtain a calibration curve as precisely as possible the complete standardization was accomplished in one day. Ceric sulfate solution was standardized with arsenious oxide. A hydrogen peroxide solution was standardized with ceric sulfate solution and then aliquoted and diluted along with an acid uranyl sulfate solution and 1 *N* potassium chloride solution to form a series of dilutions — 10, 50, 100, 300, 500  $\mu$ moles/liter — all containing the same concentration of uranyl sulfate (1000  $\mu$ moles/liter), sulfuric acid (200  $\mu$ moles/liter), and potassium chloride (100 mmoles/liter). The current flow for a sensitivity of 0.030  $\mu$ a/mm at 1.20 volts vs. a saturated calomel electrode with a particular dropping mercury electrode and mercury height was determined after purging the solutions with oxygen-free hydrogen for 10 min. The calomel electrode and test mixture were thermostated at 25°C. A model XXI Sargent polarograph was used, and the wave height for the uranyl sulfate was removed by down-scale compensation. A calibration curve was obtained by plotting the concentration of hydrogen peroxide against the current (Table 3.1).

A device for maintenance of the mercury height (Fig. 3.1) for a dropping mercury electrode was constructed. A mild source of vacuum, e.g., house vacuum, is all the power required. This device, which was mounted on the same rack as the dropping mercury electrode but on an adjacent rod, has been in

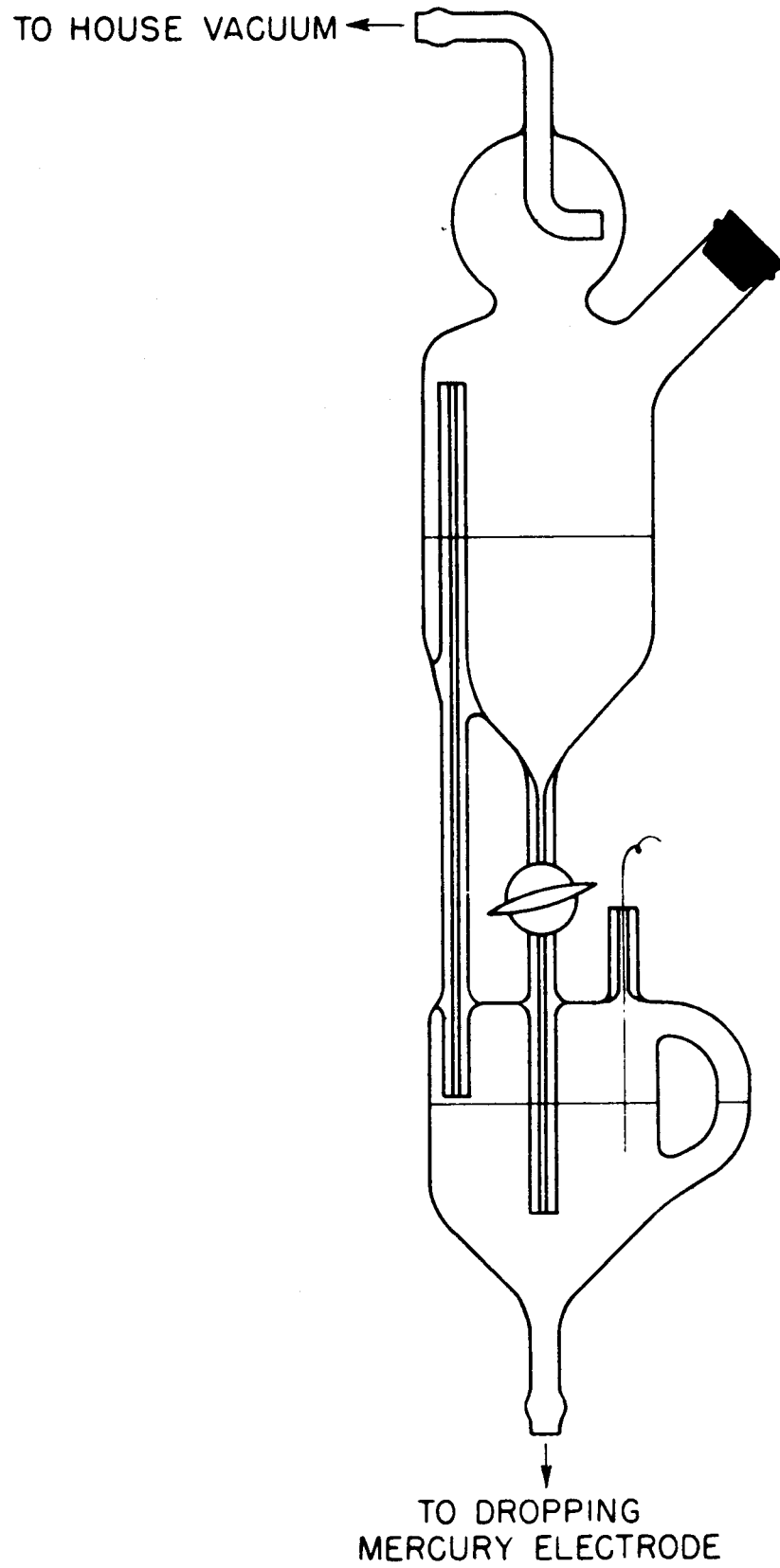


**FIG. 3.1**  
CONSTANT LEVEL DEVICE FOR  
THE DROPPING MERCURY ELECTRODE

constant use for approximately two months and has functioned satisfactorily. Occasionally, for very precise determinations of current maxima at a fixed potential, it has been advisable to close the stopcock for momentary observation. The operation of this apparatus is obvious from Fig. 3.1.

TABLE 3.1

H<sub>2</sub>O<sub>2</sub> Concentration vs. Current

CONCENTRATION OF H <sub>2</sub> O <sub>2</sub> (μmoles/liter)	CURRENT (μa)
500	7.050
300	5.100
100	3.180
50	2.730
10	2.520

**Preparative Chemistry. Methanol-C<sup>14</sup>.** A total of 690.4 mc of methanol-C<sup>14</sup> has been prepared by the high-pressure hydrogenation of carbon-C<sup>14</sup> dioxide. This material is of considerably higher specific activity than any prepared previously. The synthesis is a batch process, usually run on a 10-mmole scale. The yield was not greatly affected by increasing the amount of carbon dioxide per run to 18 mmoles, but it did suffer when the amount was increased to 24 mmoles.

A high-vacuum line was calibrated, and about 60 mc of methanol-C<sup>14</sup> was aliquoted, in quantities ranging from 0.5 to 10 mc.

**Potassium Cyanide-C<sup>14</sup>.** Approximately 70 mc of potassium cyanide-C<sup>14</sup> has been prepared by the modified Loftfield<sup>(5)</sup> procedure.

**Acetic-2-C<sup>14</sup> Acid.** Approximately 20 mc of acetic-2-C<sup>14</sup> acid was prepared by the Hess<sup>(6)</sup> procedure. It was confirmed that pure acetic acid could not be isolated by hydrolysis of the crude acetonitrile contained in the reaction

(5) R. B. Loftfield, "Preparation of C<sup>14</sup>-labeled Hydrogen Cyanide, Alanine, and Glycine," *Nucleonics* 1, No. 3, 54 (1947).

(6) D. N. Hess, "Preparation of Acetic-2-C<sup>14</sup> Acid," *J. Am. Chem. Soc.*, in press.

mixture from methyl-C<sup>14</sup> hydrogen sulfate and potassium cyanide, but that it was absolutely necessary that the acetonitrile be distilled out of the reaction mixture and separately hydrolyzed.

*Glycine-2-C<sup>14</sup>*. Two attempts were made to synthesize glycine-2-C<sup>14</sup> by the procedure of Ehrensvärd.<sup>(7)</sup> Yields of 20 and 29% of impure material were obtained.

Since it was found that chloroacetic acid could be prepared in very good yield by simply heating acetic acid containing some acetyl chloride with a slight insufficiency of chlorine in a sealed tube to 135 to 140°C for 2 hr on a 15-mmole scale, it was decided to use a modified Ostwald<sup>(8)</sup> and Sakami<sup>(9)</sup> procedure for the synthesis of labeled glycine since it would be applicable for both types of C<sup>14</sup>-labeled glycine.

Several methods for the purification of the crude glycine were tried, e.g., those of Tolbert<sup>(10)</sup> and of Siegfried.<sup>(11)</sup> Purification was accomplished by treating the water solution of crude glycine with freshly prepared silver oxide. Hydrogen sulfide was passed into the filtrate from this treatment. Norit was added to the mixture and it was concentrated slightly by evaporation on a steam bath and clarified by filtration. The pH of the filtrate was adjusted to 6.0 with dilute sulfuric acid, and the residue obtained by evaporation was sublimed at 160°C and 10<sup>-4</sup> mm Hg. Consistent overall yields of 55% of pure material, m.p. 236 to 237°C, were obtained from experiments using non-labeled glycine.

*Benzoic-7-C<sup>14</sup> Acid*. Approximately 65 mc of benzoic-7-C<sup>14</sup> acid was prepared by the carbonation of phenylmagnesium bromide.

*Malonic-2-C<sup>14</sup> Acid*. Quantitative yields were obtained during the preliminary nonradioactive experiments for the conversion of chloroacetic acid to malonic acid via cyanoacetic acid by a modification of the method of Gal and Shulgin.<sup>(12)</sup>

- (7) G. Ehrensvärd and R. Stjernholm, "An Easy Route to Methylene-labelled Glycine," *Acta Chem. Scand.* 3, 971 (1949).
- (8) R. Ostwald, "Synthesis of Chloroacetic Acid and Glycine Labeled with Radioactive Carbon in the Carboxyl Group," *J. Biol. Chem.* 173, 207 (1948).
- (9) W. Sakami, W. E. Evans, and S. Gurin, "The Synthesis of Organic Compounds Labelled with Isotopic Carbon," *J. Am. Chem. Soc.* 69, 1110 (1947).
- (10) B. M. Tolbert and D. M. Hughes, *An Improved Synthesis of Glycine-1-C<sup>14</sup> and Glycine-2-C<sup>14</sup> from C<sup>14</sup>-Labeled Acetic Acid*, UCRL-705 (May 16, 1950).
- (11) M. Siegfried, "Über die Abscheidung von Amidosäuren," *Ber.* 39, 397 (1906).
- (12) E. M. Gal and A. T. Shulgin, "Improved Syntheses of C<sup>14</sup>-Labeled Malonic Acid and Malonitrile," *J. Am. Chem. Soc.* 73, 2938 (1951).

A 25-ml bulb was blown onto one arm of an 8-mm straight-bore hollow-plug stopcock having on the other arm a 19/38 standard-taper male joint. This constituted the reaction vessel.

Through a long-stemmed funnel 1.090 g (11.54 mmoles) of monochloroacetic acid, 2.1 ml of water, and 0.64 g of sodium carbonate were added. While the temperature was maintained below 90°C, 1.1 g of potassium cyanide was added portionwise to the solution. A cold finger was attached, and the mixture was heated for 1 hr on a steam bath, during which time the color changed from a clear pale yellow to a dark cloudy brown. The contents of the reaction vessel were evaporated to dryness at 0.01 mm Hg and 50°C. To the residue was added 1.1 ml of concentrated hydrochloric acid, and the solution so obtained was evaporated in the same way to dryness. Concentrated hydrochloric acid, 3.9 ml, was added, and the bulb was immersed in liquid nitrogen. After it had been evacuated for 10 min at 0.01 mm Hg, the stopcock was closed and secured with wire.

The reaction vessel was immersed in boiling water, for 2 hr, cooled, and opened, and the contents were evaporated to dryness at 0.01 mm Hg and 50°C. The stopcock was degreased and relubricated with 100% phosphoric acid. A glass wool plug was placed in the bore of the joint surrounding the fine glass tube of a continuous extractor constructed so that the tube extended almost to the bottom of the reaction bulb. Continuous extraction with anhydrous ether was carried out for 16 hr (it was found that only 65% of the malonic acid was extracted in 6 hr). The extracted material obtained by evaporation of the ether weighed 1.149 g, m.p. 131 to 134°C (96%).

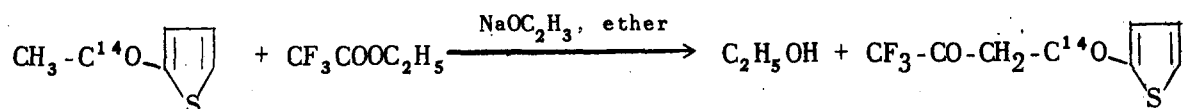
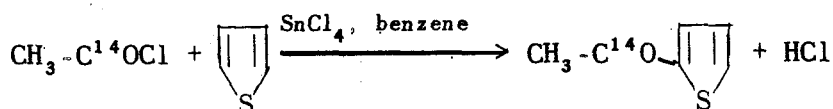
*Glycerol-1-C<sup>14</sup> (and 2-C<sup>14</sup>)*. Several attempts were made to prepare glycerol by the reaction of phosgene with diazomethane followed by reaction of the bis-diazoketone with acetic acid, reduction of the keto-diester, and hydrolysis. Although diazomethane did react with purified phosgene in ether solution even at -80°C, little evolution of nitrogen gas was noted when an ether suspension of the white solid formed in the reaction was treated with acetic acid. Either the product was not the bis-diazoketone, or the latter does not react with acetic acid.

## SYNTHESIS OF HIGH-MOLECULAR-WEIGHT COMPOUNDS CONTAINING C<sup>14</sup>

**Aromatic Polynuclear Compounds** (D. N. Hess and B. M. Benjamin). The general synthesis<sup>(13)</sup> of C<sup>14</sup>-labeled aromatic polynuclear hydrocarbons of high levels of radioactivity has been extended to phenanthrene-9-C<sup>14</sup>, 1-methyl-phenanthrene-9(10)-C<sup>14</sup> and benz(a)anthracene-5,6-C<sub>1</sub><sup>14</sup>.

Using methods previously described,<sup>(13,14)</sup> 10.6 mc of phenanthrene-9-C<sup>14</sup> (4.11 mmoles, 90% overall yield) approximately 10 mc of 1-methyl-phenanthrene-9(10)-C<sup>14</sup>, and 5.88 mc of benz(a)anthracene-5,6-C<sub>1</sub><sup>14</sup> (2.0 mmoles, 70% overall yield) have been prepared in pure form.

**2-(Thenoyl-α-C<sup>14</sup>)-trifluoroacetone (TTA)** (V. F. Raaen). TTA (0.0217 mmole, 17.3 mc) has been prepared from sodium acetate-1-C<sup>14</sup> in 65% yield by the following reactions:



The product, m.p. 40 to 41°C, had a specific activity of 3.6 μc per milligram. It was found by dilution technique to be chemically 98% pure.

**Preparation of Acetyl-1-C<sup>14</sup> Chloride.** Sodium acetate-1-C<sup>14</sup> (2.7 g, 33 mmoles, 1 mc/mmole) which had been dried in a vacuum desiccator over P<sub>2</sub>O<sub>5</sub> was treated with a fourfold excess (10.2 g) of freshly distilled POCl<sub>3</sub>, 30 ml of dry benzene was added, and the mixture was stirred vigorously. The acetyl-1-C<sup>14</sup> chloride was distilled through a short Vigreux column and collected in the 100-ml three-necked flask used in the acylation procedure which followed.

(13) C. J. Collins, "The Synthesis of Phenanthrene-9-C<sup>14</sup>," *J. Am. Chem. Soc.* 70, 2418 (1948).

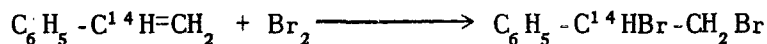
(14) C. J. Collins and J. G. Burr, "Benzo(a)-Anthracene-5,6(?) -C<sup>14</sup>," *Chemistry Division Quarterly Progress Report for Period Ending March 31, 1950. Part I. Chemical Research*, ORNL-685, p. 82 (June 16, 1950).

Preparation of 2-(Aceto-1-C<sup>14</sup>)-thiophene. The method used was that described by Johnson and May.<sup>(15)</sup>

Preparation of 2-(Thenoyl- $\alpha$ -C<sup>14</sup>)-trifluoroacetone. A dry solution of 2-(aceto-1-C<sup>14</sup>)-thiophene in ether was added to a cold, stirred solution of ethyl trifluoroacetate (4.75 g, 33 mmoles), sodium methoxide (1.88 g, 35 mmoles), and 5 ml of anhydrous ether. The mixture was kept at room temperature for two days with stirring in a nitrogen atmosphere. Ether and alcohol were removed at reduced pressure, and the residue was decomposed with a slight excess of 10% sulfuric acid. The resulting oil was extracted with ether, and the ethereal extract was treated with 35 ml of 1 M magnesium acetate. The solution was adjusted to a pH of about 6.5 by the addition of ammonia. The pasty mass was stirred vigorously for 1 hr, and the excess water and ether were removed by means of a filter stick. The solid magnesium chelate was washed twice with 20-ml portions of water, and the mixture was steam distilled using an azeotropic separator under a Friederich condenser. A solid product was obtained which melted in the range 75 to 80°C. This material was converted to a lower melting form on heating above 80°C and cooling. The product was obtained in 65% overall yield (4.82 g, m.p. 40 to 41°C, specific activity 0.80 mc/mmole). The dioxime<sup>(16)</sup> was prepared and assayed, giving an average value of 0.78 mc/mmole.

#### ISOTOPE EFFECT STUDIES

Bromination of Styrene- $\alpha$ -C<sup>14</sup> and Styrene- $\beta$ -C<sup>14</sup> (V. F. Raaen and G. A. Ropp). In the course of a search for isotope effects in addition reactions of C<sup>14</sup>-labeled organic compounds, bromine has been added to tracer-labeled styrene- $\alpha$ -C<sup>14</sup> and to tracer-labeled styrene- $\beta$ -C<sup>14</sup> at -70°C:

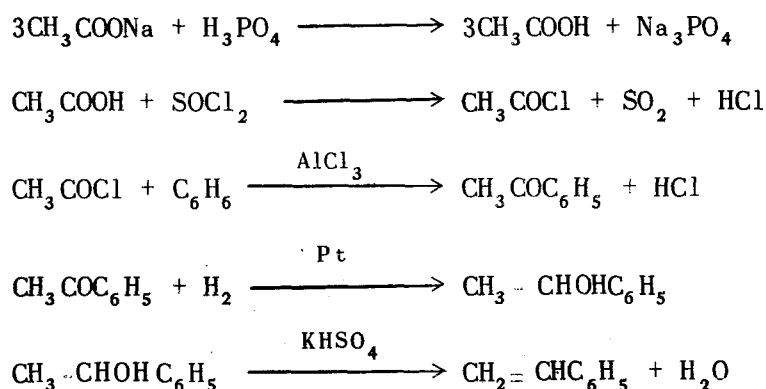


(15) J. R. Johnson and G. E. May, "2-Acethienone," *Organic Syntheses*, Collective Vol. II, ed. by A. H. Blatt, p. 8, Wiley, New York, 1943.

(16) J. C. Reid and M. Calvin, "Some New  $\beta$ -Diketones Containing the Trifluoromethyl Group," *J. Am. Chem. Soc.* 72, 2948 (1950).

In the case of each styrene, the reaction was studied in a manner analogous to that used by Stevens and Attree<sup>(17)</sup> who measured the isotope effect in the alkaline saponification of ethyl benzoate-7-C<sup>14</sup>. For each labeled styrene the bromination at -70°C was carried first to 10% completion, then to complete addition; the styrene dibromide was isolated for the 10% reaction and for the complete addition. The specific activity of the styrene dibromide obtained from 10% reaction was compared with the dibromide isolated after complete bromine addition. No isotope effect could be detected in the bromination of styrene- $\alpha$ -C<sup>14</sup> or styrene- $\beta$ -C<sup>14</sup>; for each labeled styrene the product isolated after 10% bromination had, within experimental error, the same specific activity as the product isolated after complete bromination.

The C<sup>14</sup>-labeled styrenes were prepared from the correspondingly labeled sodium acetates by the following series of reactions:



*Preparation of Styrene.* The preparation of styrene has been previously described.<sup>(18)</sup>

*Bromination of Styrene.* A three-necked 200-ml flask equipped with a stirrer, dropping funnel, and drying tube was placed in a freezing mixture of chloroform, carbon tetrachloride, and dry ice. A solution of 50 ml of dry chloroform, 50 ml of dry methylene chloride, and 3.0 g (29 mmoles, 2 to 3  $\mu\text{C}/\text{mmole}$ ) was added. The drying tube was replaced with a thermometer, and

(17) W. H. Stevens and R. W. Attree, "The Effect on Reaction Rates Caused by the Substitution of C<sup>14</sup> for C<sup>12</sup>. I. The Alkaline Hydrolysis of Carboxyl-Labeled Ethyl Benzoate," *Can. J. Res.* 27B, 807 (1949).

(18) L. A. Brooks, "Preparation of Substituted Styrenes," *J. Am. Chem. Soc.* 66, 1295 (1944).

after the temperature had reached  $-70^{\circ}\text{C}$  a solution of 0.46 g (2.9 mmoles) of bromine in 10 ml of chloroform was added in the dark over a period of 10 min. The reaction was then repeated using 1.00 g (0.00943 mmole, 2 to 3  $\mu\text{c}/\text{mmole}$ ) and 1.51 g (0.00943 mmole) of bromine.

Excess solvent and styrene were removed at reduced pressure, never permitting the temperature to rise above  $30^{\circ}\text{C}$ . Two 3-ml portions of 95% ethanol were added and then removed at reduced pressure to ensure complete removal of styrene. The white crystalline dibromide was recrystallized twice from 95% ethanol. To avoid volatilization the product was dried at  $25^{\circ}\text{C}$  and 2 mm Hg in a vacuum desiccator over  $\text{P}_2\text{O}_5$ .

*Test for Exchange of Bromine Between Labeled and Unlabeled Styrene.* In order to prove that the failure to detect an isotope effect was not caused by a rapid exchange of bromine between the styrene dibromide formed and the unreacted styrene, the following experiment was carried out: A sample of unlabeled styrene dibromide (1.00 g, 3.8 mmoles) was dissolved in a solution of labeled styrene (500 mg, 4.8 mmoles, 5  $\mu\text{c}/\text{mmole}$ ) in 50 ml of methylene chloride and 50 ml of dry chloroform. The solution was carried through the same operations as those used in the recovery of styrene dibromide from excess styrene and solvent in the earlier experiments, i.e., the excess styrene and solvent were removed under vacuum at room temperature during a period of 50 min. Since the styrene dibromide recovered was completely inactive, the possibility was ruled out that an isotope effect might be present but masked by a bromine exchange.

**TABLE 3.2**  
**Specific Activities of Styrene Dibromides**

REACTION	SPECIFIC ACTIVITY ( $\mu\text{c}/\text{mmole}$ )	
	$\alpha$ -LABELED	$\beta$ -LABELED
10% bromination	2.415	3.27
	2.428	3.28
	2.420	
	2.36	
	2.406 (avg)	3.275 (avg.)
Complete bromination	2.45	3.33
	2.43	3.24
	2.40	3.25
	2.426 (avg)	3.273 (avg.)

**The Dehydration of Formic-C<sup>14</sup> Acid** (G. A. Ropp, A. J. Weinberger, and O. K. Neville). By refinements of methods previously described<sup>(19)</sup> mean values of the isotope effect,  $100(k_{12} - k_{14})/k_{12}$ , and their 95% confidence intervals at four temperatures were obtained for the isotope effect in the dehydration of formic acid to carbon monoxide in sulfuric acid solution. These values are reported in Table 3.3. Table 3.4 gives estimates of the slopes and their variances obtained from the 26 plots by the method<sup>(20)</sup> of least squares. From the values of  $100(k_{12} - k_{14})/k_{12}$  at 0 and 24.75°C was calculated a value of  $\Delta E$ , the difference in the Arrhenius activation energies for C<sup>12</sup> and C<sup>14</sup> formic acid:

$$\Delta E = 2.30 \times 1.987 \frac{298.0 \times 273.2}{24.75} \log \frac{0.9141}{0.8889} = 183 \pm 18 \text{ calories per mole}$$

Figure 3.2 shows two sample plots, of logarithm of specific activity vs. time and logarithm of number of millimoles of unreacted formic acid vs. time.

**TABLE 3.3**

**Values of the Rate Constant and the Isotope Effect at Different Temperatures**

RUN NO.	TEMPERATURE (°C)	$k_{12}$ (min <sup>-1</sup> × 10 <sup>4</sup> )	$k_{12} - k_{14}$ (min <sup>-1</sup> × 10 <sup>4</sup> )	$100(k_{12} - k_{14})/k_{12}$	$100k_{14}/k_{12}$
1	0.00 ± 0.05	34.45	4.247	12.32	87.68
2		34.29	3.544	10.34	89.66
3		34.50	4.058	11.76	88.24
4		33.58	3.556	10.59	89.41
5		33.99	3.501	10.30	89.70
6		34.98	3.915	11.19	88.81
7		33.99	3.692	10.86	89.14
8		34.59	3.996	11.55	88.45
Mean		34.30 ± 0.11		11.11 ± 0.20	88.89 ± 0.20
9	14.75 ± 0.05	216	19.2	8.88	91.12
10		221	21.1	9.54	90.46
Mean		219		9.21	90.79
11	18.75 ± 0.05	380	34.6	9.11	90.89
12		359	31.4	8.75	91.25
Mean		370		8.93	91.07
13		24.75 ± 0.05	755.6	65.68	8.69
14	733.0		63.79	8.70	91.30
15	730.3		60.85	8.33	91.67
16	764.1		58.82	7.70	92.30
17	763.9		72.77	9.53	90.47
Mean		749.3 ± 4.9		8.59 ± 0.15	91.41 ± 0.15

(19) G. A. Ropp, A. J. Weinberger, and O. K. Neville, "Isotope Effect in Decomposition of Formic Acid-C<sup>14</sup>," *Chemistry Division Quarterly Progress Report for Period Ending December 31, 1950*, ORNL-1036, p. 47 (to be issued); G. A. Ropp and A. J. Weinberger, "The Isotope Effect in the Decomposition of Formic Acid-C<sup>14</sup>," *Chemistry Division Quarterly Progress Report for Period Ending September 30, 1950*, ORNL-870, p. 64 (Mar. 1, 1951).

(20) The curve-fitting operations and the statistical evaluation of the experiments were performed by Dr. A. W. Kimball of the Oak Ridge National Laboratory Mathematics Panel.



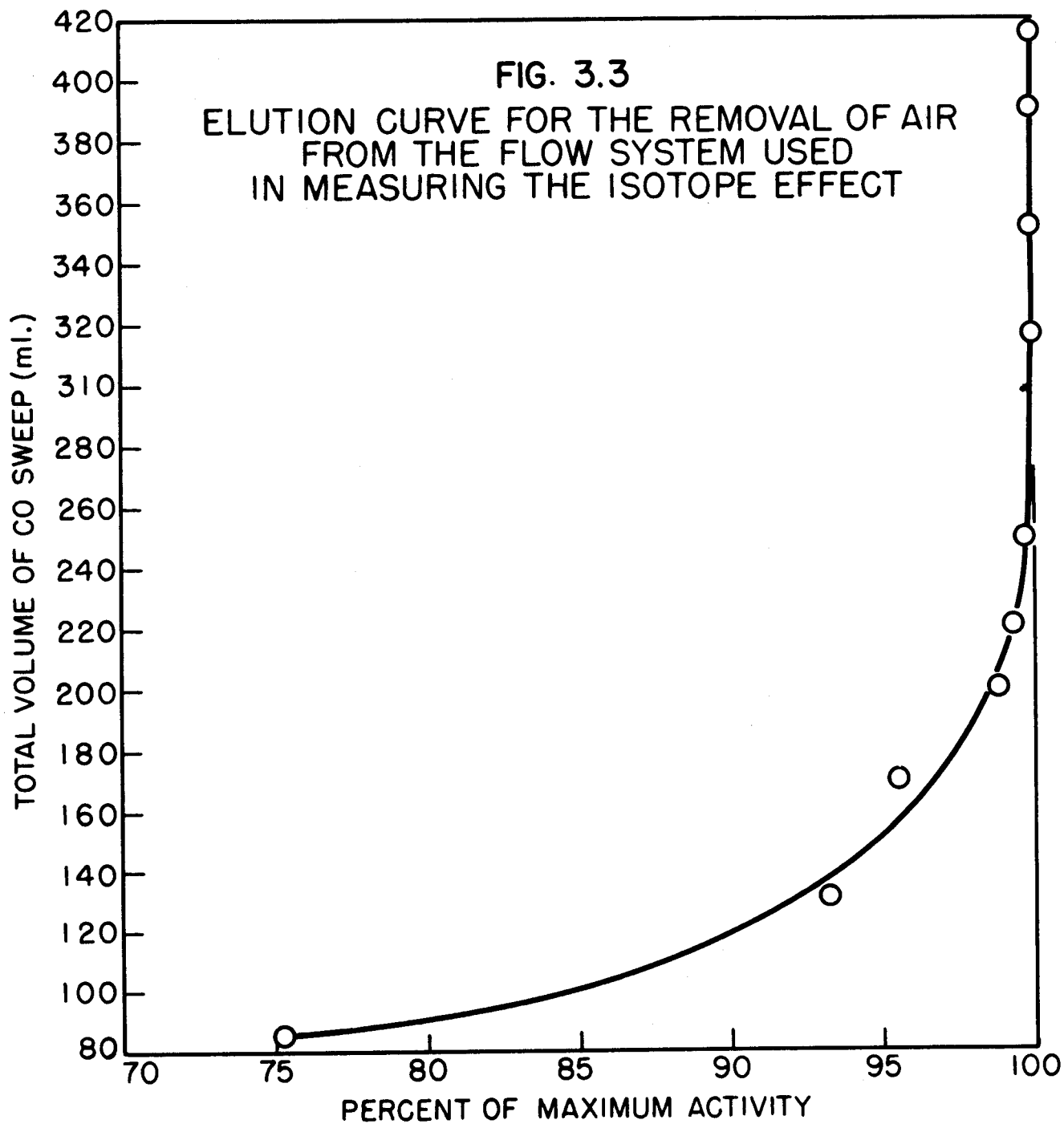
TABLE 3. 4

Estimates of Slopes and Their Variances in the Calculation of  
Values of  $k_{12}$  and of  $100(k_{12} - k_{14})/k_{12}$

RUN NO.	TEMPERATURE (°C)	KINETIC PLOT OF $\log C^{12}$ vs. $t$		DETERMINATION OF $k_{12} - k_{14}$ , $\log S$ vs. $t$	
		SLOPE	SLOPE VARIANCE $\times 10^{10}$	SLOPE	SLOPE VARIANCE $\times 10^{10}$
1	0.00 ± 0.05	-0.001496	0.4089	0.001844	0.1452
2		-0.001489	0.1947	0.001539	0.3492
3		-0.001498	1.2934	0.001762	0.2392
4		-0.001458	0.0638	0.001544	0.3158
5		-0.001476	0.2684	0.001520	0.1025
6		-0.001519	0.1081	0.001700	0.0984
7		-0.001476	0.9477	0.001603	0.1405
8		-0.001502	0.1114	0.001735	0.0252
13	24.75 ± 0.05	-0.03281	404.7	0.002852	46.21
14		-0.03183	310.1	0.002770	11.59
15		-0.03171	920.6	0.002642	32.17
16		-0.03318	816.7	0.002554	20.74
17		-0.03317	331.8	0.003160	39.51

*Supplementary Experiments.* For the reasons indicated in the following discussion, certain supplementary experiments were necessary.

1. At the beginning of each run the flow system contained air in its 60 ml dead volume. During each run this air was slowly swept from the system by the carbon monoxide produced from formic acid. Proof that all the air was swept out with the first 30% of the carbon monoxide produced in the dehydration was necessary in order that the true specific activity of the carbon monoxide subsequently produced could be measured. This proof was obtained by setting up the flow system in the usual way. No formic acid was used; instead, labeled carbon monoxide was bubbled through the sulfuric acid and out through the chamber while the activity level in the chamber was recorded. As the elution curve in Fig. 3.3 shows, the air was completely removed when 300 ml of carbon monoxide (equivalent to 30% of the volume of carbon monoxide produced in a run) had been bubbled through the sulfuric acid.
2. In each run the percent oxygen in the gas leaving the ion chamber was measured by the Pauling oxygen meter and plotted against time. The resulting air-elution curves confirmed the conclusion that the carbon monoxide was essentially free of air at the time when 30% of the total carbon monoxide had been collected.
3. The possibility was considered that the observed temperature coefficient of the isotope effect might be due to the different degrees of internal mixing as a result of the different reaction rates and consequently different gas flow rates at the four temperatures. It was thought that different degrees of mixing of the carbon monoxide increments with previously formed increments might alter the slope, the value of  $k_{12} - k_{14}$ , and hence the apparent isotope effect. To rule out this possibility two experiments were run under conditions which would alter the internal mixing or reduce its influence on the isotope effect. The first experiment consisted in reducing the dead space in the flow system by 90% (Table 3.3, Run No. 7; Fig. 3.2). This reduction of volume in order to reduce the extent of internal mixing, was effected by changing the shape of the reaction vessel and by removing the Drierite-Ascarite trap, the heat exchanger, and the manometer. The second experiment was designed to reduce the effect of internal mixing on the isotope effect. It consisted of a run (Table 3.3, Run No. 8; Fig. 3.2) made in the same manner as Run No. 7, except that, before the run, the air in the dead space was replaced by carbon monoxide of a higher specific activity than that of the formic acid used. As shown in Table 3.3, the values of the isotope effect were not significantly different from those calculated for other runs at the same temperature. It was therefore concluded that the variation of the degree of internal mixing with the reaction temperature in the flow system did not cause the apparent temperature coefficient of the isotope effect.



4. A final experiment was run to prove that the observed temperature coefficient of the isotope effect could not result from the difference in activity values recorded by the instruments caused solely by the difference in velocity of the gas through the flow chamber at the four temperatures. A sample of carbon- $C^{14}$  monoxide was passed through the chamber at several widely different rates. The recorded activity (millivolts) was not appreciably affected by the velocity of flow through the chamber when the pressure and temperature of the gas were held constant.

**The Absorption of  $C^{14}O_2$  in Alkaline Media** (A. J. Weinberger and G. A. Ropp). Attempts to find isotope effects in the absorption of tracer-labeled carbon- $C^{14}$  dioxide in various solutions have been made by passing the gas through a solution of dilute sodium hydroxide in one experiment and through benzylamine<sup>(21)</sup> in dibenzyl ether in a second case in such a manner as to give partial absorption of the gas. In the case of each solution the specific activity of the gas was determined before absorption by measurement in a 10-ml ion chamber at a known temperature and pressure. The gas was then bubbled through the absorber until 10 to 20% absorption had occurred; the specific activity of the unabsorbed gas was then determined in the flow chamber at the original temperature and pressure. No isotope effect was noted in the absorption of  $C^{14}O_2$  in benzylamine solution or in sodium hydroxide solution; in each case the Brown recorder reading for a chamberful of carbon dioxide was the same before and after partial absorption when the volume of the system was adjusted to keep the temperature and pressure of the gas in the chamber the same.

#### MECHANISM STUDIES OF ORGANIC REACTIONS

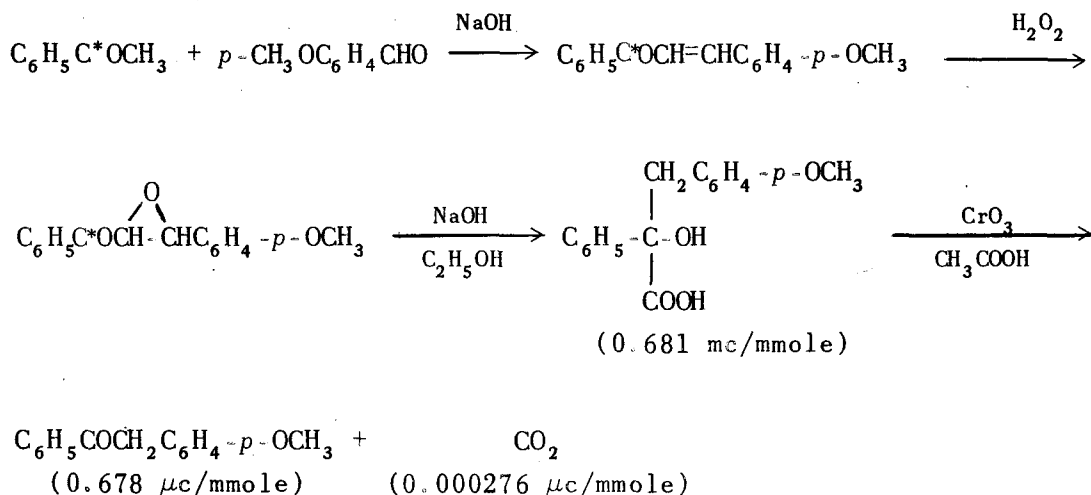
**$C^{14}$ -Tracer Studies in the Rearrangement of Unsymmetrical  $\alpha$ -Diketones** (E. C. Hendley, \* O. K. Neville, and C. J. Collins). The compound *p*-methoxybenzylideneacetophenone oxide, labeled with  $C^{14}$  in the carboxyl group, has been shown to rearrange in alkaline solution to phenyl-*p*-methoxybenzylglycolic acid. This acid contains no radioactivity in the carboxyl group, showing that

(21) H. B. Wright and M. B. Moore, "Reactions of Alkyl Amines with Carbon Dioxide," *J. Am. Chem. Soc.* 70, 3865 (1948).

\*Research participant in the program sponsored jointly by ORNL and ORINS; home address, Mississippi State College.

no migration of the phenyl group occurred. The rearrangement of this compound is thus demonstrated to be analogous to that of the unsubstituted benzylideneacetophenone oxide previously studied.<sup>(22)</sup>

The reactions and the radioactivities per millimole of the appropriate compounds are shown in the reaction scheme below. The laboratory methods have been described in detail previously.<sup>(23)</sup>



**Isotope Exchange Reactions Involving the Carbon-Carbon Bond** (Carl Douglass and O. K. Neville). As the initial part of a program on the use of  $\text{C}^{14}$  in the study of organic exchange reactions involving carbon-carbon bonds, the reversibility of the Friedel-Crafts acylation reaction is being studied.

The reversibility of the Friedel-Crafts alkylation reaction is well known.<sup>(24-26)</sup> In the presence of aluminum chloride and other similar acid catalysts, alkylated aromatic derivatives undergo reactions involving the loss, migration, or transfer of their alkyl groups. Similar transformations involving acylated aromatic compounds are rare. In the present work an attempt has been made to promote an exchange between acetyl- $1\text{-C}^{14}$  chloride and acetophenone in the presence of Friedel-Crafts catalysts:

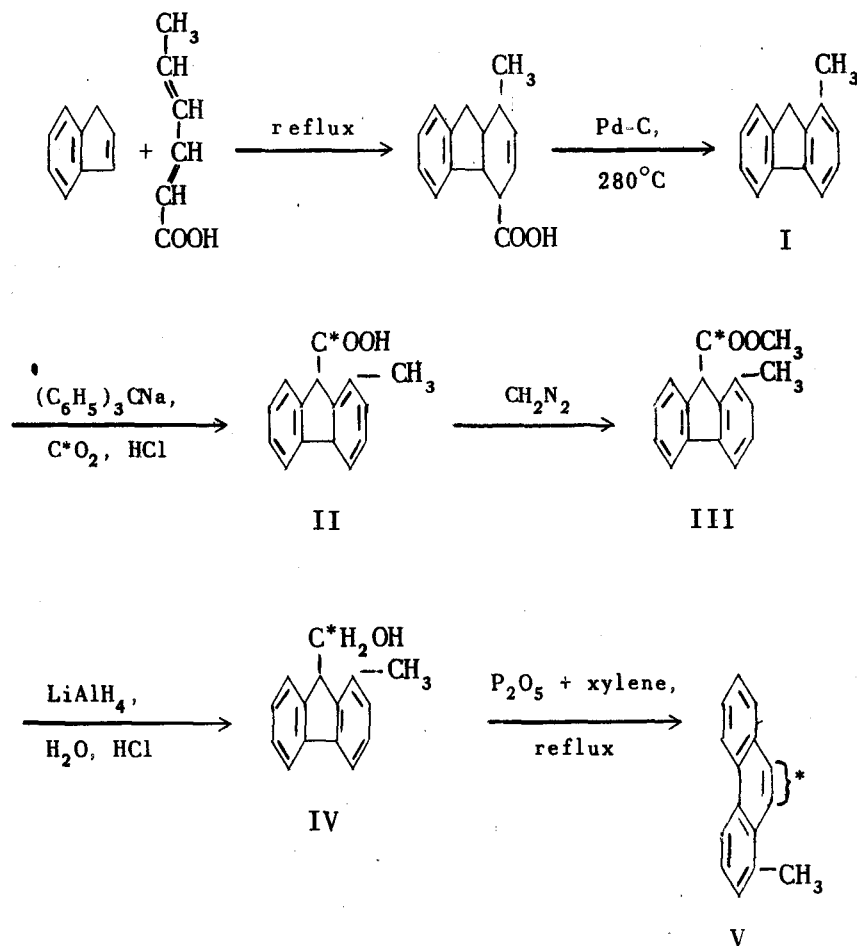
- (22) C. J. Collins and O. K. Neville, " $\text{C}^{14}$ -Tracer Studies in the Rearrangement of Unsymmetrical  $\alpha$ -Diketones. II. Benzylideneacetophenone Oxide," *J. Am. Chem. Soc.*, in press.
- (23) C. J. Collins *et al.*, "The Study of Reaction Mechanisms with  $\text{C}^{14}$ ," *Report of the Chemistry Division for the Months March, April, May, 1948*, ORNL-65; p. 85 (July 9, 1948).
- (24) E. Boedtker, "Sur quelques d $\acute{e}$ riv $\acute{e}$ s du butylbenz $\acute{e}$ ne tertiaire," *Bull. soc. chim. France* (3) 35, p. 825, esp. p. 834 (1906).
- (25) E. Boedtker and O. M. Halse, "Quelques observations sur la r $\acute{e}$ action Friedel-Crafts," *Bull. soc. chim. France* (4) 19, p. 444, esp. p. 447 (1916).
- (26) C. F. Woodward, G. T. Borchardt, and R. C. Fuson, "The Reversibility of the Friedel-Crafts Condensation. The Benzal- and Dibenzal-acetones," *J. Am. Chem. Soc.* 56, 2103 (1934).



Under a variety of laboratory conditions, exchange between acetophenone and acetyl chloride in the presence of aluminum chloride or aluminum bromide has been shown not to occur. Similar research is continuing with other aromatic derivatives.

**Synthesis and Structure Determination of C<sup>14</sup>-Labeled 1-Methylphenanthrene** (B. M. Benjamin and C. J. Collins). The syntheses of phenanthrene-9-C<sup>14</sup>,<sup>(13)</sup> benz(a)anthracene-5,6-C<sub>1</sub><sup>14</sup>,<sup>(14)</sup> and chrysene-5,6-C<sub>1</sub><sup>14</sup><sup>(27)</sup> have been described previously. The method used in these preparations has now been applied to the synthesis of C<sup>14</sup>-labeled 1-methylphenanthrene. Approximately 10 mc of this hydrocarbon has been produced.

1-Methylfluorene (I) was prepared by the method of Deno,<sup>(28)</sup> and converted to 1-methylphenanthrene (V) labeled in the 9 or 10 position by the procedure outlined in the following flowsheet.



(27) C. J. Collins and G. M. Toffel, "Chrysene-5,6-(?)-C<sup>14</sup>," *Chemistry Division Quarterly Progress Report for Period Ending March 31, 1950. Part I. Chemical Research*, ORNL-685, p. 85 (June 16, 1950).

(28) N. C. Deno, "The Diels-Alder Reaction with  $\alpha,\beta,\gamma,\delta$ -Unsaturated Acids," *J. Am. Chem. Soc.* 72, 4057 (1950).

**Model Runs with Nonradioactive Materials.** *1-Methyl-9-fluorene-carboxylic Acid (II).* By the procedure previously outlined<sup>(13)</sup> 1.10 g of 1-methylfluorene (I) was carbonated with 28 ml of 0.20 N ether solution of triphenylmethylsodium and CO<sub>2</sub> from 1.2238 g of reagent-grade BaCO<sub>3</sub>. A yield of 1.161 g of 1-methyl-9-fluorene-carboxylic acid (93.3%) was obtained, m.p. 221 to 225°C. Recrystallization from benzene gave white needles, m.p. 222 to 225°C.

*Methyl 1-Methyl-9-fluorene-carboxylate (III).* To 1.08 g of 1-methyl-9-fluorene-carboxylic acid in 25 ml of ether at 5 to 10°C was added an ether solution of diazomethane until the yellow color persisted. The solution was warmed to room temperature. When the ether was removed and the compound dried, 1.14 g of solid remained in the flask. Recrystallization from benzene-petroleum gave crystals melting at 95.5 to 97°C. A second recrystallization did not change the melting point.

The acid was not converted to the ester by methanol and a catalytic amount of acetyl chloride.

*1-Methyl-9-fluorene-methanol (IV).* The ester, 0.967 g, was reduced in dry ether by adding an excess of 0.15 N ether solution of lithium aluminum hydride. The yield of unpurified 1-methyl-9-fluorene-methanol was 0.865 g, m.p. 77 to 80°C. The melting point was not raised by adsorption of the alcohol from anhydrous benzene on alumina and recovering with absolute methanol. One recrystallization from benzene-petroleum ether raised the melting point to 83 to 87°C, and this was not improved by a second recrystallization.

*1-Methylphenanthrene (V).* A solution of 0.567 g of 1-methyl-9-fluorene-methanol in 20 ml of dry xylene was treated with 4.0 g of phosphorus pentoxide and refluxed for 30 min. A yellow solid weighing 0.530 g was recovered which did not lose color upon recrystallization from methanol. When a benzene solution of the solid was passed through an alumina column a greenish color remained at the top of the column but the effluent liquid was yellow. A fresh column removed no more color. An ethanol solution of the compound was decolorized with Norit. Addition of water to the hot alcoholic solution precipitated 0.288 g of colorless plates, m.p. 119.5 to 120°C. An additional 0.04 g was recovered from the solvent. The yield of pure 1-methylphenanthrene from 1-methyl-9-fluorene-methanol was 64%.

## PUBLICATIONS

During the past quarter the Radio-organic Group has published the following papers in the open literature:

1. J. G. Burr, Jr., "The Reaction of 9-Formylfluorene with Formaldehyde," *J. Am. Chem. Soc.* **73**, 823 (1951).
2. R. H. Mayor and C. J. Collins, "The Use of Double Dilution for the Simultaneous Determination of Yield and Activity of Radioactive Compounds," *J. Am. Chem. Soc.* **73**, 471 (1951).
3. C. J. Collins, "Carbon-14 Synthetic Studies. 2-Methyl-1,4-naphthoquinone-8-C<sup>14</sup>," *J. Am. Chem. Soc.* **73**, 1038 (1951).

## 4. CHEMISTRY OF SEPARATIONS PROCESSES

### VOLATILITY STUDIES

**Removal of Pa<sup>233</sup> from Neutron-Irradiated ThF<sub>4</sub>** (P. A. Agron). Fluorine extraction experiments at Brookhaven<sup>(1)</sup> indicate that the rate of removal of Pa<sup>233</sup> from a porous thorium fluoride lattice falls off markedly in a relatively short time. The controlling step here appears to be the rate of movement of Pa<sup>233</sup> within the crystallites to the surface of the particles. To obtain reasonable values for the protactinium diffusion rate high temperatures are required which lead to sintering with a resulting increase in holdup time.<sup>(1)</sup> A simple chemical regeneration treatment which brings about a breakdown into smaller particles would be desirable, since the shorter mean distance of diffusion involved should lead to a faster rate of removal. For example, it was hoped that compounds might be formed between ThF<sub>4</sub> and one of the phosphorus fluorides which could be converted back to ThF<sub>4</sub> by lowering the pressure of the gas phase.

In attempts to form complexes of the phosphorus fluoride gases with ThF<sub>4</sub><sup>(2,3)</sup> several indications of reaction were observed. Color changes were most marked while the samples were under high pressures of these gases. Electron micrographs of the treated samples indicated an increase in fine particles ranging from 0.02 to 0.05  $\mu$ .\* The extent of this breakdown appears to be most marked for the PF<sub>3</sub>(g) treatments. The mechanism by which this effect is brought about is not known at present. However, it appeared likely that the extent and effectiveness of these treatments could be tested directly on irradiated thorium fluoride.

Granular pieces of sintered ThF<sub>4</sub> obtained from F. T. Miles were exposed in the ORNL reactor at a flux of  $5 \times 10^{11}$  for 16 hr. This material had been previously heated at 750°C for 1000 hr in dilute F<sub>2</sub>, resulting in a material which had a surface area of 0.077 square meters per gram. The irradiated material was divided into two portions for the subsequent treatments listed in Tables 4.1 and 4.2.

- (1) "Continuous Processing Breeder Blanket Studies," *Classified Progress Report of the Reactor Science and Engineering Department, January 1 - March 31, 1950, ENL-52* (no date).
- (2) P. A. Agron and E. G. Bohlmann, "Volatility," *Chemistry Division Quarterly Progress Report for Period Ending December 31, 1950, ORNL-1036*, p. 55 (to be issued).
- (3) P. A. Agron and E. G. Bohlmann, "Breeder Blanket Studies," *Chemistry Division Quarterly Progress Report for Period Ending September 30, 1950, ORNL-870*, p. 73 (Mar. 1, 1951).

\*Micro-scale surface-area measurements were not effective for this determination because of the continual evolution of traces of gas.

TABLE 4.1

## Preliminary Run on Sample A

GAS	MAXIMUM PRESSURE (psi absolute)	FURNACE TEMPERATURE (°C)	TIME (hr)
PF <sub>5</sub> + F <sub>2</sub> *	65	350-400	2-1/4
PF <sub>3</sub>	100	400	2
PF <sub>5</sub> + F <sub>2</sub> *	102	400-450	3/4
	108	525	1
	100	575	2

\*Partial pressure of F<sub>2</sub>(g) was about 5 psi absolute.

*Apparatus.* The experiments were carried out in a 1-in.-diameter monel tube. A 12-in. sleeve of 5-mil nickel foil was inserted, and a boat containing the irradiated sample was moved to the center of the tube. A 4-in. furnace was used to heat the central section of the reaction tube. At a furnace temperature of 600°C, the temperature of the portions of the reaction tube just beyond the furnace was 350°C; at the positions corresponding to the ends of the nickel foil, temperatures of the order of 100°C were obtained. Gauges and U traps were connected to each end of the reactor, and the gases employed were moved back and forth across the heated sample.

At the end of a run the foil was removed from the furnace and unfolded, and the boat containing the active sample was removed. The foil was then cut into 1-in. strips and the activity was counted in a crystal counter. Standard samples were used for calibrating the crystal counter against a 4π ionization counter for this activity. The activity of the material in the boat was checked periodically on the 4π geometry counter.

No activity was observed on the foil strips within the furnace region. The activity also fell off rapidly in the region of 100°C. Thus the major portion of the protactinium was deposited on the foil in the region between 350 and 100°C. The activity found in one of the traps was a negligible fraction, 0.004%, of the activity in the sample. The activity material balance

TABLE 4.2

Removal of Pa<sup>233</sup> from ThF<sub>4</sub> with Phosphorus Fluoride Regeneration Treatments

SAMPLE	RUN NO.	GAS	MAXIMUM PRESSURE (psi absolute)	FURNACE TEMPERATURE (°C)	TIME (hr)	FRACTION OF ACTIVITY REMOVED, <i>f</i>
A	A-1*	PF <sub>5</sub> + F <sub>2</sub> **	106 - 113	600	4	0.009
	A-2*	F <sub>2</sub>	15	600	3½	0.058
	A-3	F <sub>2</sub>	15	600	3½	0.011
	A-4	PF <sub>5</sub>	87	400	3	
		PF <sub>5</sub>	87	375	4	
		PF <sub>5</sub> + F <sub>2</sub> **	109	600	4	0.0017
B	B-1	F <sub>2</sub>	25	600	4	0.0024
	B-2	F <sub>2</sub>	30	600	4	0.0002
	B-3	PF <sub>5</sub>		400		
		PF <sub>5</sub> + F <sub>2</sub> **	100	600	4	0.0001
	B-4	PF <sub>3</sub>	60	400	2	
		F <sub>2</sub>	30	600	4	0.0011
	B-5	F <sub>2</sub>	40	600	4	0.0001
	B-6	PF <sub>3</sub>	325	350	4	
		F <sub>2</sub>	48	600	4	0.0004
	B-7	F <sub>2</sub>	40	650	4	0.00075

\*In these runs a platinum boat was used. The boat was almost completely burned up in the A-2 run. In the following treatments a nickel boat was used.

\*\*Partial pressure of F<sub>2</sub> was approximately 10 psi absolute.

for these runs indicated that no appreciable amount of protactinium was pumped out of the system.

*Experiments.* The first irradiated sample, designated as "A," was given a series of preliminary treatments with  $\text{PF}_3$ ,  $\text{PF}_5$ , and  $\text{F}_2$  gases under a range of pressures and temperatures. Unsuccessful attempts were made with an external Geiger counting probe to follow the movement of activity out of the furnace. The conditions used for these treatments are given in Table 4.1.

Following the treatments given in Table 4.1, sample A was subjected to a sequence of runs, as indicated in Table 4.2. It was assumed that the previous treatments (Table 4.1) at the lower temperatures would not have removed any appreciable quantity of activity from the sample but might have caused reactions which it was hoped would subsequently increase the removal of protactinium. The interpretation of the activity fractions removed in runs A-1 and A-2 is at present uncertain. In run A-2 the platinum boat was almost completely converted to  $\text{PtF}_4$ . The relative importance of the heat of reaction developed by the conversion of platinum to  $\text{PtF}_4$ , the carrying power of the  $\text{PtF}_4$  vapor, and the pretreatments given in Table 4.1 is not known. Some of these variables were removed in runs A-3\* and A-4 in which the platinum was replaced by a nickel boat. Run A-4 indicates that the  $\text{PF}_5$  pretreatment is not effective at that stage in regenerating the rate of protactinium removal.

In the sample B series preliminary extractions with  $\text{F}_2$  were used in runs B-1 and B-2. It is observed that the fractions of activity removed here are apparently smaller than those removed in treatments A-3 and A-4 of the A series. The sharp decrease in rate of removal in run B-2 indicates that most of the easily removable "surface" protactinium had been previously volatilized. Run B-3 again indicates the ineffectiveness of the  $\text{PF}_5$  treatment in accelerating the removal of protactinium. The regeneration indicated by the  $\text{PF}_3$  treatment in run B-4 shows a substantial increase. However, this regeneration is of short duration, as indicated by the return to the lower rate in the next extraction. It also appears that the second exposure to  $\text{PF}_3$  is not so effective as the first. A final extraction at  $650^\circ\text{C}$  is indicated in run B-7.

*Discussion.* The rates of removal of protactinium were also followed on two pelleted samples of similar material ( $\sigma = 0.077$  square meters per gram) at Brookhaven.<sup>(4,5)</sup> One sample was first irradiated and then treated with

(4) "Reactor Chemistry; Thorium Fluoride Breeder Blanket," *Classified Progress Report of the Reactor Science and Engineering Department, July 1 - September 30, 1950*, ENL-88 (no date).

(5) Private communication, April 13, 1951.

PF<sub>3</sub>(g); the second sample was given similar treatments but in the reverse order. The first experiment showed an accelerated removal of 5% of the protactinium activity for a short initial period whereas the rate in the second, i e., much smaller removal, corresponded to that which would normally be expected for particles of this size.

As indicated in BNL-52, the mean holdup time,  $\tau$ , may be calculated from the equation

$$\tau = \frac{3}{5(\rho\sigma)^2 D} = \frac{3}{5[d(\rho\sigma)^2 Dt] / dt} = \frac{0.6}{(dy/dt)} \quad (1)$$

where

$t$  = time

$\rho$  = density of particles

$\sigma$  = total surface area

$D$  = diffusion constant

$y = (\rho\sigma)^2 Dt$

For small fractions of activity removed, it can be shown that, where  $f$  = fraction of protactinium removed,

$$y = 0.785 f^2 \quad (2)$$

The  $\tau$  values for the runs on sample B, calculated from Eqs. (1) and (2), are listed in Table 4.3. Approximate values were obtained using  $\Delta y/\Delta t$  in Eq. (1). On substituting the correct values for  $\rho$  and  $\sigma$  in Eq. (1), assuming that  $D_{600^\circ\text{C}} = 10^{-17}$  cm<sup>2</sup>/sec, a theoretical value of  $4 \times 10^4$  days is obtained for  $\tau$ , which is in fair agreement with the values in Table 4.3.

TABLE 4.3

Mean Holdup Times for Sample B

RUN NO.	$f$	$y$	$\Delta y/\Delta t$	$\tau$ (days)
B-1	0.0024	$4.52 \times 10^{-6}$	$1.1 \times 10^{-6}$	$2.2 \times 10^4$
B-2	0.0026	5.30	$1.85 \times 10^{-7}$	$1.4 \times 10^5$
B-3	0.0027	5.72	$1.05 \times 10^{-7}$	$2.4 \times 10^5$
B-4	0.0038	$1.13 \times 10^{-5}$	$1.4 \times 10^{-6}$	$1.8 \times 10^4$
B-5	0.0039	1.19	$1.5 \times 10^{-7}$	$1.7 \times 10^5$
B-6	0.0043	1.45	$6.5 \times 10^{-7}$	$3.9 \times 10^4$

*Future Work.* A pellet of  $\text{ThF}_4$  on which extensive data have been collected was obtained from the Brookhaven group ( $\sigma = 0.48$  square meters per gram). This sample should serve as a better means for evaluating the effectiveness of any regeneration treatments studied here. A study of the relative effectiveness of  $\text{PF}_3(g)$  and  $\text{PF}_3(l)$  treatments on this material will be undertaken.

An attempt to get equilibrium dissociation pressures of  $\text{PF}_3(g)$  over high-surface-area  $\text{ThF}_4$  samples is planned. It is also planned to investigate whether  $\text{PtF}_4$  is a carrier for the protactinium activity.

### SOLVENT EXTRACTION

*Organic Chemistry of Solvents* (W. H. Baldwin and C. E. Higgins). Among the organic orthophosphates that have been tested for extracting uranium from aqueous solutions, tri-*n*-butyl phosphate was found to compare favorably with the others when considering the factors distribution ratio of uranium, separation of uranium from fission products, and solvent stability. Tri-*sec*-propyl phosphate, tri-*sec*-butyl phosphate, and dibutylphenyl phosphonate did, however, extract somewhat more uranium than did tri-*n*-butyl phosphate under a standard set of conditions.

The use of tri-*n*-butyl phosphate containing radioactive  $\text{P}^{32}$  has materially facilitated the analytical problems associated with the determination and estimation of TBP and the products from its decomposition. Further refinements in radiochemical analyses should increase the speed, sensitivity, and precision of these determinations.

The commercial TBP being tested was found to contain at least 98% normal butyl radicals.

*Structural Effects in Extractions by Organic Phosphates.* In previous<sup>(6)</sup> work relatively little difference was noted in the extent of extraction of uranium from 3 *M*  $\text{HNO}_3$  by various trialkyl phosphates. The results obtained using these solvents for extracting uranium and plutonium from aqueous mixtures of uranium(VI), plutonium(IV), and fission products are summarized in Table 4.4. The trialkyl phosphates of secondary, propyl and butyl alcohols are outstanding, the extraction coefficients for uranium and plutonium for these

(6) C. E. Higgins, J. M. Ruth, and W. H. Baldwin, "The Organic Chemistry of Solvents," ORNL-870, *op. cit.*, p. 76, esp. pp. 86-87.

TABLE 4.4

## Decontamination Tests with Trialkyl Phosphates

ALKYL GROUP	DISTRIBUTION RATIO, <sup>(a)</sup> ORGANIC/AQUEOUS		DECONTAMINATION FACTOR <sup>(b)</sup>	
	U(VI)	Pu(IV) <sup>(c)</sup>	BETA <sup>(d)</sup>	GAMMA <sup>(e)</sup>
Ethyl	5.1	1.2	1500	1800
	4.8	1.1	1600	1500
<i>n</i> -Propyl	7.5	1.7	1400	1300
	7.4	2.0	1400	1800
<i>sec</i> -Propyl	12.3	4.3	2900	2100
	12.6	3.5	2800	2600
<i>n</i> -Butyl	8.2	2.2	1300	1300
	8.0	2.2	1300	2100
	8.5	1.8	1700	2100
	8.5	2.1	1600	1500
<i>iso</i> -Butyl	8.12	2.1	2300	3500
	8.12	2.0	2400	1500
<i>sec</i> -Butyl	12.6	3.2	9300	
	12.6	4.3	9300	2100
<i>n</i> -Amyl	9.2	1.3	1300	600
	9.2	1.4	1200	500

(a) The distribution ratio is the ratio of the concentration in the organic phase to that in the aqueous phase. The aqueous phase is uranyl nitrate, 0.2 M; HNO<sub>3</sub>, 3 M; plutonium, 1.3 x 10<sup>5</sup> alpha c/min/ml; mixed fission products, 5 x 10<sup>6</sup> beta c/min/ml prepared from x-12 feed supplied by W. B. Lanham, Chemical Technology Division. The organic phase was 0.75 M trialkyl phosphate in CCl<sub>4</sub>. Equal volumes of the two phases were tumbled end-over-end at 25°C for 30 min and separated after centrifuging.

(b) The decontamination factor is the ratio of counts per minute per milliliter in aqueous feed to that in the organic extract.

(c) Counted at 52% geometry.

(d) Counted at 11% geometry.

(e) Measured in the high-pressure-argon ionization chamber.

solvents being higher than for other alkyl phosphates while the decontamination factors for beta and gamma activities are as high as or higher than those obtained with the other alkyl phosphates.

The trialkyl phosphates tested previously<sup>(6)</sup> were compared at lower acidity (0.6 M HNO<sub>3</sub>) and lower uranyl nitrate concentration (0.1 M). At 0.6 M HNO<sub>3</sub> a distribution ratio of about 1 was obtained with 0.75 M tri-*n*-butyl phosphate in carbon tetrachloride. These conditions greatly magnified the differences found earlier (see Table 4.5). The trialkyl phosphates of secondary propyl and butyl alcohols extracted more uranium than did the others. The presence of ether linkages in the chain reduced the amount of uranium extracted. However, with the compound in which a single phenyl group was attached directly from carbon to phosphorus and two butyl groups were attached from carbon to oxygen to phosphorus (i.e., dibutylphenyl phosphonate), more uranium was extracted than with tri-*n*-butyl phosphate (70% compared with 55%).

Very poor extraction was obtained with trichloroethyl phosphate, which removed only 5% of the uranium; triethyl phosphate extracted 38%. Dibutyl phosphoric acid extracted 98%; however, this solvent is not very useful in uranium processing when other factors are considered.

*Utilization of Labeled TBP.* The preparation of labeled tri-*n*-butyl phosphate<sup>(7)</sup> (specific activity about 1 mc per millimole) offers a means of analysis for TBP and for the fragments from its decomposition which is limited by the specific activity and the methods available for counting the P<sup>32</sup>. Two methods of counting were tried, one including hydrolysis to orthophosphoric acid and carrying by magnesium ammonium phosphate or ammonium phosphomolybdate and counting the precipitate, and the other involving direct counting of liquid samples.

1. Hydrolysis by HI and Precipitation. Liquid samples up to 1 ml in volume can be successfully hydrolyzed by 1 ml of 55% HI after the addition of unlabeled TBP to supply carrier phosphorus. Boiling under reflux for 1 hr caused complete hydrolysis (attempts to concentrate the TBP in the original sample by evaporation of the water resulted in significant loss of TBP; hence such a concentration step before hydrolysis does not appear to be feasible.

Kerosene solutions up to 0.1 ml can be successfully hydrolyzed in this manner also.

(7) W. H. Baldwin and C. E. Higgins, *The Preparation of Tri-*n*-butyl Phosphate P<sup>32</sup>*, ORNL-887 (Feb. 5, 1951).

TABLE 4.5

## Extraction of Uranium with Phosphorus Compounds

URANIUM EXTRACTED (%)			
R <sub>3</sub> PO			
R			
C <sub>2</sub> H <sub>5</sub> O	38		
<i>n</i> -C <sub>3</sub> H <sub>7</sub> O	54		
<i>sec</i> -C <sub>3</sub> H <sub>7</sub> O	68		
<i>n</i> -C <sub>4</sub> H <sub>9</sub> O	55, 53		
<i>iso</i> -C <sub>4</sub> H <sub>9</sub> O	55		
<i>sec</i> -C <sub>4</sub> H <sub>9</sub> O	72		
<i>n</i> -C <sub>5</sub> H <sub>11</sub> O	56		
<i>n</i> -C <sub>4</sub> H <sub>9</sub> OC <sub>2</sub> H <sub>4</sub> O	23		
2-C <sub>2</sub> H <sub>5</sub> - <i>n</i> -C <sub>4</sub> H <sub>8</sub> OC <sub>2</sub> H <sub>4</sub> O	33		
(R)(R')(R'') PO			
R	R'	R''	
<i>n</i> -C <sub>4</sub> H <sub>9</sub> O	<i>n</i> -C <sub>4</sub> H <sub>9</sub> O	<i>n</i> -C <sub>4</sub> H <sub>9</sub> O	57
<i>n</i> -C <sub>4</sub> H <sub>9</sub> O	C <sub>6</sub> H <sub>5</sub> O	C <sub>6</sub> H <sub>5</sub> O	4
C <sub>6</sub> H <sub>5</sub> O	C <sub>6</sub> H <sub>5</sub> O	C <sub>6</sub> H <sub>5</sub> O	0.004
<i>n</i> -C <sub>4</sub> H <sub>9</sub> O	C <sub>8</sub> H <sub>17</sub> O	C <sub>6</sub> H <sub>5</sub> O	11
C <sub>8</sub> H <sub>17</sub> O	C <sub>8</sub> H <sub>17</sub> O	C <sub>6</sub> H <sub>5</sub> O	11
C <sub>8</sub> H <sub>17</sub> O	C <sub>6</sub> H <sub>5</sub> O	C <sub>6</sub> H <sub>5</sub> O	0.3
ClCH <sub>2</sub> CH <sub>2</sub> O	ClCH <sub>2</sub> CH <sub>2</sub> O	ClCH <sub>2</sub> CH <sub>2</sub> O	5
<i>n</i> -C <sub>4</sub> H <sub>9</sub> O	<i>n</i> -C <sub>4</sub> H <sub>9</sub> O	C <sub>6</sub> H <sub>5</sub>	70
<i>n</i> -C <sub>4</sub> H <sub>9</sub> O	<i>n</i> -C <sub>4</sub> H <sub>9</sub> O	HO	98

The aqueous phase was 0.1 M uranyl nitrate plus 0.6 M HNO<sub>3</sub>. The organic phase was 0.75 M phosphorus compound in CCl<sub>4</sub>. Equal volumes of the two phases were tumbled end-over-end at 25°C for 30 min. and separated after centrifuging.

It has been the practice, before precipitation, to distill off the organic solvents and the butyl iodide formed during the reaction.

After the hydrolysis carrier phosphorus equivalent to 20 to 30 mg of  $\text{MgNH}_4\text{PO}_4 \cdot 6\text{H}_2\text{O}$  per square centimeter was added to carry the  $\text{P}^{32}$ , and magnesium ammonium phosphate was precipitated from alkaline solution and counted. This method cannot be used with solutions containing uranyl nitrate since additional absorbing material would accompany the phosphate precipitate. When uranyl nitrate was present, ammonium phosphomolybdate was precipitated from acid solution and counted.

2. Direct Counting of Solutions. Solutions up to 1 ml in volume can be counted directly in the standard Geiger-Mueller counter fitted with a mica-end-window tube. However, continued use with aqueous solutions materially shortened the life of the tube. Preliminary tests, with glass-walled Geiger-Mueller tubes dipping into the solutions, have been encouraging.

*Distribution of Phosphate-Labeled TBP Between Kerosene and Water.* Kerosene containing 1.13 moles of phosphate-labeled TBP per liter was equilibrated with an equal volume of distilled water. The resulting aqueous phase contained about  $10^{-3}$  mole of labeled TBP per liter (observed distribution coefficients were 1100 to 1300 in favor of the organic phase). The concentration in the aqueous phase approached the solubility of TBP in water.

The aqueous phase, containing  $10^{-3}$  mole per liter, was equilibrated with a fresh portion of kerosene. Distribution coefficients of 50 to 68 in favor of the kerosene phase were observed. This indicates that TBP can be removed from aqueous process solutions by extraction with kerosene.

Labeled TBP is now being used to study the decomposition of this solvent by  $\text{HNO}_3$  and by solutions containing  $\text{HNO}_3$  and uranyl nitrate hexahydrate. Samples of labeled TBP have been furnished to members of the Chemical Technology Division for studying processing problems, including the estimation of the amount of TBP lost in aqueous solutions, the fate of TBP when these aqueous solutions are distilled, and the decomposition of TBP by various process solutions.

*Qualitative Identification of the Butyl Groups in TBP.* Tri-*n*-butyl phosphate is currently being obtained from the Commercial Solvents Corporation by the Chemical Technology Division for testing. It was considered desirable

to see what fraction of the R radicals in the compound  $R_3PO_4$  were not *n*-butyl, since other species might be expected to be less stable with respect to reaction with nitrate ion and  $HNO_3$  and might give undesirable products. Consequently, a sample of TBP was hydrolyzed to ROH and  $H_3PO_4$ , and the liberated alcohol was identified. It was found to be at least 98% normal butyl.

**Zirconium in Aqueous HCl-HClO<sub>4</sub>** (J. P. McBride and R. W. Stoughton). Studies on zirconium complexing by chloride have been continued using the TTA-benzene solvent extraction method. The experiments have been complicated by the fact that equilibrium has not been reached even after nine days of shaking for chloride concentrations of 0.1 to 1.0 M at an ionic strength ( $M HClO_4 + M NaClO_4 + M NaCl$ ) of 3.0 and a hydrogen ion concentration of 1.0 M. At zero chloride and at 2 M chloride, however, at the same ionic strength and acidity as above, the zirconium partition did not change appreciably after the first day. No grease was used on the glass stoppers of the extraction tubes.

Previous experiments, similar to those above but using silicone grease on the glass stoppers of the extraction tubes, have shown no changes in distribution after two days of equilibration.<sup>(8,9)</sup> Efforts to explain these discrepancies are continuing.

## ION EXCHANGE

**Ion-Exchange Kinetics** (B. A. Soldano and G. E. Boyd). During the past six months basic investigations have continued on the various processes which determine the rate of the achievement of equilibrium in ion-exchange resins. These studies will be described in report ORNL-908, to be issued shortly. The following abstract may serve to indicate the scope and some of the salient findings of this work:

The success with which measurements of self-diffusion have been employed in solid state physics has suggested that analogous measurements on ion exchangers might serve to elucidate the mechanism of ionic permeation in these materials. Radioactive isotopes of sodium, potassium, rubidium, cesium, zinc, strontium, yttrium, thorium, chlorine, bromine, iodine, sulfur, tungsten, and phosphorus were employed to follow ionic self-diffusion rates in several cation and anion exchangers based on a polystyrene-divinyl benzene copolymer

(8) J. P. McBride and R. W. Stoughton, "Zirconium in Aqueous HCl-HClO<sub>4</sub>," ORNL-870, *op. cit.*, p. 88.

(9) J. P. McBride and R. W. Stoughton, "Zirconium in Aqueous HCl-HClO<sub>4</sub>," *Chemistry Division Quarterly Progress Report for Period Ending December 31, 1950*, ORNL-1036, p. 21 (to be issued).

network. The influence of polymer cross-linking at constant ion-exchange capacity and of capacity at constant cross-linking were determined. The effect of varying ionic size, holding charge constant, was also examined. The apparent diffusion coefficients observed were invariably found considerably smaller than for the same ions in water.

A pronounced dependence of diffusion rate on ionic charge was revealed. Coefficients decreasing from  $10^{-7}$  for singly charged down to  $10^{-11}$   $\text{cm}^2/\text{sec}$  for quadruply charged ions were observed. Self-diffusion rates also diminished 100- to 1000-fold with increasing polymer cross-linking from a nominal 1 to 24% divinyl benzene content. Lowering of the exchange capacity, keeping the cross-linking constant, at first served to increase the self-diffusion until a critical capacity was reached, after which a dramatic slowing down occurred. Measurements of the temperature dependence of self-diffusion in the interval 0 to  $60^\circ\text{C}$  were performed. Activation energies varying from 4 to 11 kcal/mole were found which increased with increase in cross-linking and ionic charge.

An interpretation based on the idea that the exchanger is a relatively concentrated homogeneous solution in which the diffusion rate is governed by the work to form a "hole" plus the work to separate "ion pairs" will be given. In addition, evidence for the presence of steric or entropy of activation effects will be indicated.

**Ion-Exchange Separations** (R. W. Atteberry and G. E. Boyd). A number of new separations of elements either among the uranium fission products or of elements outside of the heavy element range which were of radiochemical interest have been achieved since our last report.<sup>(10)</sup> Some of these, including halide separations by both frontal and elution analysis, separation of manganese, technetium, and rhenium by elution with nitrate ion, separation of molybdenum and technetium, of arsenic and antimony, of selenium and tellurium, of manganese, iron, cobalt, nickel, copper, and zinc, and of zinc and cadmium were reported at the 118th Meeting of the American Chemical Society in Chicago, September 4-8, 1950. Since that time a very much improved separation of Tc(VII) and Re(VII) by elution with alkaline perchlorate solutions has been devised, and rapid and efficient separations of tin and indium and of cadmium and indium have been attained. Attempts to separate the fission product transition triad ruthenium, rhodium, and palladium have thus far been only partially successful. Unfortunately, no good long-lived gamma-emitting

(10) Q. V. Larson, G. E. Boyd, and R. W. Atteberry "Separation of Fission Product Anions by Ion-Exchange Chromatography," *Chemistry Division Quarterly Progress Report for Period Ending June 30, 1950*, ORNL-795, p. 124 (Oct. 3. 1950).

rhodium isotopes occur in fission so that it has been necessary to obtain a pure cyclotron-produced radionuclide of this element.

**Electrochemical Ion-Exchange Separations** (J. H. Gross and R. E. Wacker). Investigation of the electrochemical properties of beds of Dowex-50 has been continued in an effort to obtain data from which to design a series of separation experiments using countercurrent electromigration in a fixed bed of an ion exchanger. The pair of ions chosen for the separation work is lithium and sodium.

The conductance of a bed of an ion exchanger containing an electrolyte solution is a nonlinear function of the electrolyte concentration. Conduction may be regarded as taking place in three parallel branches: (1) entirely through the resin, (2) entirely through the solution, and (3) through interstitial solution elements and resin particles in series. The first quantity may be measured alone by substituting distilled water for the electrolyte solution. This has been done for various forms of Amberlite IR-100 by Heymann and O'Donnell.<sup>(11)</sup> The second branch of the network is the sum of the channels filled only with solution which are traversed by current passing through the bed. The magnitude of the conductance in this branch will vary linearly with concentration at reasonably low concentrations. For the usual rather tightly packed bed the contribution of this branch to the overall conductance should be quite small. The third branch of the network is of principal importance in determining the overall conductance. The variation of the conductance in this branch with electrolyte concentration is strongly dependent upon the mode of packing in the bed, distribution of particle size, and possible variation of specific conductance of the resin with varying external electrolyte concentration. These factors contribute to the relative magnitudes of the three branches.

Because of the serious uncertainty in the geometrical arrangement of a bed and because of the large number of variables present in the complete electrical network which represents the bed, we are unable to derive expressions for the overall bed conductance as a function of electrolyte concentration without oversimplification. However, an experimental determination presents no great difficulty.

Conductances of beds of Dowex-50 in the lithium, sodium, and hydrogen forms containing external electrolyte solutions of the chlorides of the

(11) E. Heymann and I. J. O'Donnell, "Physicochemical Investigations of a Cation Exchange Resin (Amberlite IR100). 2. Resin Conductance," *J. Colloid Sci.* 4, 405 (1949).

respective cations have been determined. Conductances of the solutions without the resin bed have also been measured. The electrolyte concentrations varied from zero to 0.5 M for LiCl and NaCl, and to 0.6 M for HCl. All measurements were at 25°C with 60 cycles/sec current between platinized electrodes. The resin bed covered the electrodes.

At zero electrolyte concentration (distilled water) the beds exhibited a specific conductance of approximately  $10^{-3}$  ohm<sup>-1</sup> cm<sup>-1</sup>, with the hydrogen form significantly higher. The values measured were found to be very sensitive to any pressure on, or other disturbance of, the bed, and hence are obviously dependent upon the contacting areas of the particles. The sensitivity to packing disturbance lessens rapidly as the concentration of external LiCl, NaCl, or HCl increases.

There exists a particular concentration of electrolyte at which the specific conductance of the solution is equal to the specific conductance of the resin particle equilibrated with the solution. We shall call this the "isoconductive" concentration. At this concentration the conductance of the system is independent of mode of packing, particle size, and even of the presence of resin in the apparatus. From a determination of the isoconductive concentration, and from published or measured values of the specific conductance of the solution at this concentration, the specific conductance of the resin may be obtained.

Below are listed the isoconductive concentrations for the three electrolytes studied; the values were obtained by plotting cell conductance against electrolyte concentration, with and without a resin bed in the cell, and taking the intersection of the two curves in each case:

CATION ON DOWEX-50	ISOCONDUCTIVE CONCENTRATION
Na <sup>+</sup>	0.14 M NaCl
Li <sup>+</sup>	0.10 M LiCl
H <sup>+</sup>	0.41 M HCl

These data show that the cation mobilities or dissociations in the resin are restricted. For example, in the case of sodium the specific conductance of the resin is equal to that of 0.14 M NaCl. At 0.14 M there is a negligible

amount of (Donnan)  $\text{Cl}^-$  within the resin, and it is justifiable to assume the sodium transport number in the resin to be 1.0. Then, the specific conductance of the resin is  $\lambda_{\text{Na}^+}^{\text{NaR}} C_{\text{Na}^+}^{\text{NaR}} / 1000$ , where  $\lambda_{\text{Na}^+}^{\text{NaR}}$  is the apparent equivalent ionic conductance of sodium in the resin and  $C_{\text{Na}^+}^{\text{NaR}}$  is the apparent sodium concentration in the resin. The sodium resin value of  $\lambda_{\text{Na}^+}^{\text{NaR}} C_{\text{Na}^+}^{\text{NaR}}$  is approximately 14.5, the volume concentration of sodium in the resin is approximately 3.5 M. The value 14.5 may also be calculated for an aqueous NaCl solution in which the  $\text{Na}^+$  concentration is 0.37 M, or for an aqueous  $\text{Na}_2\text{SO}_4$  solution 0.43 M in  $\text{Na}^+$ . It is seen that, if the sodium resin is completely dissociated, the ionic conductance, and therefore the mobility, of  $\text{Na}^+$  in the resin is depressed from the solution value by about one order of magnitude. On the other hand, in the unlikely case that the ionic conductance in the resin is not at all depressed, the degree of dissociation of the resin will be 0.1 or higher.

During this quarter measurements have also been made of the distribution constant  $K_D$  for  $\text{Li}^+$  and  $\text{Na}^+$  on Dowex-50, and of the value of the separation factor  $\alpha$  in electromigration of mixed  $\text{Na}^+$  and  $\text{Li}^+$  through a short bed of Dowex-50. In determining the value of  $\alpha$  it is also possible to obtain the overall cation transport number at various external electrolyte concentrations, and it is thus possible to estimate current efficiencies for a separation process based on electromigration in a fixed bed.

For the equilibrium  $\text{Na}^+ + \text{LiR} \rightleftharpoons \text{NaR} + \text{Li}^+$ ,

$$K_D = \frac{(\text{Na}/\text{Li})_R}{(\text{Na}^+/\text{Li}^+)_S} = 2.3$$

The values for  $\alpha$  and the transport numbers are not yet firm.

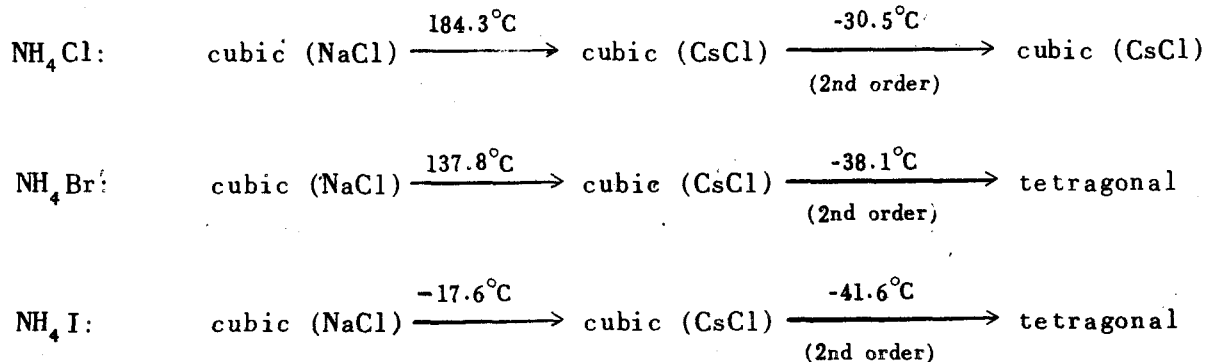
During the next quarter attempts will be made to perfect the data on  $\alpha$  and the cation transport number for the  $\text{Li}^+ - \text{Na}^+ - \text{Dowex-50}$  system. A practical separation of the cations on a small scale will then be undertaken. Time and equipment limitations permitting, the conductance of single electrolyte beds as a function of frequency will be investigated. By this means it may be possible to estimate the relative influences of partial resin dissociation and restricted cation mobility in the resin phase.

## 5. CHEMICAL PHYSICS

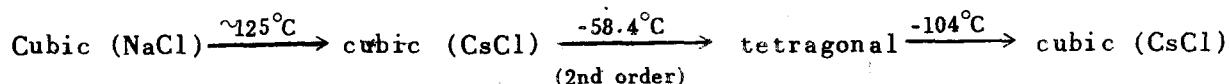
### NEUTRON DIFFRACTION STUDIES

**Neutron Diffraction Study of the Crystal Structure of Ammonium Bromide\***

(Henri A. Levy and S. W. Peterson). The crystal structure of the ammonium halides has been a popular field of investigation, especially since the time it was shown that second-order phase transitions<sup>(1)</sup> occurred in this group of compounds at temperatures somewhat below room temperature. Through the combined efforts of a number of workers<sup>(2-5)</sup> it has been established that the following series of transformations occur in the structures of the ammonium halides as the temperature is lowered:



The deuterium-substituted ammonium halides<sup>(6)</sup> have also been investigated. These, with the exception of deuterio-ammonium bromide, have shown the same transformations as the hydrogen compound but at somewhat different temperatures. Deuterio-ammonium bromide<sup>(6)</sup> has been shown to undergo the following changes:



- (1) F. Simon and C. L. von Simson, "Ein Umwandlungspunkt der Ammoniumsalze zwischen -30 und -40 Grad," *Naturwissenschaften* 14, 880 (1926).
- (2) F. Simon and R. Bergmann, "Thermisch erregte Quantensprünge in festen Körpern. IV. Messung der thermischen Ausdehnung im Gebiet der Anomalie," *Z. physik. Chem.* B8, 255 (1930).
- (3) J. A. A. Ketelaar, "Crystal Structure of the Low Temperature Modification of Ammonium Bromide," *Nature* 134, 250 (1934).
- (4) A. Smits, J. A. A. Ketelaar, and G. J. Muller, "The Transformation of Ammonium Bromide at About -39°," *Z. physik. Chem.* A175, 359 (1936).
- (5) J. Weigle and H. Saini, "La structure du bromure d'ammonium à basses températures," *Helv. Phys. Acta* 9, 515 (1936).
- (6) A. Smits and D. Tollenaar, "Die Art der Tieftemperaturumwandlung von ND<sub>4</sub>J," *Z. physik. Chem.* B52, 222 (1942).

\*This work was performed for the United States Atomic Energy Commission.

While X-ray-diffraction methods have established the existence of the above crystallographic phases and structure types, evidence of their precise nature is not obtainable by this means. Evidence obtained by means of the many other physical methods applied to this interesting problem is, on the whole, incapable of providing a comprehensive and precise picture of the subtle structural differences between the several phases, although the infrared and Raman spectral studies of Wagner and Hornig<sup>(7)</sup> and others provide strong evidence for certain characteristics of these structures which are in the main confirmed by the present study. The newly developed neutron-diffraction method provides a most suitable tool for this type of investigation, primarily because hydrogen atoms can be located by this means.

Deutero-ammonium bromide was selected for investigation because of its special interest and because deuterium lends itself better to neutron diffraction studies than does hydrogen. Reagent grade ammonium bromide was deuterated essentially to completion by means of repeated solution in 99.8% heavy water followed by evaporation of the solvent. The chemical purity of the vacuum-dried sample was established by chemical analysis and the isotopic purity by neutron transmission measurements.

Diffraction patterns were obtained on the finely powdered sample by means of an automatically recording neutron spectrometer similar to the one described by Wollan and Shull,<sup>(8)</sup> but differing from it in that scattered neutron intensities were measured with a count-rate meter and recorded on a strip chart. A servo mechanism held the incident neutron intensity constant. Diffraction data were obtained at temperatures both above and below room temperature, using an aluminum cryostat within which the sample could be cooled or heated while in vacuum. Diffraction data on powdered nickel were also obtained under identical conditions in order to allow adjusting the intensities of the ammonium bromide reflections to an absolute scale.

Integrated intensities of the reflections were determined directly from the chart record using the trapezoid rule checked occasionally by a triangle approximation. A rather large uncertainty is attached to many of the intensity values. This is due to the large statistical error inherent in low counting

(7) E. L. Wagner and D. F. Hornig, "The Vibrational Spectra of Molecules and Complex Ions in Crystals. III. Ammonium Chloride and Deutero-Ammonium Chloride," *J. Chem. Phys.* 18, 296 (1950).

(8) E. O. Wollan and C. G. Shull, "The Diffraction of Neutrons by Crystalline Powders," *Phys. Rev.* 73, 830 (1948).

rates, to incomplete resolution of peaks, and to uncertainty in the background level. The background uncertainty is accentuated by the often unsatisfactory peak height-to-background ratio and by the rather considerable structure apparent in the diffuse background.

Observed integrated reflections  $P_{hkl}$  from several patterns were averaged and values of  $jF^2$  were computed from the following formula appropriate to the case of a cylindrical sample bathed in radiation:

$$P_{hkl} = P_0 \left[ \frac{Vl\lambda^3}{8\pi rA} \right] \frac{\rho'}{\rho} \frac{N^2}{\sin \theta \sin 2\theta} B_{abs} jF_{hkl}^2$$

The quantity in parentheses was evaluated numerically from the measured integrated reflections of nickel powder. The notation follows the usual conventions for X-ray scattering.<sup>(9)</sup> The absorption correction  $B_{abs}$  was evaluated from measured values of the linear absorption coefficient for neutrons of wavelength 1.15 Å, the wavelength used throughout this investigation.

Calculated values of  $jF^2$  were obtained by adaptations of the usual formula,<sup>(9)</sup>

$$F = \sum f_0 \exp [-B(\sin \theta/\lambda)^2] \exp [2\pi i (hx + ky + lz)]$$

where in the neutron case  $f_0$  is given by  $\sqrt{\sigma_{coh}/4\pi}$ . The coherent cross-section  $\sigma_{coh}$  has been experimentally determined for many substances by Shull and Wollan.<sup>(10)</sup>

*Low-Temperature Cubic Phase.* Previous X-ray studies of deuterio-ammonium bromide at -140°C have shown<sup>(6)</sup> that the nitrogen and bromine atoms are arranged according to a CsCl type structure consistent with space group

(9) *Internationale Tabellen zur Bestimmung von Kristallstrukturen*, rev. ed., Edwards Brothers, Ann Arbor, Michigan, 1944.

(10) C. G. Shull and E. O. Wollan, "Coherent Scattering Amplitudes as Determined by Neutron Diffraction," *Phys. Rev.* 81, 527 (1951).

symmetry  $O_h^1$ , the unit cell length being 3.98 Å. The placement of four hydrogen atoms tetrahedrally around nitrogen, however, requires a space group of symmetry no higher than  $T_d^1$ .

The neutron-diffraction powder pattern of  $\text{ND}_4\text{Br}$  obtained at  $-195^\circ\text{C}$  is illustrated in Fig. 5.1. The pattern was indexed on the basis of a cubic unit with  $a_0 = 3.96$  Å, consistent with the X-ray value above in view of the lower temperature. The importance of deuterium scattering is illustrated by the (100) peak, which would be hardly observable by neutron diffraction if it were not for the considerable scattering amplitude of deuterium.

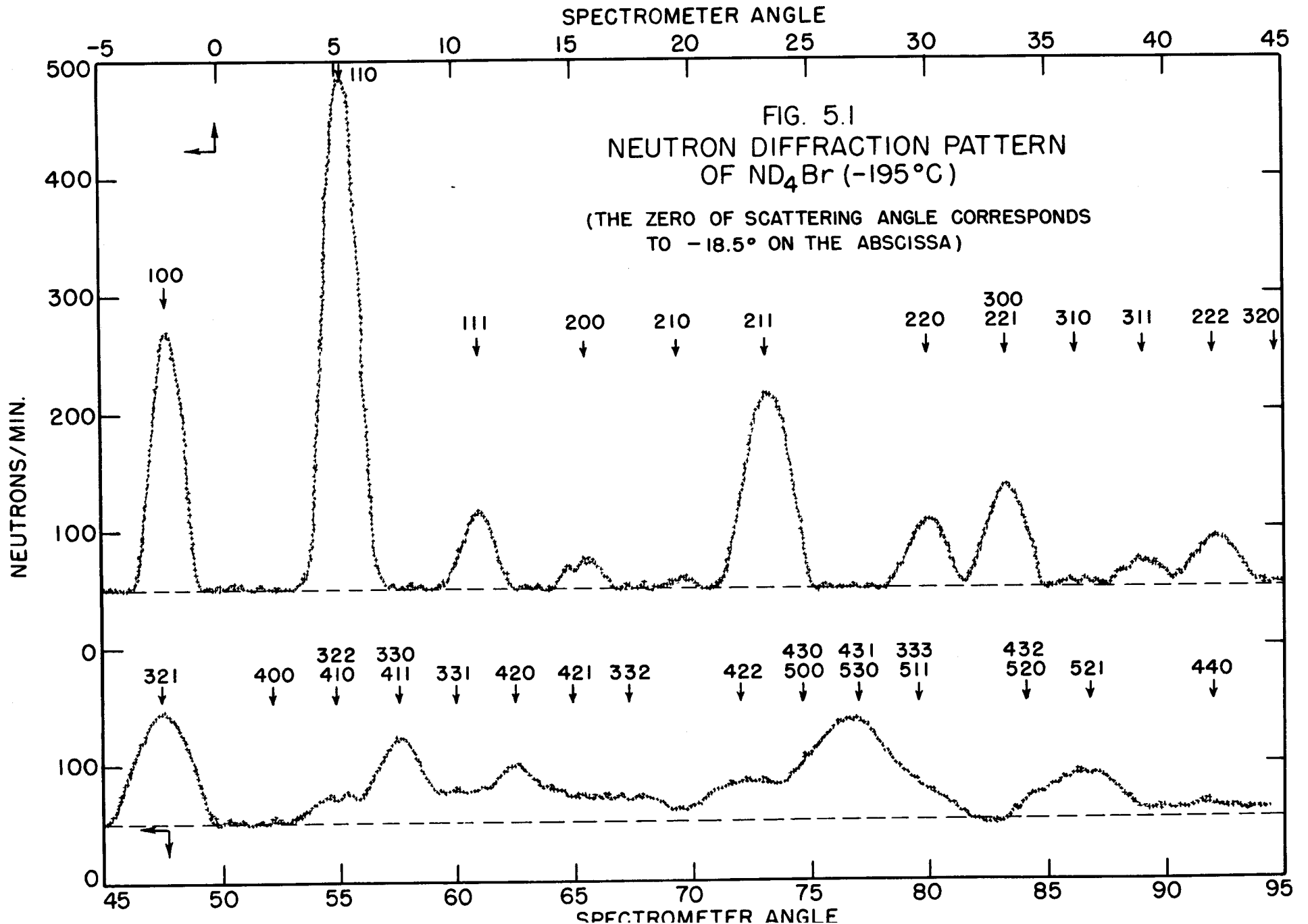
Structure factors were calculated for a  $T_d^1$  model with N and Br placed in positions<sup>(9)</sup>  $a$  and  $b$ , respectively, and four deuterium atoms in positions  $e$  involving one parameter  $x$ . A more severe Debye-Waller temperature factor for D than for N and Br was found necessary to give agreement with the observed data. Satisfactory agreement, shown in Table 5.1, was achieved with the following parameter and temperature factor coefficient values:

$$x = 0.144 \pm 0.003, \quad B(\text{D}) = 1.4, \quad B(\text{N}) = B(\text{Br}) = 0.17$$

The corresponding N—D bond distance is  $0.988 \pm 0.020$  Å. The rather severe temperature factor for D corresponds to a spherically symmetrical amplitude with a root mean square of 0.14 Å. The effect of greater amplitude perpendicular to than along the N—D link was also investigated, using a method similar to that described in the next section; agreement essentially as good as that presented in Table 5.1, but no better, was obtained for a characteristic angle of deviation  $\alpha$  up to  $5^\circ$ ,  $B(\text{D}) = 1.2$ ,  $B(\text{N}) = B(\text{Br}) = 0$ , and  $x = 0.145$ .

*Room-Temperature Cubic Phase.* The neutron-diffraction pattern of  $\text{ND}_4\text{Br}$  obtained at  $23^\circ\text{C}$  is shown schematically in Fig. 5.2. This pattern was indexed on the basis of a cubic unit with  $a_0 = 4.047$  Å, in agreement with X-ray determinations.<sup>(11)</sup> That there are marked differences between this pattern and the low-temperature pattern is immediately apparent. The marked decrease in peak intensity at large angles is due in part to structural differences and in part to increased temperature motion.

(11) R. W. G. Wyckoff, *Crystal Structures*, p. 7, Interscience, New York, 1948.



SPECTROMETER ANGLE

-5 0 5 10 15 20 25 30 35 40 45

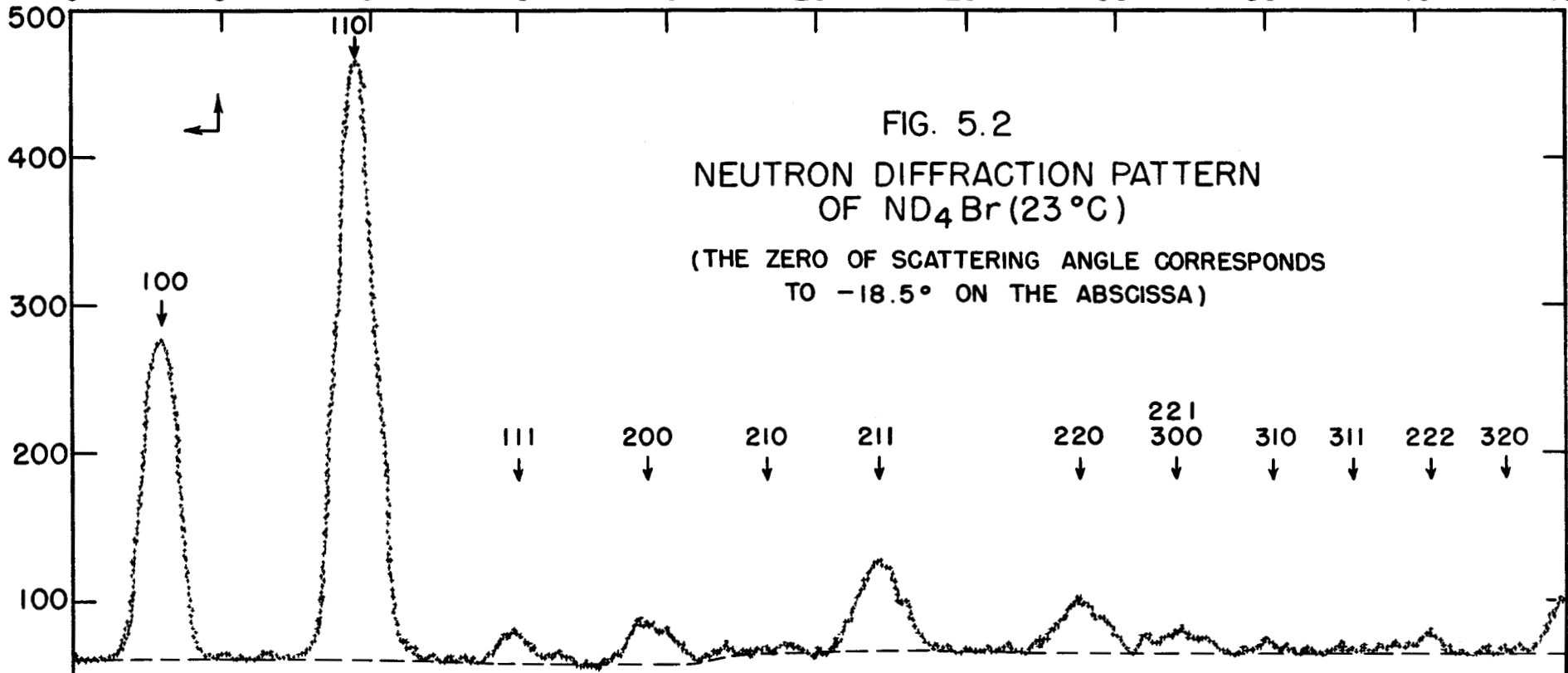
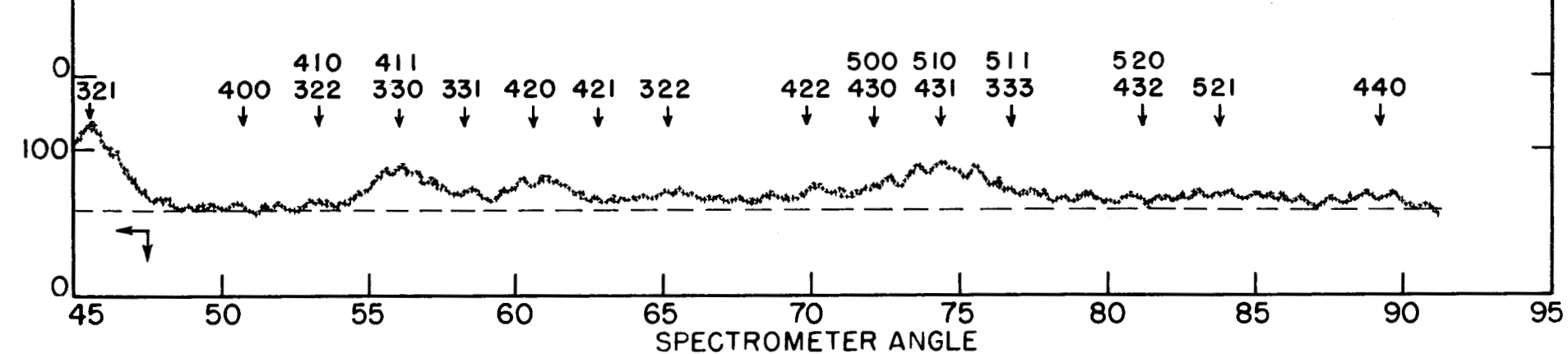


FIG. 5.2  
NEUTRON DIFFRACTION PATTERN  
OF  $\text{ND}_4\text{Br}$  ( $23^\circ\text{C}$ )  
(THE ZERO OF SCATTERING ANGLE CORRESPONDS  
TO  $-18.5^\circ$  ON THE ABCISSA)

86

NEUTRONS/MIN.



SPECTROMETER ANGLE

45 50 55 60 65 70 75 80 85 90 95

TABLE 5.1

ND<sub>4</sub>Br Data at -195°C

<i>hkl</i>	<i>jF</i> <sup>2</sup> OBSERVED	ESTIMATED UNCERTAINTY IN <i>jF</i> <sup>2</sup>	<i>jF</i> <sup>2*</sup> CALCULATED
100	17.9	± 0.4	17.9
110	72.3	1.4	72.0
111	16.1	0.8	15.4
200	5.0	0.6	5.4
210	1.7	1.0	0.6
211	87.1	2.4	84.5
220	30.8	2.0	31.1
221	76.0	3.5	60.8
300			18.3
310	4.1	2.1	2.4
311	13.3	3.5	13.1
222	41.5	8	43.3
320	5.8	4	8.4
321	163.2	8	159.5
400	0	1	0.2
410	27.4	3	15.4
322**			11.8
411	117.5	15	23.6
330			100.5
331	33.4	15	27.5
420	93.2	15	77.7
421	40.9	15	23.4
332	25.0	10	32.0
422	92.7***	10	54.7
500			0.1
430			46.2
510	252.5	25	37.4
431			225
511	43.7	20	18.5
333			6.9
520	143.5***	14	1.3
432			3.6
521			150.3

\*Parameter:  $x = 0.144$ .

\*\*Peaks beyond this one are incompletely resolved.

\*\*\*Unresolved peaks.

No agreement was found possible with a model in which the deuterium atoms were placed in positions  $e$  of space group  $T_d^1$ , even with severe temperature motion included. Since the transition at  $-58^\circ\text{C}$  has alternatively been considered as the advent of free rotation<sup>(12)</sup> or as an order-disorder transition,<sup>(13)</sup> models involving freely rotating ammonium ions and disordered ammonium ions were among those tested. Structure factors for the free rotation model were computed with a deuterium contribution of

$$\left[4f_0(\text{D})/2\pi ah_0\right] \sin 2\pi ah_0$$

where  $a$  is the radius of the spherical shell containing the deuterium atoms expressed as a fraction of the unit cell length  $a_0$ , and  $h_0$  is  $\sqrt{h^2 + k^2 + l^2}$ . Models involving orientational disorder are described by placing four deuterium atoms at random in the eightfold positions  $g$  of space group  $O_h^1$ .

Table 5.2 compares the experimental  $jF^2$  values for a number of key reflections with those calculated for a simple ordered  $T_d^1$  model, an  $O_h^1$  model involving disorder, and an  $O_h^1$  model involving free rotation of the ammonium ion. It is apparent that the disordered model shows the best approach to agreement with experiment, while the free-rotation model has some points in its favor. The application of Debye-Waller temperature factors, especially to deuterium, brought improvement but was not sufficient to give satisfactory agreement.

The comparison in Table 5.2 suggests that a more satisfactory model might be achieved by superposing on the orientational disorder a severe temperature motion corresponding to a torsional oscillation of the ammonium ion. This sort of model was approximated by considering that each hydrogen is distributed not only in a spherical cloud corresponding to the usual temperature factor, but also around a circle centered at one of the positions  $g$  of  $O_h^1$ . If  $\alpha$  is the central half-angle of the cone defined by the nitrogen position and this circle, the corresponding contribution of deuterium to the structure factor is

$$\sum \frac{1}{2} f_0(\text{D}) \exp \left[ -B \left( \frac{\sin \theta}{\lambda} \right)^2 \right] \exp \left[ 2\pi i \cos \alpha (hx_0 + ky_0 + lz_0) \right] J_0 (2\pi \sqrt{S} \sin \alpha)$$

(12) L. Pauling, "The Rotational Motion of Molecules in Crystals," *Phys. Rev.* 36, 430 (1930).

(13) J. Frenkel, "Über die Drehung von Dipolmolekülen in festen Körpern," *Acta Physicochim.* U.R.S.S. 3, 23 (1935).

where  $x_0$ ,  $y_0$ , and  $z_0$  describe in turn the eight positions corresponding to  $\alpha = 0$ , the summation is over these positions,  $S = (hy_0 - kx_0)^2 + (lx_0 - hz_0)^2 + (kz_0 - ly_0)^2$ , and  $J_0$  is the Bessel function of zero order. This expression is adapted from a more general one given by Lipscomb.<sup>(14)</sup> While the use of a single value of  $\alpha$  is artificial and a weighted average over a distribution in  $\alpha$  is doubtless to be preferred, the sensitivity of the neutron intensities to this parameter did not justify the more elaborate procedure.

With appropriate choices of the parameters  $x_0$  and  $\alpha$ , and temperature factor coefficients for D, N, and Br, a satisfactory fit was obtained.

TABLE 5.2  
Selected ND<sub>4</sub>Br Data at 23°C

<i>hkl</i>	CALCULATED $jF^2$			EXPERIMENTAL $jF^2$
	ORDERED $T_d^{-1}$	DISORDERED $O_h^{-1}$	FREE ROTATION	
100	19.7	19.7	20.1	17.7
110	78.7	78.7	73.2	67.3
111	17.7	5.6	2.9	3.6
200	6.5	6.5	14.5	6.8
211	96.0	42.2	26.4	32.1
220	31.0	31.0	11.3	19.5
221	88.2	1.3	3.3	
300	25.6	25.6	0.8	7.8
311	25.7	12.9	1.8	3.0
222	65.2	18.1	10.5	11.3
321	195.3	153.6	83.6	77.8
400	4.5	4.5	13.3	0

\*No temperature factors were applied.

The final values of the parameters and temperature coefficients are:

$$x_0 = 0.142 \pm 0.002, \quad \alpha = 10 \pm 3^\circ, \quad B(D) = 3.05, \quad B(N) = B(\text{Br}) = 1.44$$

(14) M. V. King and W. N. Lipscomb, "Formulas for X-Ray Scattering from Atoms in Various Spatial Probability Distributions," *Acta Cryst.* 3, 318 (1950).

Table 5.3 presents a comparison of experimental  $jF^2$  values with those calculated for the final model for all reflections in the available angular range. The N—D distance is  $0.995 \pm 0.015$  Å.

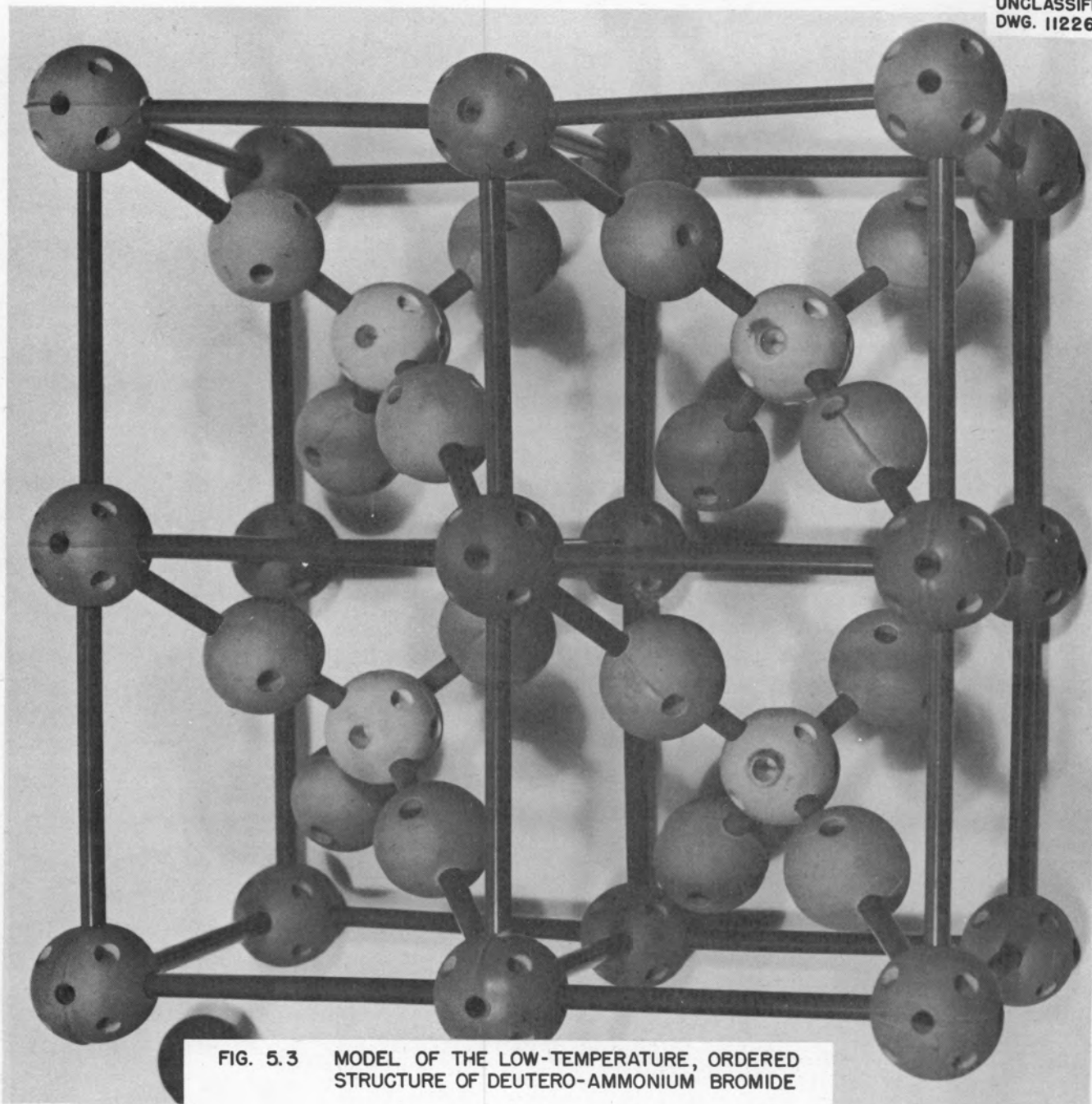
*Discussion.* This investigation confirms decisively the conclusion, previously based on indirect evidence, that at low temperatures the structure of  $\text{ND}_4\text{Br}$  is ordered and at room temperature involves orientational disorder of the ammonium ions. The low-temperature structure is entirely similar to that recently reported for low-temperature  $\text{ND}_4\text{Cl}$  from a neutron diffraction study; however, our structure for the room-temperature phase contrasts with that for room temperature  $\text{ND}_4\text{Cl}$  in which, according to the same investigators, no disorder was found.

The structure of both phases of ammonium bromide is based on the CsCl type lattice. Thus each nitrogen is surrounded by eight bromide ions at the corners of a cube. In the ordered phase, the hydrogen atoms surround the nitrogen tetrahedrally, the N—D links are directed toward four of the eight surrounding bromide ions, and all ammonium ions are in parallel orientation. This structure is shown in Fig. 5.3. In the disordered phase the N—D links are again directed toward the surrounding bromide ions, but over any extended region of the crystal all eight of these positions are occupied with equal probability. This is achieved if the ammonium ions are arranged at random in the two possible orientations in which the hydrogens approach most closely to the bromide ions.

The structures indicate that an attraction between hydrogen and bromine is effective in determining the arrangement of atoms in this crystal. The ordered phase is probably stabilized by weak repulsive forces between hydrogen atoms of neighboring ions. This stabilization is overcome at higher temperatures by the increased entropy of the disordered structure.

Table 5.4 presents values of the N—H or N—D distance found in ammonia, ammonium chloride, and ammonium bromide by various methods. The differences between these values are small but may be significant.

The rather large value of the temperature factor coefficient  $B$  for bromine in the room-temperature phase suggests that there may actually be some randomness in the bromine position, in accord with a suggestion made by Wagner and Hornig<sup>(7)</sup> that a particular bromine position would be expected to depend on



The dark balls represent bromine and the light ones nitrogen. The disordered structure may be visualized by rotating half the ammonium ions

ninety degrees about the cubic axis nearly perpendicular to the plane of the photograph.

TABLE 5.3  
ND<sub>4</sub>Br Data at 23°C

<i>hkl</i>	<i>jF</i> <sup>2</sup> OBSERVED	ESTIMATED UNCERTAINTY IN <i>jF</i> <sup>2</sup>	<i>jF</i> <sup>2*</sup> CALCULATED
100	17.7	± 0.35	17.8
110	67.3	1.3	67.5
111	3.6	0.4	3.9
200	6.8	0.7	6.2
210	0	1.0	0.2
211	32.1	1.6	32.0
220	19.5	1.4	18.9
221	7.8	0.8	0.5
300			8.2
310	3.7	1.8	3.9
311	3.0	1.5	3.0
222	11.3	1.7	11.3
320	3.7	1.8	2.0
321	77.8	5.8	72.8
400	0	1.0	0.1
410	6.1	3.0	4.2
322			0.6
411	48.0	4.8	12.1
330			33.8
331	9.6	4.8	6.8
420	36.9	5.5	31.3
421	5.2	2.6	2.5
332	18.1	2.7	18.8
422	17.8	2.6	19.3
500	93.4***	13.0	0
430			9.9
510			14.4
431			63.6
511			0.4
333			0.3
520	4.1	2.0	0.8
432			1.3
521	25.5	7.7	32.8
440	10.4	5.2	13.6

88.6

\*Parameters:  $x_0 = 0.142$ ,  $\alpha = 10^\circ$

\*\*Peaks beyond this one are incompletely resolved.

\*\*\*Unresolved peaks.

the number and distribution of hydrogen atoms close to it. Explicit incorporation of randomness into the model, however, did not improve agreement between calculated and observed intensities. The value of  $B$  corresponds to a root mean square deviation of 0.13 Å, a value numerically close to the observed shift of bromine in the tetragonal phase structure from the ideal position.<sup>(3)</sup>

TABLE 5.4  
N—H or N—D Distances

SUBSTANCE	N—H or N—D DISTANCE <sub>0</sub> (Å)	METHOD	REFERENCE
NH <sub>4</sub> Cl	1.01	Nuclear magnetic resonance	(16)
NH <sub>4</sub> Cl	1.025	Nuclear magnetic resonance	(17)
NH <sub>4</sub> Br	1.039	Nuclear magnetic resonance	(17)
ND <sub>4</sub> Cl	1.03	Neutron diffraction	(15)
ND <sub>4</sub> Br	0.995	Neutron diffraction	This research
NH <sub>3</sub> , ND <sub>3</sub>	1.01	Spectroscopy	

#### EXPERIMENTS IN CHEMICAL KINETICS WITH MOLECULAR BEAMS

S. Datz and E. H. Taylor

This research has been restarted after a lapse of about six months. Recent improvements in counting techniques have suggested some changes in the separation and counting of radiobromine, and some preliminary experiments were done to assess the possibilities. At present, the beam apparatus is being started up for the purpose of calibrating the neutron activation analysis of bromine against the surface ionization gauge for potassium, using a beam of KBr.

- (15) G. H. Goldschmidt and D. G. Hurst, "The Structure of Ammonium Chloride by Neutron Diffraction," *Bull. Am. Phys. Soc.* 26 (No. 1), 28 (1951).
- (16) H. S. Gutowsky and G. E. Pake, "Nuclear Magnetism in Studies of Molecular Structure and Rotation in Solids: Ammonium Salts," *J. Chem. Phys.* 16, 1164 (1948).
- (17) H. S. Gutowsky, G. B. Kistiakowsky, G. E. Pake, and E. M. Purcell, "Structural Investigations by Means of Nuclear Magnetism. I. Rigid Crystal Lattices," *J. Chem. Phys.* 17, 972 (1949).

## RADIOFREQUENCY SPECTROSCOPY

R. Livingston

**Magnetic Moment of  $I^{129}$ .** The  $I^{129}$  magnetic moment study, a cooperative program with H. E. Walchli of the Stable Isotopes Research and Production Division (Y-12) and G. M. Hebert of the Chemistry Division (X-10), has been completed. The final results, essentially the same as those reported previously (ORNL-1036, p. 58), appeared in *Physical Review*.<sup>(18)</sup>

**Spin of  $I^{131}$ .** The cooperative studies with Duke University on the  $I^{131}$  spin problem have not been active for several weeks. It is expected that active work will be resumed during the coming quarter. The Operations Division has agreed to purify, by solvent extraction, iodine solutions used in future experiments.

**Quadrupole Moment Ratio of  $Cl^{35}$  and  $Cl^{37}$ .** Resonance absorption lines due to nuclear quadrupole splittings were first observed by Dehmelt and Krüger<sup>(19)</sup> for chlorine in solid trans-dichloroethylene at 90°K. The splitting is caused by the interaction of the chlorine nuclear electric quadrupole moment with the gradient of the electric field at the nucleus. The electric field gradient can be considered to arise from charge distribution within the molecule and from other charge distributions in the crystal lattice.

Equipment for observing this phenomenon has been assembled by making minor circuit changes in available proton magnetic resonance equipment. Resonances for  $Cl^{35}$  and  $Cl^{37}$  were initially found and measured in five compounds at 77°K. These are listed in Table 5.5. In some cases two absorption lines were present for each isotope, which effect is presumed to be due to crystallographically different sets of chlorine atoms in the crystal lattice. Hence, each chlorine set experiences its own particular electric field gradient. The frequency ratios in Table 5.5 should be the ratio of the quadrupole moments of the two chlorine isotopes. The average gives  $Q(Cl^{35})/Q(Cl^{37}) = 1.26878 \pm 0.00015$ . The agreement of the eight ratios, to within  $\pm 0.00015$ , is

(18) H. Walchli, R. Livingston, and G. Hebert, "Nuclear Magnetic Moment of  $I^{129}$ ," *Phys. Rev.* 82, 97 (1951).

(19) H. G. Dehmelt and H. Krüger, "Nuclear Quadrupole Frequencies in Solid Dichloroethylene," *Naturwiss.* 37, 111 (1950).

quite significant. Recent studies<sup>(20,21)</sup> by microwave spectroscopy gave values for the ratio that varied slightly from molecule to molecule. The effect was explained by assuming a nuclear polarization by the external electric field gradient. Such an effect is absent in the measurements reported here. Details of this work will appear in *Physical Review*.<sup>(22)</sup>

**TABLE 5.5**  
**Measured Frequencies and Ratios for Solid Chlorine Compounds**

COMPOUND	$\nu(\text{Cl}^{35})$ (megacycles)	$\nu(\text{Cl}^{37})$ (megacycles)	$Q(\text{Cl}^{35})/Q(\text{Cl}^{37})$
SOCl <sub>2</sub>	32.0908	25.2935	1.26874
	31.8874	25.1331	1.26874
POCl <sub>3</sub>	28.9835	22.8432	1.26880
	28.9378	22.8067	1.26883
CH <sub>2</sub> Cl <sub>2</sub>	35.9912	28.3673	1.26876
CHCl <sub>3</sub>	38.3081	30.1921	1.26881
	38.2537	30.1500	1.26878
C <sub>6</sub> H <sub>5</sub> Cl	34.6216	27.2872	1.26879

**Electronic Nature of Chlorine Bonds in Covalently Bonded Chlorine Compounds.** Quadrupole coupling data, usually obtained by microwave spectroscopy on gaseous molecules, have recently become of great interest in the attempts to understand the electronic nature of chemical bonds. However, the technique has been limited to a small number of molecules where observed hyperfine structure could be analyzed. Observations of pure quadrupole spectra can be made on a large variety of compounds. In many cases simplifying assumptions can be made that will allow the calculation of an approximate quadrupole coupling which may be compared with microwave data. In the present study

- (20) S. Geschwind, R. Gunther-Mohr, and C. H. Townes, "Ratio of the Quadrupole Moments of Cl<sup>35</sup> and Cl<sup>37</sup>," *Phys. Rev.* 81, 288 (1951).
- (21) G. R. Gunther-Mohr, S. Geschwind, and C. H. Townes, "Polarization of the Nucleus by Electric Fields," *Phys. Rev.* 81, 289 (1951).
- (22) R. Livingston, "Quadrupole Moment Ratio of Cl<sup>35</sup> and Cl<sup>37</sup> from Pure Quadrupole Spectra," *Phys. Rev.* 82, 289 (1951).

resonances have been measured in a variety of covalent chlorine compounds. In most, if not all, of the solids studied, it may be assumed that the error introduced is small by ignoring the crystal lattice contribution to the electric field gradient at the chlorine nucleus. This is strongly suggested by the nature of an electric field gradient which is a  $1/r^3$  function. Townes and Dailey<sup>(23)</sup> have made a theoretical evaluation of contributions to electric field gradients at nuclei, and, for typical microwave cases, they concluded that one electronic charge a distance of 1 Å from an atom of interest gave a negligible effect when compared with the effect of a P bonding orbital. Their original treatment was to demonstrate that in typical gaseous molecules studied by microwave spectroscopy the electric field gradient at a nucleus could be considered to arise almost exclusively from properties of the covalent chemical bond. The experimental data also strongly suggest that the crystal field gradients are small. In most cases splittings are seen which are usually small. It is quite reasonable that the crystal lattice effects will become more important when compounds are studied which have a high degree of ionic character. In such cases there would be little contribution from chemical bonding, and, correspondingly, the resonance frequencies observed should be much lower than those found in the compounds reported here.

The energy levels for pure quadrupole spectra are given by

$$E_m = \frac{1}{4}[eqQ/I(2I - 1)] [3m^2 - I(I + 1)]$$

The observed transition frequencies for the two chlorine isotopes with spin  $I = 3/2$  should be one-half the quadrupole coupling,  $eqQ$ . This equation is valid for the case of axial symmetry for the electric field gradient,  $q = \partial^2 V / \partial Z^2$  and  $\partial^2 V / \partial X^2 = \partial^2 V / \partial Y^2$ . There is no information on the symmetry properties of the field gradient in the compounds studied here. Side gradients within the molecule would be expected in cases in which the chlorine bond had some double-bond character. It is felt that side gradient effects from the crystal lattice are small.

Table 5.6 contains the results of all measurements. The third column is the average of the corresponding frequencies appearing in the second column, and the fourth column is the coupling obtained by doubling the values of the

(23) C. H. Townes and B. P. Dailey, "Determination of Electronic Structure of Molecules from Nuclear Quadrupole Effects," *J. Chem. Phys.* 17, 782 (1949).

TABLE 5.6

## Pure Quadrupole Transitions for Solid Chlorine Compounds at 77°K

COMPOUND	MEASURED FREQUENCY (megacycles)	AVERAGE FREQUENCY (megacycles)	$eqQ$ (megacycles)	$ X _{Cl} -  X $
Cl <sub>2</sub>	54.248	54.248	108.50	0.0
CH <sub>2</sub> Cl <sub>2</sub>	35.991	35.991	71.98	0.5
CHFC1 <sub>2</sub>	36.479 36.508	36.493	72.99	0.5
CF <sub>2</sub> Cl <sub>2</sub>	38.450	38.450	76.90	0.5
CHCl <sub>3</sub>	38.254 38.308	38.281	76.56	0.5
CFC1 <sub>3</sub>	39.161 39.517 39.703	39.460	78.92	0.5
CCl <sub>4</sub>	40.463 40.520 40.542 40.609 40.640 40.653 40.720	40.592	81.18	0.5
C <sub>6</sub> H <sub>5</sub> Cl	34.622	34.622	69.24	0.5
C <sub>6</sub> H <sub>5</sub> CH <sub>2</sub> Cl	33.627	33.627	67.25	0.5
SOCl <sub>2</sub>	31.887 32.091	31.989	63.98	0.5
POCl <sub>3</sub>	28.938 28.984	28.961	57.92	0.7
PCl <sub>3</sub>	26.107 26.202	26.154	52.31	0.7
AsCl <sub>3</sub>	24.960 25.058	25.009	50.02	1.0
SnCl <sub>4</sub>	23.719 24.140 24.226 24.294	24.095	48.19	1.3
GeCl <sub>4</sub>	25.451 25.714 25.736 25.746	25.662	51.32	1.3
BCl <sub>3</sub>	21.580 21.585	21.583	43.17	1.0
SiCl <sub>4</sub>	20.273 20.408 20.415 20.464	20.390	40.78	1.2
SbCl <sub>3</sub>	19.304 20.912	20.108	40.22	1.2

third column. The last column lists the electronegativity difference of chlorine and the atom to which it is bonded.<sup>(24)</sup> All measurements were at liquid-nitrogen temperature and only  $\text{Cl}^{35}$  values are given. The  $\text{Cl}^{37}$  values may be obtained by dividing by 1.26878. The measurements on  $\text{CCl}_4$  are preliminary. Fourteen very weak lines were seen, and preliminary values for seven are given. The chlorine couplings are negative, but since the sign is not determined by this method, it will be understood that all coupling values reported should have a negative sign.

Perhaps the most significant single measurement is the 108.50-megacycle coupling value for  $\text{Cl}_2$ . Atomic beam measurements on Cl, which lacks one P electron from having a closed shell, gave a coupling of 110.4 megacycles.<sup>(25)</sup> If chlorine was bonded in a molecule with a P bonding orbital and there was no ionic character, the quadrupole coupling should be essentially the same as that of atomic chlorine.<sup>(23)</sup> The measurement reported here indicates that bonding in molecular chlorine is predominantly P type with little or no S character. This is in contrast to Townes' and Dailey's earlier work<sup>(23)</sup> on other chlorine compounds which they interpreted as having at least 15% S character. Molecular chlorine is a particularly good case because the problem of assessing the amount of ionic character in the bond is at a minimum. The ionic character problem is one of the major difficulties in a complete appraisal of data of this type.

The one-carbon-chlorine compounds form an interesting sequence. The  $\text{CH}_2\text{Cl}_2$  coupling of 71.98 megacycles increases to 72.99 megacycles in  $\text{CHFCl}_2$  where one hydrogen is replaced by a fluorine atom. The change is in the expected direction since fluorine is much more electronegative than hydrogen. The fluorine will have a tendency to assume a negative charge, which will make the carbon appear a little more electronegative to the chlorine atoms. Hence the bond will be a little less ionic or more covalent in character and the coupling should increase. In other words, the CHF group is more electronegative than the  $\text{CH}_2$  group. Similarly the coupling for  $\text{CF}_2\text{Cl}_2$ , 76.90 megacycles, is still higher, and the coupling for  $\text{CFCl}_3$ , 78.92 megacycles, is higher than that for  $\text{CHCl}_3$ , 76.56 megacycles. In comparing the couplings for

(24) L. Pauling, *Nature of the Chemical Bond and the Structure of Molecules and Crystals*, Cornell University Press, Ithaca, N. Y., 1939.

(25) L. Davies, Jr., B. T. Feld, C. W. Zabel, and J. R. Zacharias, "The Hyperfine Structure and Nuclear Moments of Chlorine," *Phys. Rev.* 73, 525 (1948).

$\text{CH}_2\text{Cl}_2$ , 71.98 megacycles, for  $\text{CHCl}_3$ , 76.56 megacycles, and for  $\text{CCl}_4$ , 81.18 megacycles, the frequencies increase when hydrogen is replaced by chlorine, but the effect is noticeably greater than when hydrogen is replaced by fluorine. This trend is unexpected since fluorine is more electronegative than chlorine and should give a larger effect in a purely inductive phenomenon. This suggests that in addition to the inductive phenomenon some other effect is superimposed. It is hoped that by studying other mixed halogen compounds, such as  $\text{CHBrCl}_2$  and  $\text{CBr}_2\text{Cl}_2$ , additional information will be obtained. The coupling for  $\text{CH}_3\text{Cl}$  from microwave data<sup>(26)</sup> is 75.15 megacycles. The reason for its coming between  $\text{CH}_2\text{Cl}_2$  and  $\text{CHCl}_3$  is unexplained. It should be noted, however, that it is below  $\text{CCl}_4$ , while the microwave value of 38 megacycles<sup>(27)</sup> for  $\text{SiH}_3\text{Cl}$  is below that of  $\text{SiCl}_4$ , 40.78 megacycles, and the microwave value of 46 megacycles<sup>(28)</sup> for  $\text{GeH}_3\text{Cl}$  is appropriately below  $\text{GeCl}_4$ , 51.32 megacycles. The silicon and germanium analogs to the carbon molecules should be interesting cases for further study.

There also appears to be an inductive effect in the expected direction when  $\text{PCl}_3$  is compared with  $\text{POCl}_3$ .  $\text{PSCl}_3$  should be an interesting case since sulfur is less electronegative than oxygen and the coupling should fall between those of  $\text{PCl}_3$  and  $\text{POCl}_3$ . Unfortunately, resonances have not been seen in all compounds tried. The very important cases of  $\text{CH}_3\text{Cl}$ ,  $\text{CH}_2\text{BrCl}$ , and  $\text{CHF}_2\text{Cl}$  gave negative results. It is felt that in some cases the resonance is not seen because of an unsatisfactory crystal structure. This is quite reasonably the case for *tert*-butyl chloride and *tert*-amyl chloride, which gave negative results. These molecules were of interest since they are cases in which chlorine is bonded to one carbon which in turn is bonded only to carbon atoms.

It may be possible to correlate observed splittings with crystallographic data. For example, there is a striking similarity between the splittings for  $\text{SnCl}_4$ ,  $\text{GeCl}_4$ , and  $\text{SiCl}_4$ . Each consists of four lines, three of which are close together with the fourth noticeably off at a lower frequency. It would indeed be interesting if these crystals were found to be isomorphous. Some consideration has been given to obtaining X-ray diffraction patterns of these three crystals.

(26) W. Gordy, J. W. Simmons, and A. G. Smith, "Microwave Determination of the Molecular Structures and Nuclear Couplings of the Methyl Halides," *Phys. Rev.* 74, 243 (1948).

(27) A. H. Sharbaugh, "Microwave Determination of the Molecular Structure of Chlorosilane," *Phys. Rev.* 74, 1870 (1948).

(28) J. M. Mays and C. H. Townes, "The Nuclear Spins and Quadrupole Moments of Stable Germanium Isotopes," *Phys. Rev.* 81, 940 (1951).

## CALORIMETRY OF RADIOACTIVITY

G. H. Jenks and F. H. Sweeton

**Test for Storage of Absorbed Beta-Ray Energy in Charcoal.** As described previously,<sup>(29)</sup> the total power generated by two different samples of  $C^{14}O_2$  adsorbed on charcoal have been measured with the liquid-helium calorimeter. However, the possibility existed that the measured power did not represent the true decay energy because of a storage of part of the energy in the charcoal at the low temperature. Measurements were, therefore, undertaken which were designed to establish whether such a storage occurred. These measurements have been completed. Within the sensitivity of the measurements, no storage of energy was detected.

*Procedure and Results.* The search for the existence of storage of absorbed beta-ray energy in charcoal was carried out as follows: A source of radioactive  $Au^{198}$  was placed in the liquid-helium calorimeter in such a manner that part of the beta radiations were absorbed in aluminum and the remaining part in other metallic sections of the calorimeter. The heat generated in the calorimeter by the source was then measured. Subsequently, the aluminum absorber was replaced by a charcoal absorber of the same mass and geometry, and the heat generated by a gold source was again measured. The resulting values for the heat generated per unit source strength in each measurement were then compared. The storage of energy in the charcoal should have produced a decrease in the measured power in going from the aluminum to the charcoal absorber.

The charcoal absorber was made to reproduce as closely as possible the adsorber used in the  $C^{14}O_2$  measurements. It was sealed from the liquid helium in the calorimeter, and  $CO_2$  and helium gases in amounts equivalent to those used in the previous measurements were adsorbed on it.

The gold sources used were activated just prior to each measurement, and the relative activities of the sources were determined by means of the  $4\pi$  ionization chamber which has been calibrated and described by Cobble.<sup>(30)</sup>

(29) G. H. Jenks and F. H. Sweeton, "Calorimetry of Radioactivity," *Chemistry Division Quarterly Progress Report for Period Ending December 31, 1950*, ORNL-1036, p. 60 (to be issued).

(30) J. W. Cobble, *Calibration of the  $4\pi$  High Pressure Ion Chamber*, ORNL Memorandum CF-50-6-114 (June, 1950).

The results of the measurements with the different absorbers are shown below:

ABSORBER	POWER GENERATED PER UNIT OF ACTIVITY (watts x 10 <sup>8</sup> )
Aluminum	4.96 <sub>5</sub>
Charcoal No. 1	4.94 <sub>5</sub>
Charcoal No. 2	5.00 <sub>3</sub>

The average value for the two measurements with charcoal is 0.2% higher than that obtained with the aluminum absorber, and the deviation of the values for charcoal from the average is  $\pm 0.6\%$ . Thus, no significant difference was observed between the power generated per unit source activity in the different absorbers.

In using the data to decide within what limits the absence of energy storage was demonstrated, the fraction of the measured power which originated in the charcoal must be estimated. That part of the power which resulted from absorption of gamma-ray energy and that from absorption of beta-ray energy between the source and the charcoal will decrease the sensitivity.

The geometry and mass of the calorimeter were such that 3 to 4% of the gamma-ray energy emitted by the gold was absorbed. This is equivalent to 4 to 5% of the total power measured. Variation in the gamma-ray absorption between different measurements was made negligible by careful reproduction of the geometry and mass of the calorimeter in each case.

The mass of metal absorber between the gold source and the charcoal amounted to  $7.4 \times 10^{-2}$  g/cm<sup>2</sup>, including the mass of the source. The fractional loss of beta-ray energy in this absorber was estimated by computing the energy loss for homogeneous electrons in different regions of the spectrum and integrating to find the total energy not absorbed. The estimate indicated a value of about 54% for the fraction absorbed.

On the basis of the estimated value for the fraction of the total power not absorbed in the charcoal, the sensitivity with which the absence of storage of energy was demonstrated was 1.0%. Allowance for possible error in the estimation of the fraction not absorbed would raise the uncertainty to 1.3%.

*Present Program.* A determination of the abundance of  $C^{14}$  in the  $C^{14}O_2$ - $C^{12}O_2$  mixture from which the calorimetric samples were prepared has been undertaken. It is planned to carry out the determination by a method similar to that used previously<sup>(31)</sup> for the determination of the abundance of tritium in a tritium-hydrogen mixture, i.e., by measuring the density of the purified gas by means of a small gas-density balance. Mass spectrographic analyses of two different samples of the mixture have been made at Y-12, but the results of the measurements indicated concentrations of  $C^{14}$  which differed by 2.5%. Because of this rather large variation in the mass spectrographic results and because there is a possibility that the ionization efficiency of  $C^{14}O_2$  and  $C^{12}O_2$  may differ significantly and thus be a source of error in any mass spectrographic analysis, it was decided to make use of the density technique in analyzing the mixture. Apparatus for use in the measurements is being assembled and perfected.

#### SOLIDS AND HIGH-TEMPERATURE CHEMISTRY

M. A. Bredig

A research program dealing with chemical and certain physical properties of solids, largely chemical compounds, and especially at high temperatures, is being initiated. In some respects this is a continuation of work started previously (see, for example, the preliminary study of the beryllium oxide-nitride system, ORNL-336, and previous ORNL Chemistry Division reports). It is planned to expand it to cover investigation of physical properties other than crystal structure, such as electrical and thermal conductivity, reactions in molten salt systems, unusual valence states stable at elevated temperatures, and crystal structure at elevated, including highest possible, and subnormal temperatures. As a continuation of work previously performed under the Physics Division program (ORNL-865, p. 77), some irradiation experiments on chemical compounds are also included.

**X-Ray-Diffraction Apparatus.** The greatly expanding needs for X-ray-diffraction work at ORNL, both of a research and of a more routine nature, led to the establishment of an additional facility in the chemistry building.

(31) G. H. Jenks, F. H. Sweeton, and J. A. Ghormley, "A Precise Determination of the Half-Life and Average Energy of Tritium Decay," *Phys. Rev.* 80, 990 (1950).

The new, console type, General Electric X-ray-generating equipment has been set up and operated in conjunction with an Ohio X-ray spectrometer. Modifications in both were necessary in order to allow this combination. The latter instrument, besides being furnished with an unsatisfactory collimating-slit system which has now been altered, has a vertical goniometer circle, whereas the General Electric X-ray tube mounting was originally designed for the horizontal General Electric goniometer. The vertical circle is desirable for the work with the high-temperature furnace mentioned below. Cameras for recording X-ray diffraction on photographic film will also be operated with this unit.

**Vacuum Chamber for High (and Subnormal) Temperature X-Ray Diffraction.**

The construction of a vacuum, or controlled-atmosphere, chamber has been started and is nearing completion. It is expected to permit taking X-ray-diffraction patterns in conjunction with the Geiger counter spectrometer at temperatures in excess of 2000°C, as well as at the temperature of liquid air. It consists of a horizontal water-cooled brass tube, 8 in. in diameter and 15 in. long, in which beryllium windows approximately  $\frac{3}{4}$  in. wide and 17 mils thick will permit the radial entrance of the primary X-ray beam and the observation, by means of a Geiger counter scanning around the cylinder, of the diffracted beams. Preliminary experiments led to a design of a U-shaped graphite heating element specifically suited for the heating of a flat specimen while permitting observation of the diffracted X-ray beams over an arc of 180°. Possible difficulties with a high rate of evaporation of carbon in the vacuum at temperatures above 1600°C may be overcome by changing to an atmosphere of an inert gas, or to wolfram metal for the heating element. Power will be supplied by a high-current, maximum 300 amp, low-voltage welding transformer of 8 kilowatts maximum output.

**Remote-Control X-Ray-Diffraction Spectrometer for High-Level Radioactive Specimens** (with B. S. Borie, Metallurgy Division). The design of this instrument was completed during this quarter, and work on the construction has been started in the Research Shops. For a general description of the principles employed see the Physics Division quarterly report ORNL-782, p. 89. A detailed description will be given when the instrument has been installed and tested in one of the "hot" cells of the new Physics of Solids Institute Building.

The new model of the Hilger X-ray-diffraction equipment which will be used in this connection is also being assembled. It has been selected because of its unusually high maximum output of 160 mamp, which will be useful in case the operation of a high-power rotating-anode X-ray tube becomes necessary or desirable for the study of high-level radioactive specimens.

**Specific Gravity of Hafnium and Zirconium.** In Report Y-696 (F. P. Boody) the conclusion was reached that a value for the specific gravity of hafnium metal, 12.62 g/cc as measured directly, was in better agreement with a value computed according to the formula

$$\frac{\text{At. Wt. of Hf}}{\text{At. Wt. of Zr}} \times \text{density of Zr} = \text{density of Hf}$$

namely,  $(178.6/91.22) \times 6.5 = 12.73$  g/cc, than with the figure 13.3 g/cc previously reported in the literature. The writer, noticing that the value 13.3 was based on very accurate X-ray data (Van Arkel, 1939), was enabled through the courtesy of P. J. Hagelston to repeat the direct specific gravity measurements on the specimens employed by Boody and also to perform X-ray-diffraction measurements on these for comparison with both the direct density determination and with the X-ray data of the literature. The result was that both values were reproduced, i. e., 12.62 for direct physical measurement and 13.3 from the X-ray data on the same specimen. The conclusion was inevitable that the directly measured physical density was in error owing to one of several possible causes: (1) the presence of impurities, such as magnesium or calcium, which substituted for hafnium in the crystal lattice, or (2) existence of voids in the metallic matrix. The first of these two possibilities was quickly excluded when analytical data procured by P. Hagelston showed the absence of such impurities in any significant amounts. The presence of small amounts of nitride or carbide, discovered in the X-ray pattern, was not sufficient to explain the density discrepancy. The second possible cause, however, turned out to be the actual one, when photomicrographs obtained from T. E. Wilmarth (Fig. 5.4) clearly showed the existence of fissures, or voids, between metallic grains, to an estimated extent of 3 to 5 vol. %. Such voids were absent in the zirconium specimens which were examined simultaneously

Plate ME-718



Plate ME-719



FIG. 5.4

Views Showing Fissures in Hafnium Matrix

Magnification - 125X

with the hafnium specimens in both Boody's and this investigation and which did not show the discrepancy between density measured directly and X-ray-diffraction data. It is clear, then, that the true specific gravity of hafnium is 13.3 g/cc as derived from X-ray measurements, and that the mathematical formula above is not applicable because of the actual difference of more than 1% in the atomic dimensions of hafnium and zirconium (hexagonal lattice constants for Hf:  $c_0 = 5.0508$ ,  $a_0 = 3.1945$  A; for Zr:  $c_0 = 5.1486$ ,  $a_0 = 3.2312$ .<sup>(32)</sup> It is worth noting that there is a marked asymmetry in these structures, with two short distances between atoms, namely, 3.1945 and 3.1280 A for hafnium and 3.2313 and 3.1790 A for zirconium.

It would be of interest to determine the cause, and also the effect upon mechanical properties, of the intergranular voids. The former most likely is connected with the high melting point (approximately 2220°C) of hafnium, which is considerably higher than that of zirconium (1880°C).

**Effects of Radiation on Crystal Structure.** *Lead Oxide.* As described in ORNL-865, p. 77, the irradiation of the two allotropic modifications of lead oxide, PbO, is expected to shed some light on the mechanism of the effect of radiation, especially particulate radiation, on crystals. After a preliminary short test in the ORNL reactor, which gave a negative result, two groups of specimens were shipped to Chalk River for irradiation in the water-cooled fast-neutron facility there for periods of 28 and 120 days. Each group consisted of one sample of the red tetragonal low-temperature form and one of the yellow orthorhombic high-temperature modification, metastable at room temperature.

Transformation, partial or total, of the red form into the yellow form might support the theory of the so-called "heat spikes." The reverse conversion, yellow to red, might also be produced by localized temperature increases that would not go above the transition point of 489°C (this is a correction of the figure 587°C, erroneously given in ORNL-865). However, it

(32) R. B. Russel in *M.I.T. Metallurgical Project Technical Progress Report for the Period April Through June, 1950*, MIT-1052 (Sept. 8, 1950).

is doubtful that the time of such a heat spike for a thermal conversion of this type would be long enough since several weeks were found necessary for conversion of the yellow into the red form at 420°C.<sup>(33)</sup> This particular point will also be tested by irradiating metastable crystals that cannot be converted mechanically but only by heating into stable structures. In such cases conversion would support the theory of a mechanism similar to thermal annealing (heat spikes), whereas failure to transform would be indicative of a mechanism more related to cold work.

*Salts of Organic Acids* (with J. H. Crawford, Physics of Solids Institute). K. Lark-Horovitz reported last year that, according to a personal communication, W. Bothe of the University of Heidelberg, had observed destruction of the crystal structure of sodium oxalate under bombardment by alpha particles from radon ("amorphous" X-ray pattern), and its recovery on heating at 100°C. He suggested repetition of this experiment with pile radiation. Exposure for three weeks in the water-cooled hole 51 of the ORNL reactor of anhydrous sodium oxalate,  $\text{Na}_2\text{C}_2\text{O}_4$ , and of three other salts, potassium oxalate monohydrate,  $\text{K}_2\text{C}_2\text{O}_4 \cdot \text{H}_2\text{O}$ ; sodium bitartrate monohydrate,  $\text{NaHC}_4\text{H}_4\text{O}_6 \cdot \text{H}_2\text{O}$ ; and sodium potassium tartrate tetrahydrate,  $\text{NaKC}_4\text{H}_4\text{O}_6 \cdot 4\text{H}_2\text{O}$ , resulted in the destruction of the crystal lattice of only the bitartrate (Figs. 5.5 and 5.6). The test will be repeated with the bioxalate of sodium, with the hope of removing the discrepancy with Bothe's result, who may have used the acid salt instead of the neutral one, as well as with results on other salts, especially the acid salts of dicarboxylic acids. Perhaps significantly, it was the one acid salt among the four irradiated at ORNL which showed the effect. It is believed to be due to a partial decomposition of the bitartrate, possibly resulting in carbon dioxide evolution, which disrupts the crystal lattice of the remaining bitartrate. Quantitative analysis will be undertaken after future exposures. Also, the effect of gamma radiation will be studied in salts that show the effect in pile exposures.

**Carbonate and Potassium Apatites.** The problem of "carbonate apatite" has been the subject of scientific inquiry and controversy for many years. Carbonate apatite is related in composition and crystal structure to a rather large family of substances, of which fluorine apatite  $[\text{Ca}_5(\text{PO}_4)_3\text{F}]$ , often

(33) M. Petersen, "Studies of the Preparation and Allotropic Transformation of Lead Monoxide," *J. Am. Chem. Soc.* 63, 2617 (1941).

UNCLASSIFIED  
DWG. 11227

$\text{NaHC}_4\text{H}_4\text{O}_6 \cdot \text{H}_2\text{O}$   
before irradiation

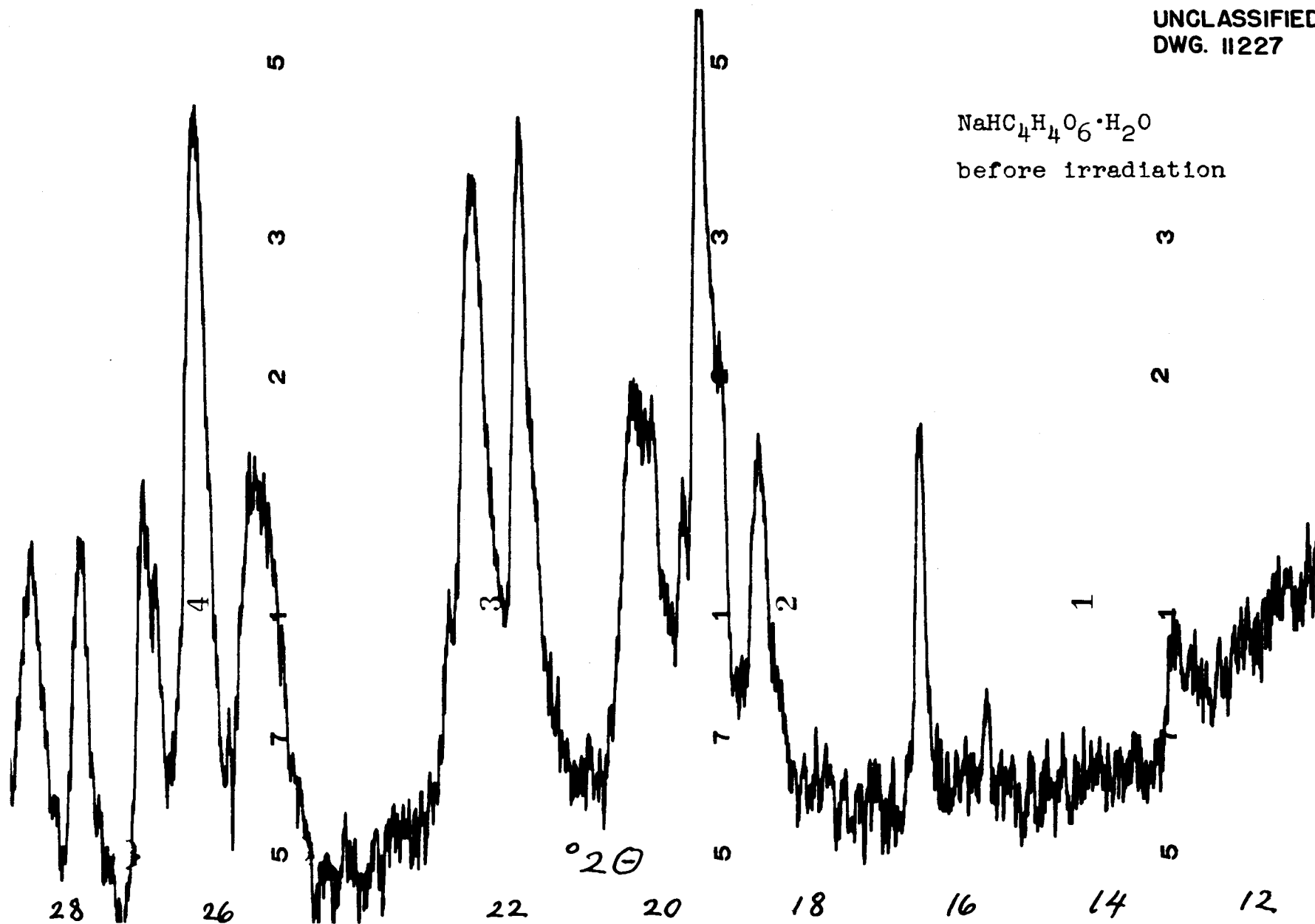


FIG. 5.5 X-RAY-DIFFRACTION PATTERNS OF SODIUM BITARTRATE HYDRATE BEFORE IRRADIATION

UNCLASSIFIED  
DWG. 11228

$\text{NaHC}_4\text{H}_4\text{O}_6 \cdot \text{H}_2\text{O}$   
after irradiation

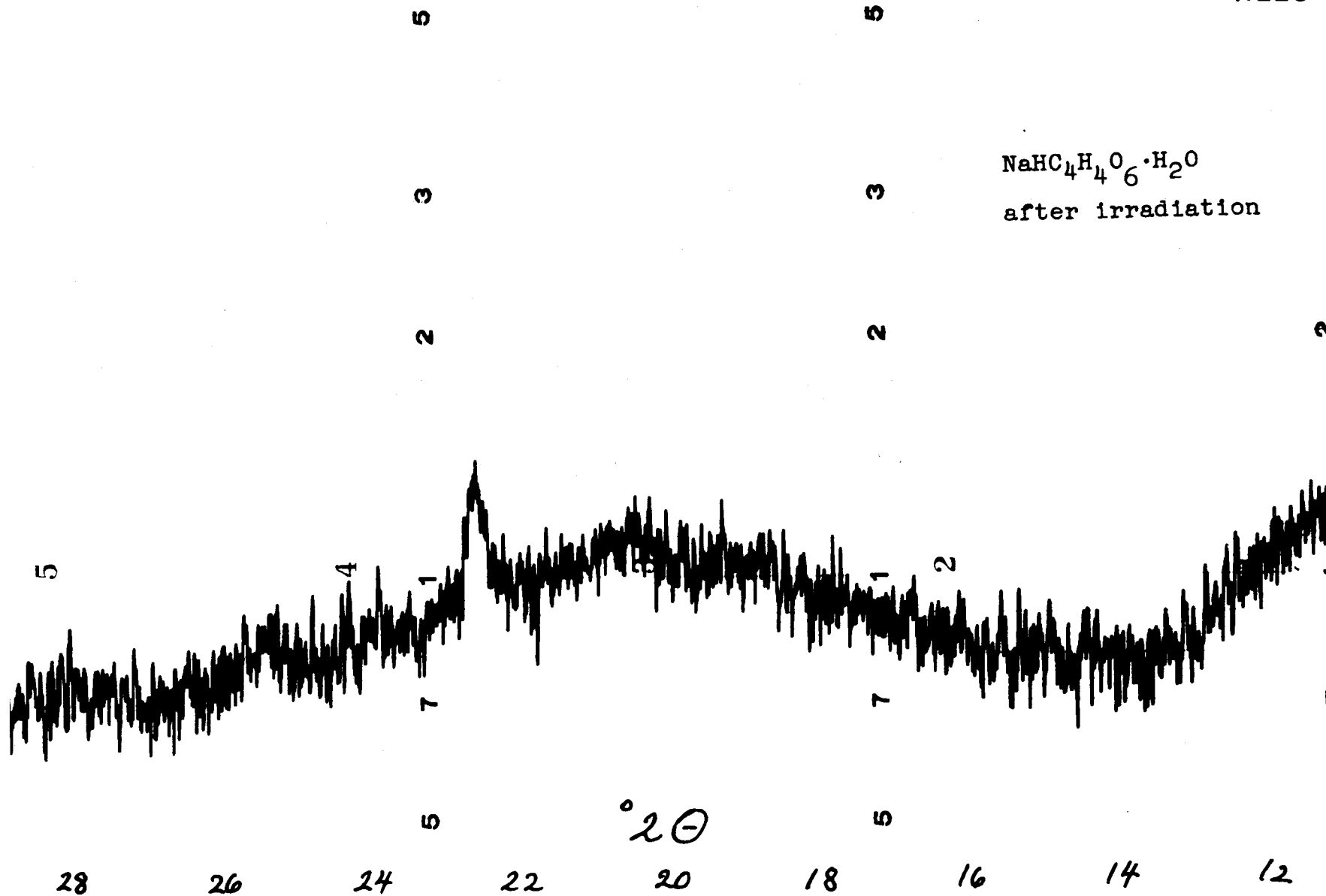


FIG. 5.6 X-RAY - DIFFRACTION PATTERNS OF SODIUM BITARTRATE HYDRATE AFTER IRRADIATION

written  $\text{Ca}_{10}(\text{PO}_4)_6\text{F}_2$ , or  $3\text{Ca}_3(\text{PO}_4)_2 \cdot \text{CaF}_2$ , principal constituent of most phosphate mineral deposits] and hydroxyapatite [ $\text{Ca}_5(\text{PO}_4)_3\text{OH}$ , main mineral constituent of animal and human bones and teeth] may be considered prototypes, but which includes as isomorphous substances phosphates, arsenates, vanadates, etc. of calcium and of other metals such as lead. While most workers agree now on the existence of carbonate apatites, i.e., of substances of hexagonal apatite structure containing carbonate ions in solid solution (molecularly dispersed), there are notable exceptions. S. B. Hendricks, of the U. S. Bureau of Plant Industry, believes that chemical and optical properties reported for carbonate apatites can well be explained by intimate mechanical mixtures, or surface combinations, of fluorine apatite, or hydroxyapatite, with microcrystalline calcium carbonate. A similar point of view has been taken by J. Thewlis and Coworkers.<sup>(34)</sup> In the course of a recent discussion at a special symposium of the American Crystallographic Association (Washington, D. C., March, 1951) the writer was asked by members of the staff of the U.S. Geological Survey laboratories, who are working on this problem in connection with the interest on the Atomic Energy Project in the recovery of uranium from low-grade sources such as rock phosphates, whether he could supply samples of synthetic preparations of carbonate apatites described in his earlier publications (1936-1938).<sup>(35)</sup> Additional interest in chemical combinations of phosphates and carbonates may arise in connection with the special behavior of uranium toward carbonate, which may be of significance in as widely separated fields as the deposition of toxic heavy and radioactive elements in parts of the human body, the recovery of uranium from rock phosphates, and the preparation of stable solutions or slurries for homogeneous reactors.

A review of the literature of the past 12 years yields the following rather confused picture of the present status of this problem:

The old formula for carbonate apatite,  $\text{Ca}_{10}(\text{PO}_4)_6\text{CO}_3$ , based on a purely formal analogy with fluorine apatite,  $\text{Ca}_{10}(\text{PO}_4)_6\text{F}_2$ , has been almost universally abandoned. Some Belgian authors<sup>(36)</sup> still use it, however, without any valid evidence. In a closely related problem, they assume the existence of "oxyapatites" [ $\text{Ca}_{10}(\text{PO}_4)_6\text{O}$ , or, with partial substitution of such elements as

(34) J. Thewlis, G. E. Glock, and M. M. Murray, "Chemical and X-Ray Analysis of Dental, Mineral, and Synthetic Apatites," *Trans. Faraday Soc.* 35, 358 (1939).

(35) H. H. Franck, M. A. Bredig, and E. Kanert, "Calcium Alkali Phosphates. II. Calcium Potassium Phosphates," *Z. anorg. us. allgem. Chem.* 237, 49 (1938); and preceding papers referred to in this article.

(36) H. A. L. Brasseur and M. J. Dallemagne, "La synthèse des apatites," *Bull. soc. chim. France*, March-April 1949, D series, p. 135; M. J. Dallemagne, H. Brasseur, and J. Mellon, "La Constitution de la substance minérale de l'os et la synthèse des apatites," *ibid.*, p. 136; and previous papers referred to in these articles.

Ni or Mn for Ca, e.g.,  $\text{NiCa}_9(\text{PO}_4)_6\text{O}$ , with no proof at all for the absence of  $\text{H}_2\text{O}$ , as  $2(\text{OH})$ ], thus disregarding the conclusive work of Trömel<sup>(37)</sup> and of Bredig and coworkers,<sup>(38)</sup> which showed oxyapatites not to exist except in dilute solid solution with hydroxy and fluorine apatite. In most publications the curious but experimentally well-supported fact,<sup>(37,38)</sup> namely, that in basic calcium phosphates water is taken up to form hydroxyapatite even from an atmosphere of normal degree of humidity at temperatures as high as  $1200^\circ\text{C}$ , has been neglected by most authors, notably also in the interpretation of analytical data (McConnell<sup>(39)</sup> and Brasseur *et al.*<sup>(36)</sup>). Gruner, McConnell, and Armstrong<sup>(40)</sup> seem to be the only authors who assume carbonate apatite with extensive substitution of  $\text{CO}_3$  for  $\text{PO}_4$  ions to be present in animal and human bones and teeth. Most others [e.g., Hirschman and coworkers<sup>(41)</sup> and Brandenberger<sup>(42)</sup>] have confirmed the writer's first X-ray data (1933),<sup>(43)</sup> which substantiated the earlier, purely chemical result, that the carbonate in these materials is not molecularly dispersed through the apatite but is present as a separate phase (or surface combination<sup>(44)</sup>) and that this apatite is either hydroxyapatite,  $\text{Ca}_{10}(\text{PO}_4)_6(\text{OH})_2$ , with some excess  $\text{H}_3\text{PO}_4$  adsorbed (Trömel<sup>(37)</sup>) or a tricalcium orthophosphate hydrate,  $\text{Ca}_9(\text{PO}_4)_6(\text{H}_2\text{O})_2$  (Brasseur *et al.*<sup>(36)</sup> and Hendricks *et al.*<sup>(44)</sup>).

On the basis of X-ray data for synthetic apatites which serve as standards, and which are discussed further below, it is possible to state rather definitely that McConnell is correct in assuming the occurrence of carbonate apatite in some minerals, such as francolite, containing varying amounts of carbonate, but errs with respect to others, e.g., dahllite, as he does with respect to bone and teeth phosphates.

Synthetic carbonate apatites were first examined by X-ray diffraction when their occurrence was observed in preparations of mixed calcium alkali

- (37) G. Trömel, "Untersuchungen über die Bildung eines halogenfreien Apatits aus basischen Calciumphosphaten," *Z. physik. Chem.* A158, 422 (1932).
- (38) M. A. Bredig, H. H. Franck, and H. Fuldner, "Beiträge zur Kenntnis der Kalk-phosphorsäureverbindungen. II," *Z. Elektrochem.* 39, 959 (1933).
- (39) D. McConnell, "The Problem of the Carbonate-Apatites: A Carbonate Oxy-Apatite (Dahllite)," *Am. J. Sci.* 36, 296 (1938); and previous papers referred to in this article.
- (40) J. W. Gruner, D. McConnell, and W. D. Armstrong, "The Relationship Between Crystal Structure and Chemical Composition of Enamel and Dentin," *J. Biol. Chem.* 121, 771 (1937).
- (41) A. Hirschman, A. E. Sobel, B. Kramer, and I. Fankuchen, "An X-Ray Diffraction Study of High Phosphate Bones," *J. Biol. Chem.* 171, 285 (1947).
- (42) E. Brandenberger and H. R. Schinz, "The Nature of the Inorganic Material of Bone," *Experientia* 4, 59 (1948).
- (43) M. A. Bredig, "The Apatite Structure of the Inorganic Substance of Bone and Tooth," *Z. physiol. Chem.* 216, 239 (1933).
- (44) S. B. Hendricks, W. L. Hill, K. D. Jacob, and M. E. Jefferson, "Structural Characteristics of Apatite-Like Substances and Composition of Phosphate Rock and Bone as Determined from Microscopical and X-Ray Diffraction Examinations," *Ind. Eng. Chem.* 23, 1413 (1931).

metal phosphates. While X-ray patterns on film showed distinct differences of structure for carbonate-containing apatites, no definite interpretation was given to this qualitative finding. With the development of the Geiger counter X-ray spectrometer techniques, a more convenient and accurate tool has become available. Results thus obtained on specimens of synthetic carbonate apatites which were prepared in accordance with previously described methods<sup>(35)</sup> are discussed below.

Intimate mixtures (pellets) of 1 mole of tribasic calcium orthophosphate with 1 mole of  $\text{Na}_2\text{CO}_3$  (or  $\text{K}_2\text{CO}_3$ ) were heated in a carbon dioxide atmosphere for several hours at  $1200^\circ\text{C}$  and then cooled slowly in the furnace. A large portion of the reaction product consisted of a solid solution of  $\text{Na}_2\text{CO}_3$  (or  $\text{K}_2\text{CO}_3$ ) in  $\text{CaNaPO}_4$  (or  $\text{CaKPO}_4$ ) and had to be removed from the apatite which was found<sup>(35)</sup> to be composed of the ions Ca, Na,  $\text{PO}_4$ , and  $\text{CO}_3$  in the ratio 10:2:6:2 for the so-called "sodium carbonate apatite," or, in the case of the potassium carbonate reaction,  $\text{Ca}:\text{PO}_4:\text{CO}_3 = 11:6:2$ , with no potassium entering this so-called<sup>(35)</sup> "dicalcium carbonate apatite." This separation is accomplished by leaching the finely pulverized material (200 mesh) with 100 parts of an aqueous solution of 2% citric acid per part of solid. Potassium, present as  $\text{CaKPO}_4$ , which is intimately mixed with the apatite and which dissolves at a rate similar to that of calcium carbonate when similarly dispersed as a separate phase in the reaction product, was almost completely removed by the leaching operation (to less than 0.5% according to a spectrographic analysis by C. Feldman). This purification of the synthetic apatite from potassium is one of the strong arguments against those doubts regarding the existence of carbonate apatite which were based on the erroneous assumption of the presence of a finely dispersed, inseparable calcium carbonate phase. The X-ray spectrometer record of the insoluble residue shows only reflections which can be indexed on the basis of an apatite structure. In Table 5.7 are listed experimental values for  $1/d^2$  for the sodium carbonate apatite as compared with the values calculated for hexagonal lattice constants,  $c = 6.91$ ,  $a = 9.33$ , and  $c/a = 0.740$ , i.e., similar, but not equal to those of hydroxyapatite ( $c = 6.87$ ,  $a = 9.41$ , and  $c/a = 0.730$ ). Figure 5.7 shows that portion of the recorded diffraction patterns in which the structural differences between carbonate apatites and hydroxyapatites can be demonstrated most clearly, namely, an intermediate region of Bragg angles, where spacings are high enough and widely enough separated for unambiguous assignment of indices but low enough for accuracy in

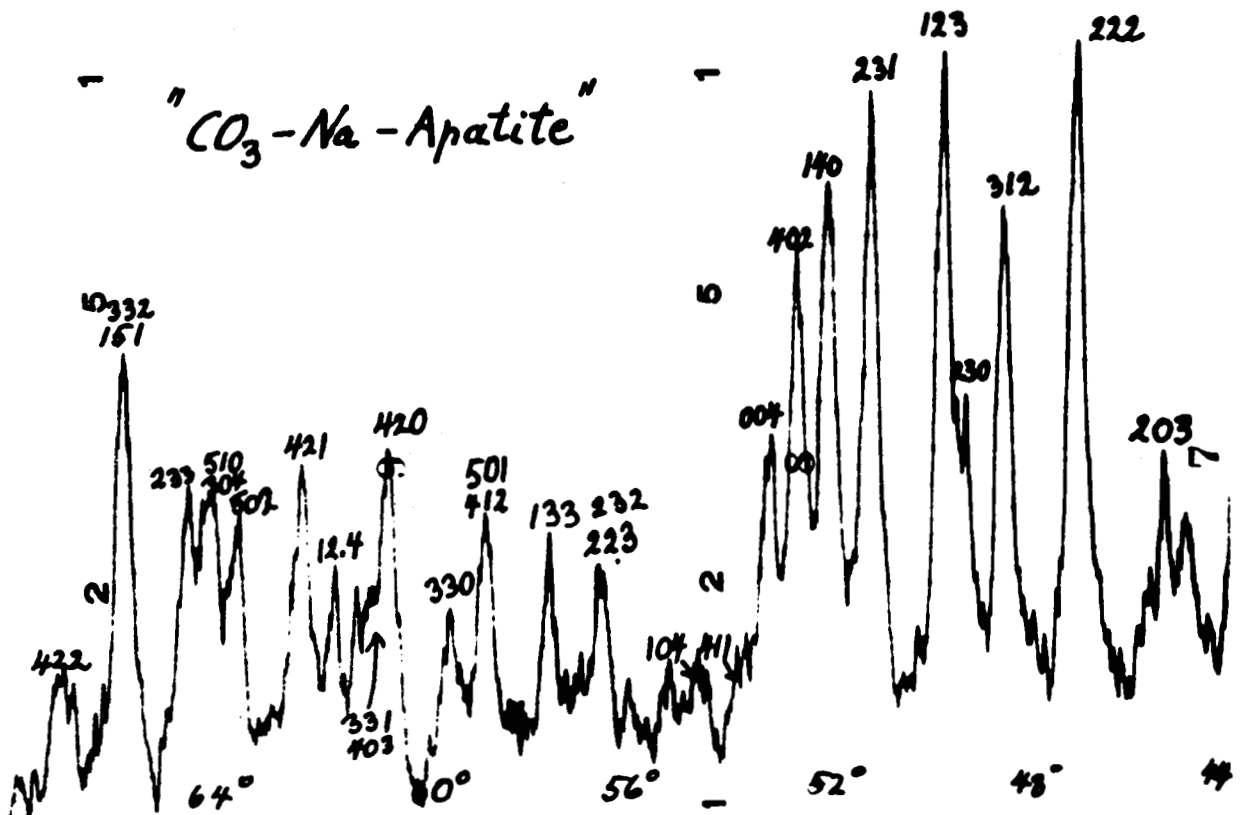
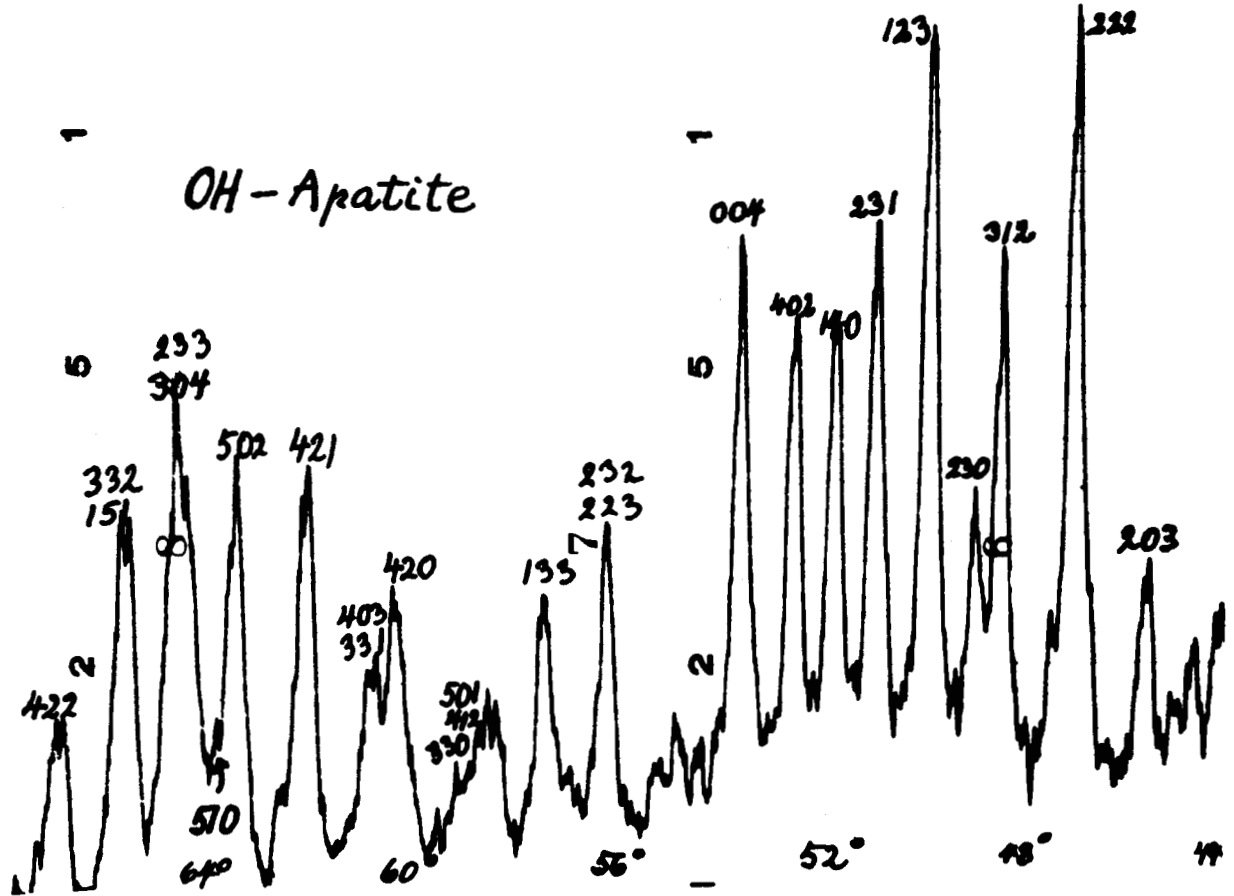


FIG. 5.7 X-RAY-DIFFRACTION PATTERNS OF CARBONATE APATITE AND HYDROXYL APATITE

TABLE 5.7

Observed and Calculated Spacings from Powder X-Ray-Diffraction  
Spectrometer Data for Sodium Carbonate Apatite

$$a = 9.33 \pm 0.01 \text{ \AA}; c = 6.90 \pm 0.01 \text{ \AA}; c/a = 0.740 \pm 0.01$$

HEXAGONAL INDICES, <i>hk.l</i>	INTENSITY	$1/d^2$		HEXAGONAL INDICES, <i>hk.l</i>	INTENSITY	$1/d^2$	
		EXPERIMENTAL	CALCULATED			EXPERIMENTAL	CALCULATED*
20.0	28	0.0614	0.0613	23.1	78	0.3120	0.3125
11.1	25	0.0672	0.0670	14.0	70	0.3220	(0.3220)
00.2	80	0.0843	0.0839	40.2	50	0.3290	0.3295
10.2	14	0.1001	0.0992	00.4	32	0.3360	(0.3360)
12.0	125	0.1081	0.1073	41.1	6	0.3430	0.3430
12.1	420	0.1280	0.1282	10.4	7	0.3510	0.3513
11.2	300	0.1295	0.1299	22.3 } 23.2 }	13	0.3735	{0.3726 {0.3752
30.0	370	0.1375	0.1380	11.4			0.382
20.2	80	0.1449	0.1452	50.0			0.383
30.1	30	0.1587	0.1590	13.3	13	0.3865	0.3890
12.2	28	0.1913	0.1913	20.4			0.3870
13.0	148	0.2000	0.1995	50.1 } 41.2 }	15	0.404	{0.404 {0.406
13.1	30	0.2200	0.2205	33.0	7	0.414	0.414
11.3	18	0.2342	0.2348	42.0	20	0.428	0.429
40.0	13	0.2450	0.2452	40.3 } 33.1 }	9	0.433	{0.434 {0.435
20.3	20	0.2491	0.2500	12.4	14	0.441	0.443
22.2	110	0.2672	0.2679	42.1	20	0.449	0.450
13.2	60	0.2830	0.2832	50.2	22	0.465	0.4674
23.0	20	0.2920	0.2913	30.4	25	0.4715	0.4737
12.3	115	0.2960	0.2963				

\*The values in parentheses were not calculated but were taken from experiments to evaluate constants for other calculated values.

measurement of Bragg angles. The calculation of the lattice constants in the table as well as a comparison, for example, of the distance of the (00.4) and (14.0) peaks from each other in each pattern of Fig. 5.7, which depends directly on the relative length of the  $c$  and  $a$  axes, shows that in this synthetic carbonate apatite, "sodium carbonate apatite," the  $c/a$  ratio is larger by more than 1% than in hydroxyapatite.

These same line shifts were observed<sup>(35)</sup> in the original films but there was no discussion, in the reference, of their meaning for the dimensions of the crystal lattice. They are also accompanied by considerable differences in intensity ratios (Fig. 5.7). McConnell<sup>(39)</sup> has correctly pointed out that a simple replacement on the hexagonal axes of  $2(\text{OH})(2\text{F})$  ions by  $2(\text{NaCO}_3)$  groups, or by  $1\text{CO}_3$  ion,<sup>(44)</sup> without substantial increases in the density and the lattice dimensions ( $a$  axis), which are not observed, is not possible. On the contrary, contraction in the direction of the  $a$  axis is found. McConnell's alternate suggestion was the random substitution of  $4\text{CO}_3$  ions for  $3\text{PO}_4$  ions. While such substitution may not be ruled out at this stage of the investigation, it seems that substitutions of the type  $1\text{CO}_3$  for  $1\text{PO}_4$  must also be considered since they are very common, for example, in solid solutions of  $\text{CaKPO}_4$  or  $\text{CaNaPO}_4$  with  $\text{K}_2\text{CO}_3$  or  $\text{Na}_2\text{CO}_3$ , respectively, or of  $\text{Na}_2\text{SO}_4$  with  $\text{Na}_2\text{CO}_3$ .<sup>(45)</sup> Vacancies in cation lattice positions, or simultaneous substitution of Na for Ca would restore the ionic charge balance. On the basis of a preliminary density determination, it seems likely that the content of the unit cell is less than  $\text{Ca}_{10}\text{Na}_2(\text{PO}_4)_6(\text{CO}_3)_2$ , or, in the case of the  $\text{K}_2\text{CO}_3$  reaction, less than  $\text{Ca}_{11}(\text{PO}_4)_6(\text{CO}_3)$ , the formulas previously suggested.<sup>(35)</sup>

While it is also assumed on the basis of the older data that hydroxyl groups are absent, this interesting point, too, would appear to need further checking. On the basis of Trömel's theory of the apatite lattice,<sup>(37)</sup> the presence of hydroxyl ions, or possibly  $\text{CO}_3$  ions and  $\text{H}_2\text{O}$  substituting for them, would be required. However, at least one case has been observed with certainty<sup>(35)</sup> in which the positions on the hexagonal axes actually were not occupied by singly charged negative ions such as  $\text{OH}$ ,  $\text{F}$ , or  $\text{Cl}$ , namely, a substance of the nominal composition  $\text{Ca}_8\text{K}_2(\text{PO}_4)_6$ , also possessing apatite structure. This fact was also reflected in the solubility of this particular

(45) M. A. Bredig, "Isomorphism and Allotropy in Compounds of the Type  $\text{A}_2\text{XO}_4$ ," *J. Phys. Chem.* 46, 747 (1942).

compound, whose synthesis has also just been repeated, in ammonium nitrate solution in which all the other apatites, including the synthetic carbonate apatites, were found to be insoluble. A further pertinent point is the result of Zambonini and Ferrari, later confirmed by Ferrari<sup>(46)</sup> against criticism by Klement,<sup>(47)</sup> that tribasic lead orthophosphate,  $Pb_3(PO_4)_2$ , which may be written  $Pb_9(PO_4)_6$ , has apatite structure like its complex compound with lead chloride,  $Pb_{10}(PO_4)_6Cl_2$  (pyromorphite), in spite of the absence of singly charged anions such as Cl, F, or OH at the hexagonal axes. It is suggested here that in the absence of such anions the presence of cations more easily polarizable (deformable) than  $Ca^{++}$  or  $Na^{++}$ , such as  $Pb^{++}$  or  $K^+$ , can lead to apatite structure. In recent attempts in this laboratory a "sodium apatite" analogous to the "potassium apatite,"  $Ca_8K_2(PO_4)_6$ , has not been obtained under conditions under which the potassium compound forms.

Potassium ions entering the apatite structure produce an increase not only in the  $c/a$  ratio somewhat similar to that produced by carbonate ions, but, in addition, an increase in the absolute magnitudes of the lattice constants. This increase must be largely due to a substitution of one-fifth of the calcium ions by potassium ions. Ionic radii are 0.98 Å for  $Ca^{++}$  and 1.33 Å for  $K^+$ . In the case of the carbonate apatites some rather striking intensity effects are evident, for example, Fig. 5.4 will be very difficult to interpret in terms of atomic positions in this complicated type of solid solution structure, with random distribution of substituents.

Conclusions based on the literature survey and the recent X-ray investigation may then be summarized as follows:

1. Very distinct changes in both the lattice constants (e.g., increase of the  $c/a$  ratio from 0.730 in hydroxyapatite to 0.737 in "dicalcium carbonate apatite" to 0.740 in sodium carbonate apatite, all  $\pm 0.001$ ) and in intensity ratios in powder X-ray patterns are final proof of the existence of carbonate apatite, of varying carbonate ion content, in synthetic preparations of simple compositions.

(46) A. Ferrari, "Lead Orthophosphate," *Gazz. chim. ital.* 70, 457 (1940); *Chem. Abs.* 37, 322 (1943).

(47) R. Klement, "Basic Phosphates of Bivalent Metals. II. Lead Hydroxyl Apatite," *Z. anorg. u. allgem. Chem.* 237, 161 (1938).

2. Although major amounts of potassium produce a similar increase in the  $c/a$  ratio (in potassium apatite,  $\text{Ca}_8\text{K}_2(\text{PO}_4)_6$ ,  $c/a = 0.742$ ), the characteristic axis ratio of carbonate apatite can be used in conjunction with analytical data which may show the absence of potassium, to determine the presence or absence of a true carbonate apatite in a given material. In this way, the occurrence in natural minerals such as francolite, or North African and North American rock phosphates, of true carbonate apatite, usually in solid solution with fluorine or hydroxyapatites, has been firmly established. Frequently such minerals contain "free" carbonate in addition to the  $\text{CO}_3$  ions of the apatite crystal phase. The concentration of the  $\text{CO}_3$  ions in solid solution also varies in different minerals.
3. Sodium and potassium behave differently with respect to apatite formation. Whereas sodium can enter the carbonate apatite, potassium has not been observed to do so under similar conditions. On the other hand, a sodium apatite,  $\text{Ca}_8\text{Na}_2(\text{PO}_4)_6$ , analogous to the potassium apatite discussed above, has not been obtained.
4. The unusually high solubility of potassium apatite,  $\text{Ca}_8\text{K}_2(\text{PO}_4)_6$ , in ammonium citrate solution is explained by the absence of the two critically important Z ions in the general apatite formula  $\text{Me}_{10}(\text{XO}_4)_2\text{Z}_2$ . A possible similar situation in tribasic lead phosphate,  $\text{Pb}_9(\text{PO}_4)_6$ , needs clarification.
5. On the basis of the definite knowledge of the effect of  $\text{CO}_3$  ions upon the apatite X-ray pattern, some minerals (e.g., dahlite), as well as the inorganic substance of animal and human bones and teeth (enamel and dentine) were established as consisting of a mechanical mixture of hydroxyapatite, of variable basicity, with "free" calcium carbonate, rather than of one homogeneous phase with molecular dispersion of  $\text{CO}_3$  ions throughout the apatite lattice (Table 5.8).
6. A decision between two alternate concepts of the apatite microstructure of compositions such as enamel or dentine, slightly less basic than  $\text{Ca}_{10}(\text{PO}_4)_6(\text{OH})_2$ , e.g.,  $\text{Ca}_9(\text{PO}_4)_6(\text{OH})_2$ , is not yet possible. We may be dealing here either with a true hydrate of tribasic calcium (or lead) phosphate possessing apatite structure, which might also be represented by a formula such as  $\text{Ca}_9(\text{PO}_4)_4(\text{PO}_4\text{H})_2(\text{OH})_2$ , corresponding to uniform distribution of the component ions in the structure, or with a true hydroxyapatite,  $\text{Ca}_{10}(\text{PO}_4)_6(\text{OH})_2$ , plus adsorbed phosphoric acid (Trömel), corresponding to a nonuniform dispersion of the component ions. Further study might involve the aid of radioactive tracer methods in the solution of this problem.

TABLE 5.8

## Crystal Lattice Constants of Apatites

COMPOUND	a (A)	c (A)	c/a
Hydroxyapatite, $\text{Ca}_{10}(\text{PO}_4)_6(\text{OH})_2$ , synthetic	9.41	6.87	0.730
Human tooth enamel	9.41	6.87	0.730
Dahlite (McConnell <sup>(38)</sup> )	9.41	6.88	0.731
Fluorine apatite	9.36	6.87	0.734
Staffelite I (low $\text{CO}_2$ )	9.33	6.87	0.736
Francolite (McConnell <sup>(38)</sup> )	9.31	6.87	0.738
"Dicalcium carbonate apatite," synthetic (Ca:PO <sub>4</sub> :CO <sub>3</sub> =11:6:2)	9.40	6.92	0.737
"Sodium carbonate apatite," synthetic (Ca:Na:PO <sub>4</sub> :CO <sub>3</sub> = 10:2:6:2)	9.33	6.90	0.740
"Potassium apatite," synthetic, $\text{Ca}_8\text{K}_2(\text{PO}_4)_6$	9.47	7.03	0.742

## 6. RADIATION CHEMISTRY

**Luminescence of Alkali Halides Subjected to Ionizing Radiation** (J. A. Ghormley with H. A. Levy). A paper discussing work to date on this problem has been written and will be submitted for publication in the *Journal of Physical & Colloid Chemistry* together with other papers presented at the Radiation Chemistry Symposium of the April ACS meeting. The paper is summarized as follows:

1. Infrared emission has been observed in irradiated or additively colored KCl during exposure to F-band light. This is thought to be associated with the transition from the excited F center to the ground state of the F center.
2. Glow curves for infrared emission during heating of additively colored KCl following exposure to F-band light at low temperature exhibit five peaks between  $-196$  and  $+25^{\circ}\text{C}$ , indicating five types of electron traps.
3. Glow curves obtained simultaneously for different emission bands indicate that at least two types of processes requiring activation energy may occur, and a single type of activation step can lead to more than one spectral emission band.
4. NaCl and LiF irradiated at  $4^{\circ}\text{K}$  and allowed to warm give maximum emission at  $66$  and  $135^{\circ}\text{K}$ , respectively, with little phosphorescence below these temperatures. The emission peaks are thought to arise from release of self-trapped electrons.
5. A temperature-independent afterglow observed in alkali halides is attributed to tunneling of trapped electrons to trapped holes.

**Effect of Radiation on Heterogeneous Catalysts** (J. A. Wethington and E. H. Taylor). Work has continued on the decrease in catalytic activity of ZnO observed after irradiation with gamma rays. As before, the catalytic activity is determined by following the rate of hydrogenation of ethylene at  $0^{\circ}\text{C}$ .

The catalytic activity of a sample of ZnO, which had been activated by evacuation for 16 hr at about  $360^{\circ}\text{C}$ , was measured after each of a series of treatments, including evacuation at  $0^{\circ}\text{C}$ , evacuation at  $100^{\circ}\text{C}$ , and irradiation with  $\text{Co}^{60}$  gamma rays at an intensity of about 15,000 r/min. The results are given in the following tabulation:

ZnO TREATMENT	CATALYTIC ACTIVITY (half-time for $2\text{H}_2 + \text{C}_2\text{H}_4$ at $0^\circ\text{C}$ ) (hr)
Preliminary*	26.9
Evacuated 2 hr at $0^\circ\text{C}$	27.6
Evacuated 2 hr at $0^\circ\text{C}$ , irradiated 10 days	41.0
Evacuated 2 hr at $0^\circ\text{C}$	40.9
Evacuated 2 hr at $100^\circ\text{C}$	36.5
Evacuated 2 hr at $100^\circ\text{C}$	41.7
Evacuated 2 hr at $0^\circ\text{C}$	42.7
Evacuated 2 hr at $100^\circ\text{C}$	47.7
Evacuated 2 hr at $100^\circ\text{C}$	48.3
Evacuated 4 hr at $100^\circ\text{C}$	48.6
Evacuated 2 hr, at $100^\circ\text{C}$ , reirradiated 10 days	52.5
Evacuated 2 hr at $0^\circ\text{C}$	54.3

\*Activated by 16-hr evacuation at  $360^\circ\text{C}$ .

There is a marked decrease in catalytic activity upon irradiation, followed by what appears to be a complicated annealing process occurring at  $100^\circ\text{C}$  but not at  $0^\circ\text{C}$ .

The effect of simply standing at room temperature in vacuo was measured on another sample of the same ZnO and was found to be about one-fourth as large as the above irradiation effect, namely, an increase in half-time from 35.4 to 38.2 hr after 11 days. Another sample, evacuated at  $0^\circ\text{C}$  between runs, showed virtually no change after standing 11 days, the half-times being 25.2 and 27.3 hr before standing and 25.3 after standing.

There is still no evidence that the observed effects, which are certainly real, are the result of changes in the catalyst itself. The chief alternative possibilities are (1) radiation decomposition of adsorbed ethylene (that ethylene not removed by the standard evacuation technique) to either carbon or polymer, both of which would poison the catalyst; and (2) radiation release of adsorbed water from the glass followed by poisoning by re-adsorption in the ZnO. Some evidence against the latter was obtained in an experiment in which the usual 1 g of ZnO was mixed with 6.67 g of pyrex helices to afford a

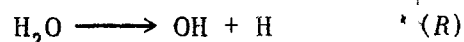
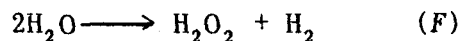
highly increased glass surface. The increase in half-life after a 10-day irradiation was 8.3 hr, clearly no larger than the effect observed without the added glass.

Experiments are underway which are designed to prove which possible explanation is correct. A considerable difficulty is the common one in catalysis of unreproducibility of separate samples of the same material.

**Radiation Decomposition of Water and Aqueous Solutions** (C. J. Hochanadel). Recent work on this problem was presented at the Radiation Chemistry Symposium at the spring meeting of the American Chemical Society in Cleveland, and will be published subsequently. A summary of the paper follows:

The radiation decomposition of water and the radiation-induced back reaction of the products  $H_2$  and  $H_2O_2$  have been studied using a cobalt gamma-ray source. Absolute yields were determined by comparison with an acid ferrous sulfate actinometer which had been calibrated calorimetrically. The measured yield for oxidation of  $Fe^{++}$  in air-saturated 0.4 M  $FeSO_4$  was  $15.5 \pm 0.3 Fe^{++}$  oxidized per 100 ev absorbed.

The decomposition of water by any ionizing radiation is treated as occurring in two separate reactions



The value of 0.46  $H_2O_2$  (and presumably  $H_2$ ) per 100 ev for  $k_F$  was determined from the  $H_2O_2$  yield in oxygen-free acid bromide solutions.

The value of 2.74 H and OH per 100 ev for  $k_R$  was determined from the  $H_2O_2$  yield in solutions containing  $H_2$  and  $O_2$ . The minimum yield for decomposition of water by gamma radiation is then 3.66  $H_2O$  per 100 ev or 1  $H_2O$  per 27 ev.

The radiation-induced reaction between dissolved product molecules  $H_2$  and  $H_2O_2$  was studied under a variety of conditions. The kinetics are discussed in terms of reactions with free radicals H, OH, and  $HO_2$ .

**Radiation Chemistry of Aqueous Organic Solutions** (T. J. Sworski). In order to obtain an understanding of the mechanism of protective action of

many organic solutes in biological systems, an investigation of the mechanism of radiation chemical effects in aqueous organic solutions has been initiated. The immediate objective of this investigation is to examine protective action in simple aqueous solutions.

An aqueous benzene solution, with its resultant phenol formation upon irradiation,<sup>(1)</sup> is now under investigation.

**Radiation Stability of HRE Components** (J. W. Boyle, F. J. Fitch, J. F. Manneschildt, H. F. McDuffie, D. M. Richardson, M. D. Silverman, C. H. Secoy, A. W. Smith, and F. H. Sweeton). During the past quarter work has been continued on uranyl sulfate solutions in contact with type 347 stainless steel which had been pretreated with nitric or chromic acid to produce a passivated surface. Since all this work is connected with the homogeneous reactor program, detailed reports with full discussion and tabulation of data have been included in the HRE quarterly report for the period ending February 28, 1951 (ORNL-990). Major findings of interest during the quarter were as follows:

1. Analytical results on hot solutions from previously reported in-pile experiments and examinations of corrosion specimens from these experiments support the classifications of experiments as "good" or "bad" based on pressure-temperature data obtained in the course of the irradiations.
2. Additional support was found for the association of failures in the in-pile experiments with conditions during pile shutdowns (i.e., the absence of a neutron flux).
3. Several nonradiation factors were discovered which, in the absence of radiation, consistently caused reduction of uranium to insoluble oxides. These factors could have been responsible for the failures observed in experiments in which there were pile shutdowns.
4. Increasing support for the idea that radiation is beneficial rather than harmful with respect to corrosion and solution stability was obtained. A low but effective level of hydrogen peroxide (or oxidizing radicals associated with peroxide formation and decomposition) appears to be maintained during neutron irradiation even at temperatures of 250 to 300°C.
5. At temperatures above 100°C and fluxes up to  $5 \times 10^{11}$  there appears to be little risk of precipitation of uranium peroxide.

(1) G. Stein and J. Weiss, "Chemical Actions of Ionising Radiations on Aqueous Solutions. Part II. The Formation of Free Radicals. The Action of X-Rays on Benzene and Benzoic Acid," *J. Chem. Soc. London* 1949, p. 3245 (1949).

During the next quarter it is planned to extend irradiation experiments using uranyl sulfate to the higher fluxes obtainable in the LITR. Ampoule and metal-bomb experiments with uranyl nitrate will be continued in the graphite pile. Work with other uranium compounds, soluble and insoluble, is also underway. Preliminary irradiations of slurry systems are in progress in cooperation with members of the Chemical Technology Division. Long-term radiation-corrosion tests on uranyl sulfate and passivated 347 stainless steel will be continued.

Out-of-pile tests of bomb-fitting-tubing assemblies will be continued in order to establish the effectiveness of various passivation techniques in the absence of radiation. Ampoule experiments complementing these out-of-pile experiments and extending toward fundamental studies of protective film formation and breakdown in the absence of radiation are being carried out in cooperation with other groups studying the mechanism of corrosion as applied to uranyl sulfate--stainless steel systems.

*Analytical Results for Irradiated Solutions.* In an earlier HRE quarterly report (ORNL-990, Tables 12, 13, and 14) it was stated that the results of 22 in-pile irradiation experiments were classified as "good," "indeterminate," or "bad" on the basis of pressure-temperature data obtained during the course of the experiment; for example, an experiment in which the total pressure ( $H_2 + O_2 + H_2O$ ) was maintained substantially in excess of steam pressure was classified as "good."

During the past quarter analytical results on the radioactive solutions from these experiments have become available and have been set forth in detail in the HRE quarterly report for the period ending February 28, 1951 (ORNL-990). A summary of these results may be of interest:

1. Solutions from "good" experiments were found to have consistently low chloride ion contents. (Chloride ion is known to be very damaging to protective films on stainless steel.) These solutions contained substantially all their original uranium content in a soluble form.
2. Solutions from "indeterminate" experiments contained very little uranium in solution and had high chloride ion concentrations.
3. One of the two solutions from "bad" experiments was found to contain substantially all its uranium in soluble form. This was, however, expected, since the solution had been "reactivated" while still in the pile by the combined effect of a high flux and a low temperature, which produced a high peroxide concentration and reoxidized the reduced uranium to the uranyl state.

4. Examination of corrosion specimens for surface condition and for weight changes showed marked correlation between "good" experiments and lack of change in the specimen.
5. Re-examination of pressure-temperature data for experiments showing loss of pressure led to support for the idea that failures can be associated with pile shutdowns. It seems probable that the concentration of hydrogen peroxide or of oxidizing radicals is maintained, during neutron irradiation, at a level which prevents corrosion and reduction of the uranium. If the neutron flux is removed and high temperatures are retained, the peroxide quickly decomposes, permitting corrosion of the passive film on the stainless steel and destabilizing the uranium in solution.

*Nonradiation Factors Affecting Stability.* Results from the irradiation experiments suggested that some of the failures were not due to radiation but possibly to other, nonradiation, factors. This was confirmed by subsequent out-of-pile control tests in which bomb-fitting-tubing assemblies loaded with uranyl sulfate solution were heated. Every such test resulted in complete reduction of the uranium to an oxide coating on the stainless steel within a period of a few days. These results, in sharp contrast to the findings of the Engineering Corrosion Group of the Reactor Technology Division that passivated 347 stainless steel was inert toward uranyl sulfate solutions, led to an intensive study of nonradiation factors which developed the following results:

1. Supposedly passivated stainless steel bombs with which our group had been furnished were found to be heavily contaminated with chloride ions. These presumably were not rinsed out after an etching treatment, and, moreover, remained through the passivation treatment and subsequent rinsing. Some of the failures observed by us under irradiation were undoubtedly caused by the presence of these chloride ions. This was confirmed by subsequent analysis of the radioactive solutions from the bombs. To eliminate chloride ions the group has taken over responsibility for passivating its own bombs, has redesigned the bomb to allow a more efficient rinsing, and has adopted the practice of analyzing the rinses from each bomb for chloride ion prior to filling with a passivating solution.
2. Defects in the previously used pressure fitting were overcome by a redesign of the fitting so as to eliminate the use of silver solder and of unpassivated stainless steel even in positions not in contact with the solution and not normally heated to temperatures above 200°C. The new fittings are passivated after assembly, thus providing a uniform treatment for all surfaces eventually in contact with uranyl sulfate solutions or its vapors and gases. Bomb performances with these new fittings have been very satisfactory both in and out of radiation.

3. It cannot be emphasized too strongly that the numerous successful experiments in the presence of radiation observed prior to the above findings become highly significant in view of the overwhelming probability that they all would have been failures if they had been conducted in the absence of radiation. Despite the combination of old-style fittings containing silver solder, of unpassivated stainless steel, and of inadequate rinsing of bombs following the etching treatment, most of the bombs maintained their content of soluble uranium and did not show excessive corrosion when in the presence of radiation. Such evidence suggests that radiation will prevent corrosion rather than cause corrosion or solution instability.

*Peroxide Precipitation Studies.* The start-up procedure for the HRE would be greatly affected if uranium peroxide were to precipitate before equilibrium conditions could be attained in the reactor. For this reason experiments were conducted to determine the effect of temperature, uranium concentration, flux, and acidity upon the precipitation of uranium peroxide in X-10 pile-irradiated solutions using quartz ampoules throughout. The results from these experiments may be summarized as follows:

1. At temperatures of 100 to 250°C enriched (93%  $U^{235}$ ) uranyl sulfate solutions in the concentration range from 10 to 40 g of uranium per liter and from zero to 2 *N* in excess sulfuric acid can be exposed to a flux of  $5 \times 10^{11}$  n/cm<sup>2</sup>/sec for at least 30 min without uranium peroxide precipitation. The combination of excess acidity and high temperature caused some precipitation of  $SiO_2$ .
2. Enriched uranyl sulfate solutions containing 30 to 120 g of uranium per liter and no excess acid have shown some (less than 20% in any case) precipitation of uranyl peroxide when exposed for 1 hr to a flux of  $5 \times 10^{11}$  n/cm<sup>2</sup>/sec, during which time the temperature rose from 25 to 90°C.
3. Natural uranyl sulfate solutions containing 120 to 200 g of uranium per liter showed no evidence of uranium peroxide precipitation when exposed for 30 min to the same flux as in (2) at 100 and at 150°C.
4. Uranyl sulfate solutions of differing enrichments (17 and 93%  $U^{235}$ , respectively) at a concentration of 120 g of uranium per liter, when exposed to the same flux as in (2) for 30 min at temperatures of 175, 200, and 250°C precipitated small amounts of silica. The more highly enriched material precipitated traces of uranium peroxide at 175 and 200°C but not at 250°C.

Thus, for the HRE, it appears that precipitation of uranium peroxide will not be a problem if start-up is conducted at temperatures of 100°C or higher. A detailed discussion of the foregoing results may be found in the HRE quarterly report for the period ending February 28, 1951 (ORNL-990).

## 7. INSTRUMENTATION

**4 $\pi$  Proportional Beta Counter for Absolute Disintegration-Rate Measurements** (C. J. Borkowski and T. H. Handley). Coincidence methods can be used for determining absolute disintegration rates of beta-emitting nuclides only if gamma rays are present and the decay scheme is known. Pure beta emitters or nuclides with complex and unknown decay schemes pose a difficult problem for determining absolute disintegration rates. Mica-end-window counters can be calibrated if a source of known disintegration rate is available. Calibration must be made over the range of energies for which the counter will be used. Factors such as shape of the beta spectrum; absorption of beta particles in the air and window of the counters; and air, sample support, and self-scattering are important and vary with energy.

The 4 $\pi$  proportional-counter method for obtaining absolute disintegration rates described here<sup>(1)</sup> requires a minimum amount of information about the decay scheme and does not have the disadvantage of the coincidence method in that it can be applied to pure beta emitters. Use of the counter in a 4 $\pi$  geometry is based on the theory that regardless of the complexity of the decay scheme only one pulse will be obtained for each atom decaying by beta emission. Since a gas amplification of  $10^4$  to  $10^5$  can be used, all ionizing events producing at least one or two ion pairs in the sensitive volume of the counter will be detected. The method does, however, require the preparation of sources of either negligible or known self-absorption on thin plastic films. For high specific activities and for maximum beta energies greater than about 0.3 Mev, absorption losses in the film can be made negligible. Absolute disintegration rates obtained with the 4 $\pi$  counter and by coincidence methods were found to agree to within 2%.

Phenomena associated with the scattering of electrons play an unimportant role in the 4 $\pi$  geometry, since electrons scattered from one counter into the other are recorded as a single event when the two counters are connected in parallel to the input of an amplifier.

(1) Previously reported by C. J. Borkowski at the Conference on Absolute Beta Counting at the National Bureau of Standards, 1949.

*Description of the Counter.* Figures 7.1 and 7.2 show the type of counter used in this study. The center wire, which is made of 1-mil stainless steel, is stretched across a diameter of a pillbox configuration as shown. An aluminum disk, 0.010 in. thick with a ½-in.-diameter hole in the center covered with a thin film of formvar upon which the source is mounted, separates two identical halves of the counter. An O-ring rubber gasket provides a vacuum-tight seal.

Two other counter configurations giving a  $4\pi$  geometry were tried. The first was similar to the one shown in Figs. 7.1 and 7.2 except that each half of the counter was hemispherical and a 1-mil wire loop in each half served as the center wire. The second was a cylindrical geometry similar to the one described by Rossi and Staub.<sup>(2)</sup>

All three counters gave essentially the same disintegration rate on the same source of  $P^{32}$  and  $Co^{60}$ .

With methane at a pressure of 1 atm as the counter gas, a voltage plateau of 200 volts or more with a slope of 1% per 100 volts was obtained at about 2600 volts. With 90% argon and 10% methane at 1 atm, the plateau occurs at 1700 volts. In general, slightly flatter plateaus are obtained with methane as the counter gas.

To obtain flat plateaus in the proportional and semiproportional regions it is important that the amplifier be able to handle pulses from 1 mv to 1 volt without overloading and producing spurious pulses. The Instrument Development Laboratory model 162 proportional amplifier with 1 mv input sensitivity is satisfactory in this application if a germanium diode is used as the counter load impedance.

No conducting coating is necessary on the formvar film if the diameter of the opening in the aluminum separator is kept below ½ in. With a 1-in. opening the collection of positive ions on the formvar reduces the electric field between the source and the wire sufficiently to result in the lowering of the counting rate with time.

(2) B. B. Rossi and H. H. Staub, *Ionization Chambers and Counters*, p. 182, NNES, Div. V, Vol. 2, McGraw-Hill, New York, 1949.

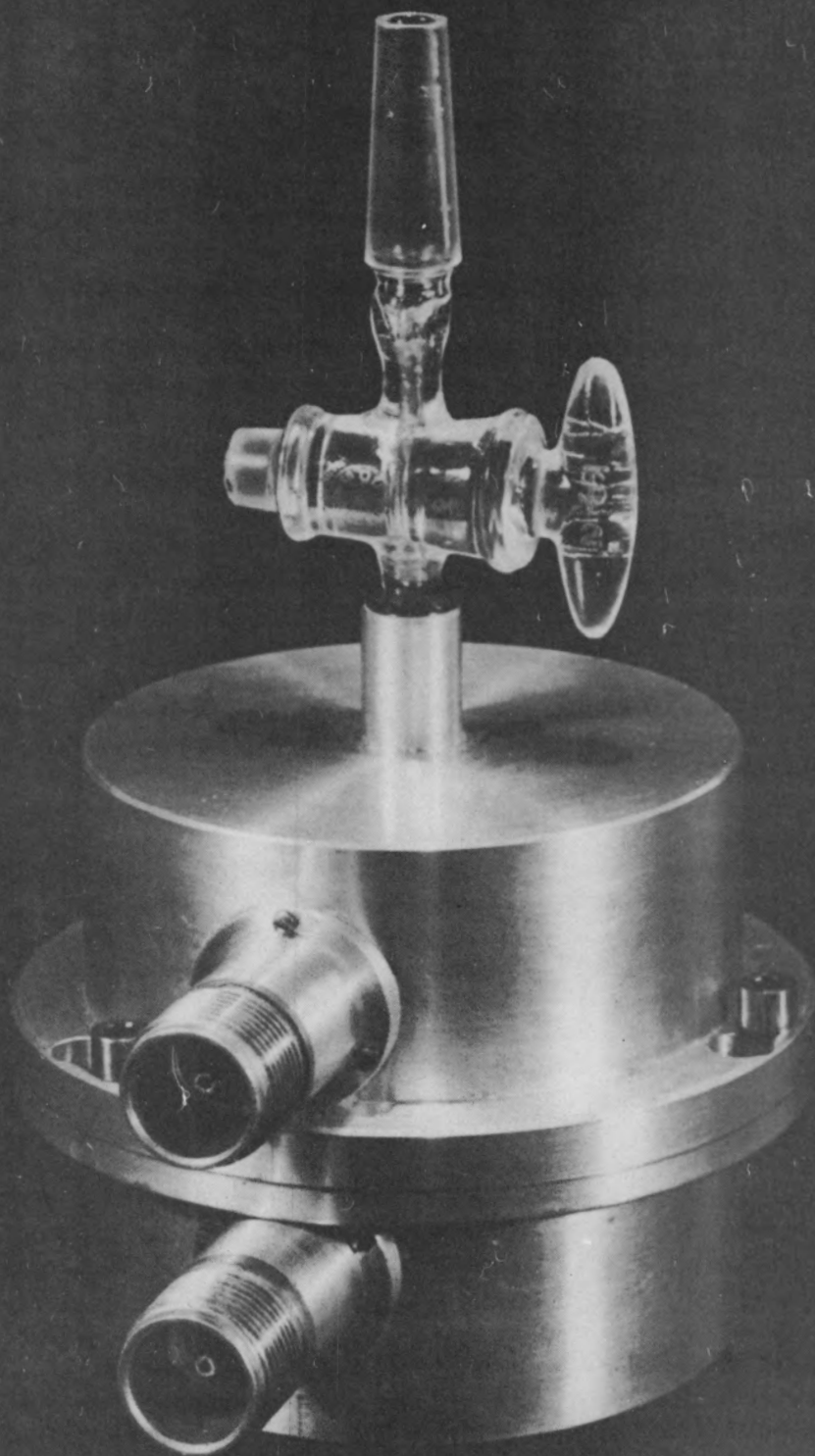


FIG. 7.1  $4\pi$  PROPORTIONAL COUNTER



UNCLASSIFIED  
PHOTO # 5290

FIG.7.2 4 $\pi$  PROPORTIONAL COUNTER

*Source Preparation.* Since the formvar film is not resistant to acids it is necessary to neutralize or make slightly ammoniacal the solution to be evaporated on the film. For beta energies above 1 Mev,  $100\text{-}\mu\text{g}/\text{cm}^2$  films can be used with negligible absorption.  $\text{Co}^{60}$  with a maximum beta energy of 0.31 Mev requires a film of  $20\ \mu\text{g}/\text{cm}^2$  to show less than 2% absorption. Uneven evaporation of the sample can result in serious self-absorption errors for soft beta rays even if the total solids is less than  $20\ \mu\text{g}$ .

After the source has been placed in the counter it is evacuated for about 5 min and then filled with methane to a pressure of 1 atm.

*Measurement Procedure and Results.* The two halves of the counter are connected in parallel to the input of the amplifier, and the sample is counted at a voltage midway on the plateau. Each half of the counter can be counted separately to determine the extent of absorption by the formvar film. Background of the counter shielded with 2 in. of lead is 100 c/m. Typical counting data for the  $4\pi$  counter using a  $\text{Co}^{60}$  source mounted on  $10\text{-}\mu\text{g}/\text{cm}^2$  formvar follows:

	COUNTING DATA (c/m)
Top half	38,600
Bottom half	38,500
Top and bottom counted together (disintegration rate)	71,200
Sum of top and bottom	77,100
Coincidence counting disintegration rate	72,600

Since the counting rate of the two halves of the counter were the same there was negligible absorption in the film. The sum of the counting rates of top and bottom is always greater than the counting rate of the two counted simultaneously because beta particles are scattered from one counter through the film into the other. When the counters are counted separately such a scattered beta particle will be recorded twice, whereas when the counters are connected in parallel only a single count is obtained for each disintegration.

Pure methane has given disintegration rates which are 3% higher for  $\text{Co}^{60}$  and 7% higher for  $\text{Nb}^{95}$  than the argon-methane mixture. For hard beta rays the

difference between the two gases is less than 1%. There is no effect of counter-gas filling pressure on the disintegration rate, as can be seen from Table 7.1.

**TABLE 7.1**  
**Effect of Methane Gas Pressure on Disintegration Rate**

PRESSURE (cm Hg)	DISINTEGRATION RATE (c/m)
10	$2.21 \times 10^5$
20	$2.21 \times 10^5$
40	$2.22 \times 10^5$
76	$2.21 \times 10^5$

The voltage plateau shifts with pressure, but the counting rate on the plateau is unchanged.

Saturation backscattering was determined (Table 7.2) for several elements, using a  $\text{Co}^{60}$  source mounted on thin formvar with the infinitely thick backscatterer in contact with the film. The upper half of the  $4\pi$  counter was used

**TABLE 7.2**  
**Saturation Backscattering Using a  $\text{Co}^{60}$  Source**

MATERIAL	$2\pi$ GEOMETRY	10% GEOMETRY END- WINDOW G-M
Be	21%	7%
Al	35%	23%
Brass	44%	52%
Pt	56%	80%

with essentially  $2\pi$  geometry. For comparison, typical values for 10% geometry using an end-window Geiger-Mueller tube are given in Table 7.3.

The large discrepancy found with the  $\text{Nb}^{95}$  source was probably due to self-absorption in the source since the specific activity was not very high and a visible amount of solid was present.

TABLE 7.3

Comparison of  $4\pi$  Disintegration Rates with Those Determined by Various Methods

ACTIVITY	MAXIMUM BETA ENERGY (Mev)	COMPARISON METHOD	DIFFERENCE
p <sup>32</sup>	1.7	End-window Geiger-Mueller counter <sup>(3)</sup>	1.0% low
Na <sup>24</sup>	1.4	Coincidence counting	1.0% low
Co <sup>60</sup>	0.31	Coincidence counting	2.0% low
I <sup>131(a)</sup>	0.6 and 0.3	Coincidence counting	5% low
Na <sup>22</sup>	0.57 $\beta^+$	$4\pi$ geometry ion chamber <sup>(4,5)</sup>	1.3% low
Nb <sup>95</sup>	0.15	Coincidence counting	16% low

(a) In the case of I<sup>131</sup> the coincidence counting rate was obtained by using the  $4\pi$  counter as the beta counter.

A useful application of the  $4\pi$  counter is its use as a beta detector in coincidence counting. It eliminates the necessity of an absorption curve when more than one beta is emitted by the nuclide and the resulting uncertain extrapolation to zero absorber which is difficult to reproduce and, in the case of very complex decay schemes, doubtful. Alpha disintegration measurements can also be made with the  $4\pi$  counter. An alpha source was evaporated on a 20- $\mu\text{g}/\text{cm}^2$  formvar film and counted in the  $4\pi$  counter, filled with argon-methane at 1 atm and operating at 1000 volts. Alpha absorption in the film was less than 1%. The following results were obtained:

	ACTIVITY (c/m)
Top	25,400
Bottom	25,100
Top and bottom counted together	50,300

Figures 7.3 and 7.4 show the construction of the chamber.

- (3) L. R. Zumwalt, *Absolute Beta Counting Using End-Window Geiger-Mueller Counters and Experimental Data on Beta-Particle Scattering Effects*, AECU-567 (Sept. 14, 1949).  
 (4) J. W. Jones, and R. T. Overman, *The Use and Calibration of a 100% Geometry Ion Chamber*, MonC-399 (March 20, 1948).  
 (5) J. W. Cobble, private communication.

NOT CLASSIFIED

MATERIALS LIST					
ITEM NO.	DWG. NO.	QTY.	NAME	SIZE	MATERIAL

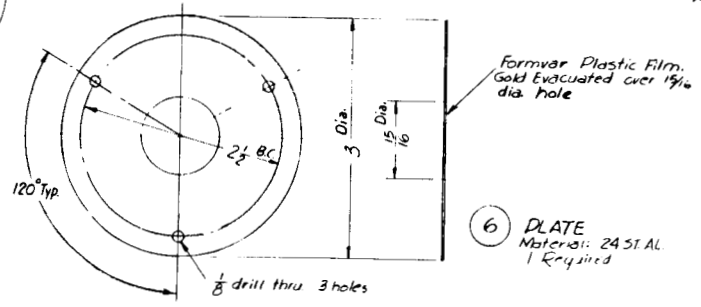
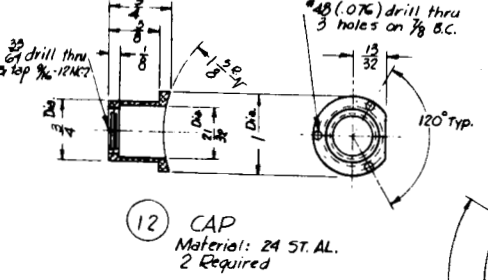
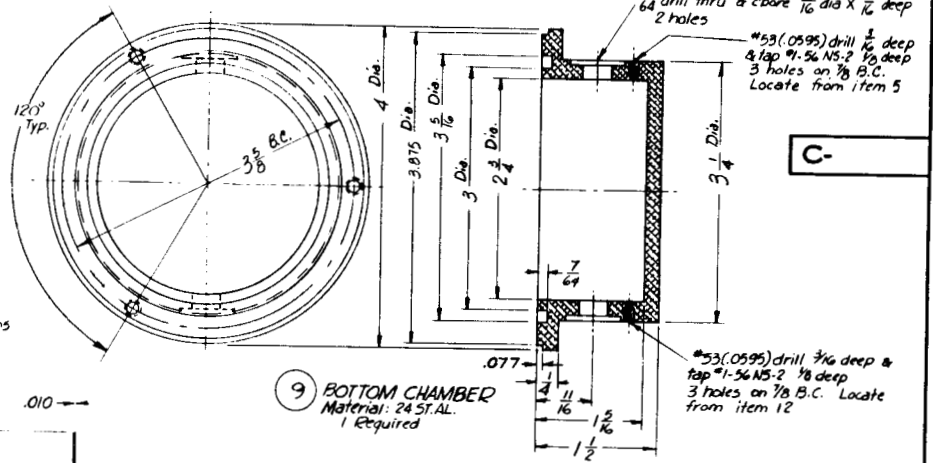
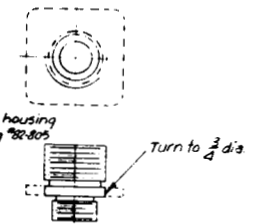
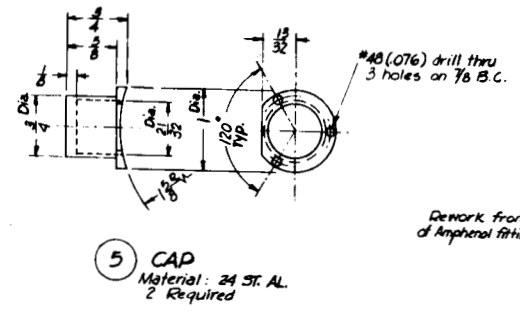
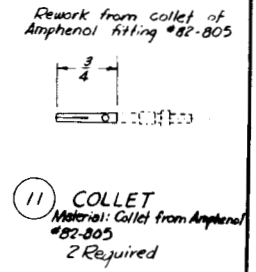
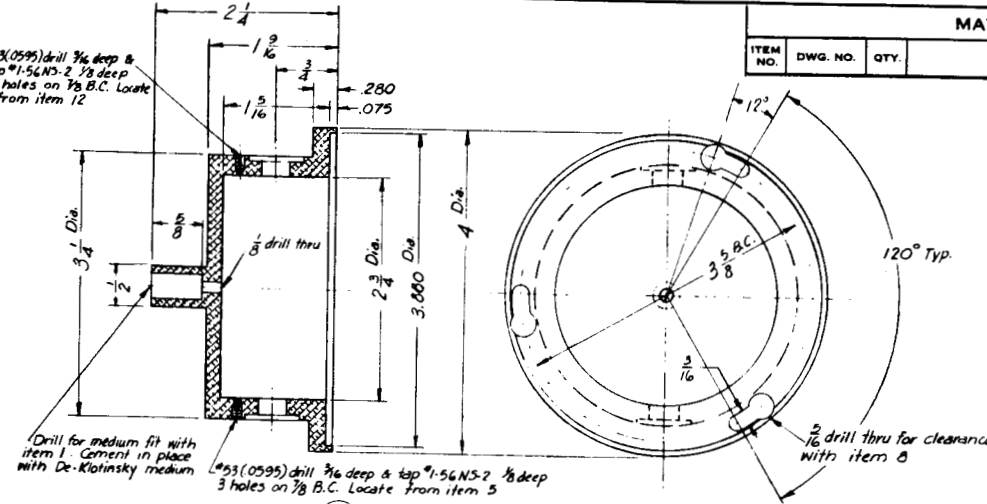
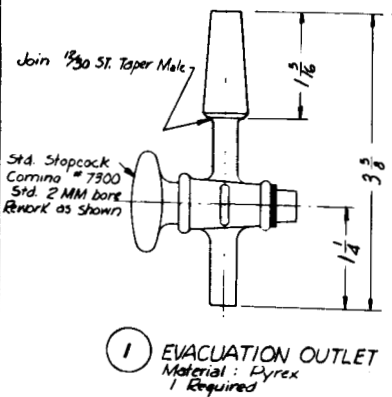
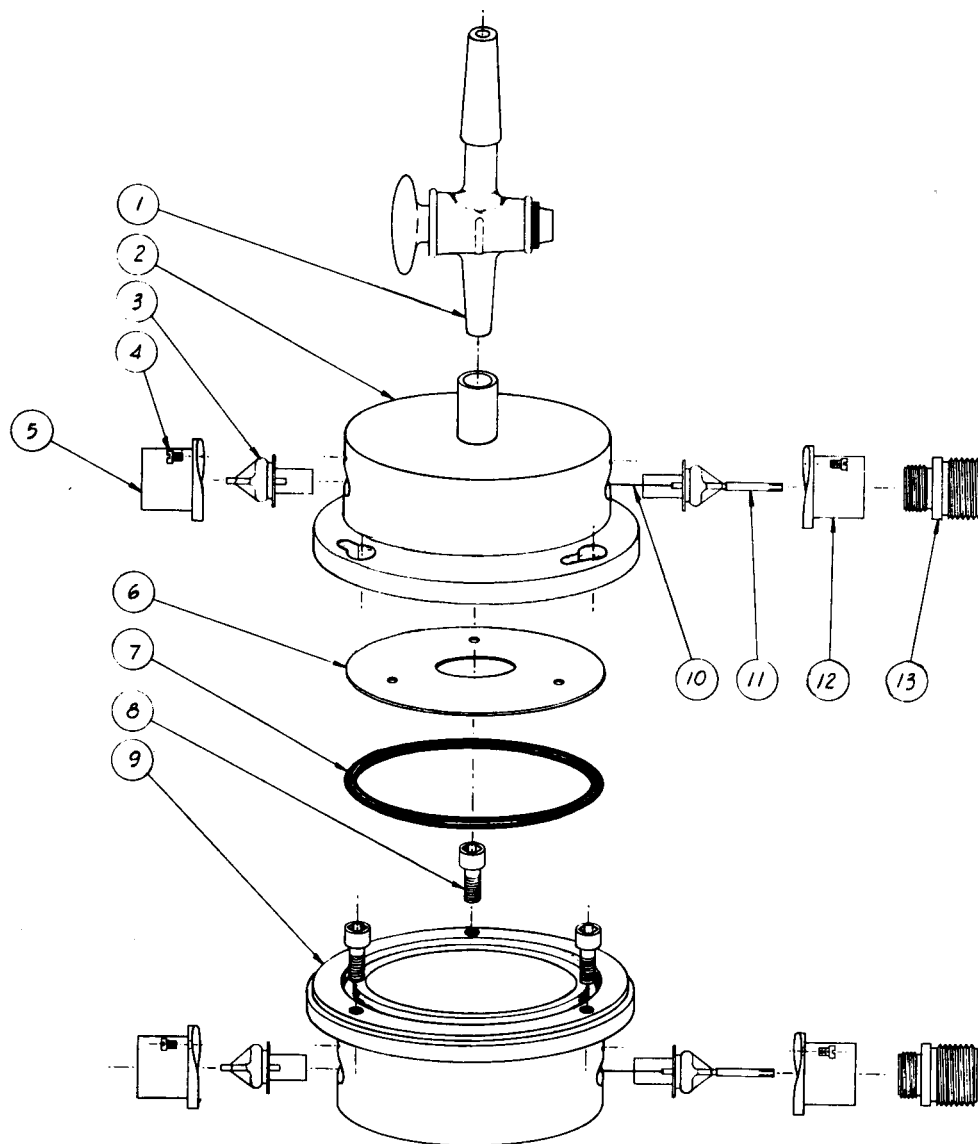


FIG. 7.3  
4TT PROPORTIONAL COUNTER  
DETAILS

NOT CLASSIFIED



MATERIALS LIST					
ITEM NO.	DWG. NO.	QTY.	NAME	SIZE	MATERIAL
1	C-7534	1	Evacuation Outlet	As Shown	Pyrex
2	C-7534	1	Top Chamber	4 Dia. x 2 1/4	24 St.Al.
3	Stock	4	Kover Seal	# 9824 Hollow Electrode	
4	Stock	12	Fillister Head Mech. Screw	# 1-56 NS-2 x 1/8	Steel
5	C-7534	2	Cap	1 Dia. x 3/4	24 St.Al.
6	C-7534	1	Plate	3 Dia. x .010	24 St.Al.
7	Stock	1	"O" Ring	# 12 Parker 5430	
8	Stock	3	Socket Head Cap Screw	# 10-32 NF-2 x 1/2	Steel
9	C-7534	1	Bottom Chamber	4 Dia. x 1 1/2	24 St.Al.
10	Stock	2	Wire	1 Mil. sig. as req'd.	8.Stl.Wire
11	C-7534	2	Collet (from Amphenol)	As Shown	
12	C-7534	2	Cap	1 Dia. x 3/4	24 St.Al.
13	C-7534	2	Housing (from Amphenol)	As Shown	

NOTE:  
Item 11 to be sweated on end of Kover seal

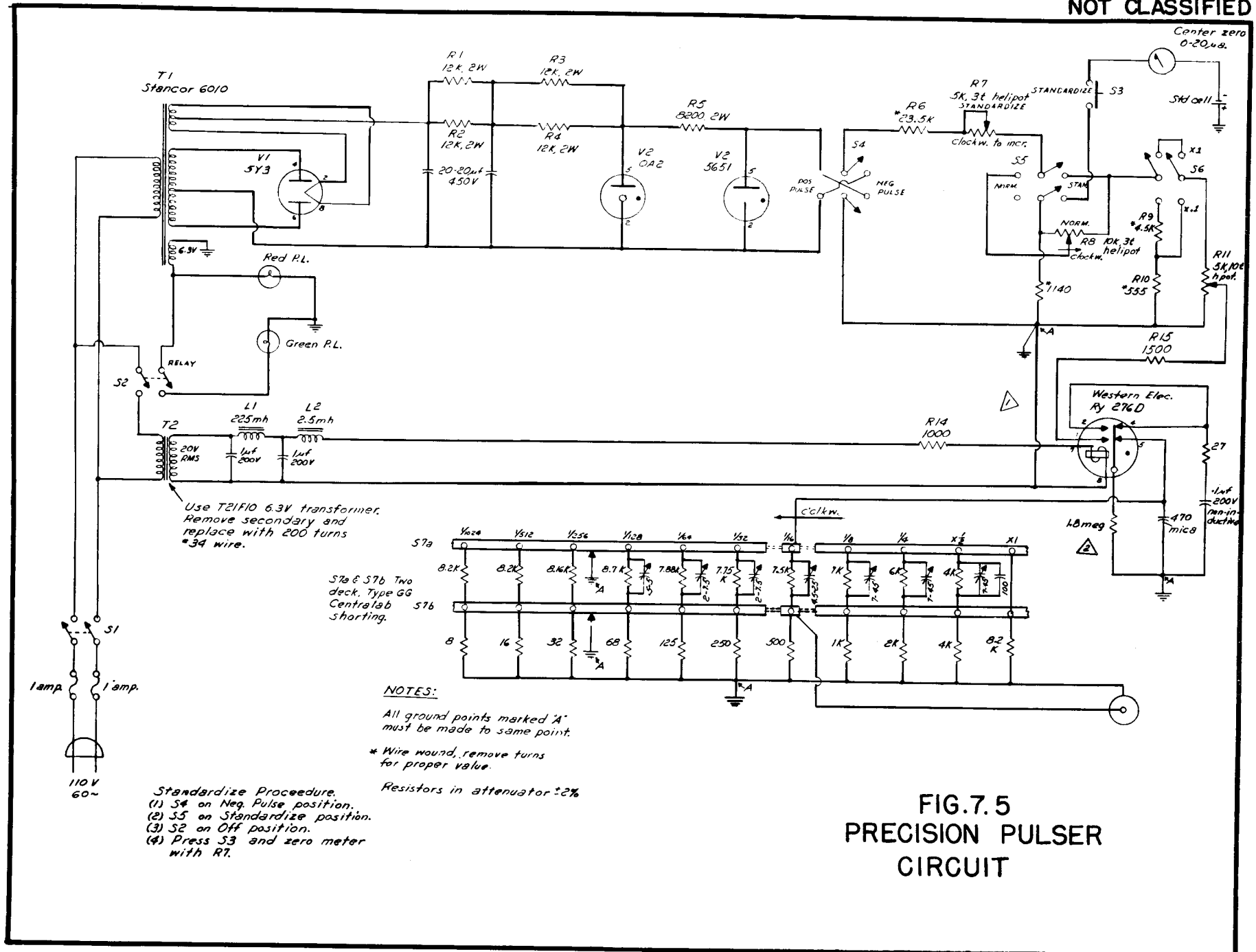
FIG.7.4  
4T PROPORTIONAL COUNTER  
ASSEMBLY

**Precision Pulser Circuit** (R. A. Dandl). The pulse generator shown in Fig. 7.5 is a modified version of the one described in the progress report ORNL-788.

The advantages of the modified circuit are improved reliability, incorporation of a system to standardize the pulse voltage, incorporation of a system to normalize the pulse voltage when calibration of the energy axis of a spectrometer is desired, finer control of the pulse voltage, and freedom from spurious pulses, which makes the generator useful for checking the overload characteristics of pulse amplifiers.

Several models of this generator have been in use for almost six months and have proved most reliable.

149



Use T21F10 6.3V transformer. Remove secondary and replace with 200 turns #34 wire.

S7a & S7b Two deck, Type GG Centralab S7b shorting.

**NOTES:**  
All ground points marked 'A' must be made to same point.  
\* Wire wound, remove turns for proper value.  
Resistors in attenuator ±2%

**Standardize Procedure.**  
(1) S4 on Neg. Pulse position.  
(2) S5 on Standardize position.  
(3) S2 on Off position.  
(4) Press S3 and zero meter with R7.

**FIG. 7.5  
PRECISION PULSER  
CIRCUIT**